INTERRADICULAR MINERALIZED TISSUE ADAPTATION IN AN ASEPTIC NECROSIS MODEL

A report submitted in partial fulfilment of the requirement for the degree of
Doctor of Clinical Dentistry (Orthodontics)

by

Andrew Chang
BDS (Hons)

THE UNIVERSITY
OF ADELAIDE
AUSTRALIA

SUB CRUCE LUMEN

Orthodontic Unit
Dental School
Faculty of Health Science
The University of Adelaide
2008

9.   RESULTS

9.1 <u>Experimental animals</u>

18/28 animals survived the application of the cold thermal stimulus and gained weight during the observation periods. 2/10 rats died in the initial session from carbon dioxide asphyxiation and the latter 8/10 died during the recovery period, where the rats were placed beneath a heat lamp. During this recovery period, involuntary fluid loss from the anaesthetized rats through frequent urinary discharge was noted. An additional 10 rats were requested and approved (under ethics number M-054-2006B) to replace the 10 deceased rats.

9.2 <u>Anaesthesia</u>

Initially, for the first 4 surviving rats {3 treatment rats (rat ID 2,4 and 5) and 1 sham rat, from Group 3}, no premedication was used prior to administering the Ketamine/Xylazine combination. However, it was found that the speed of onset and duration of anaesthesia was highly variable, due to the difficulty in accuracy of an intraperitoneal injection with a fully conscious anxious rat, which affected operator precision.

An inhalational anaesthetic (administered as an isoflurane/oxygen mixture) was used for all remaining rats prior to administration of Ketamine/Xylazine. This achieved a rapid, reliable onset of anaesthesia within 5 minutes. Small additional 0.1ml-0.2ml increments of Ketamine (50mg/kg at 0.2ml per 100grams) were also administered as a top up anaesthetic where the rat was beginning to regain consciousness during the procedure. This was to minimize anaesthetic overdose as Ketamine had a more rapid hepatic clearance rate compared with Xylazine.

During the recovery period, subcutaneous saline was occasionally administered. This, in combination with the use of cooler heating pads instead of a heat lamp, ensured the survival of the remaining rats. All treated rats except one received a 20 minute application of dry ice to their upper right first molar.

Rat number 6 in group 1 was administered the usual dose per body weight of Ketamine/ Xylazine anaesthetic. This rat started to regain consciousness after a 3 minute application of dry ice. Two top up doses were given to prolong the duration of anaethesia but this only enabled an additional 2 minutes application. It was decided to abort administering any more anaesthetic to avoid mortality and the dry ice application was terminated. No ankylosis was seen in this rat and data from this rat were excluded in the statistical analysis.

9.3 Micro-computed tomography pilot study

The two dimensional image slices obtained from the Group 2, sham rat were 11µm apart. A total of 284 images of the upper first molar teeth were obtained, spanning a distance of 3124µm. These corresponded to Z values from 546 to 829. (Fig 17)
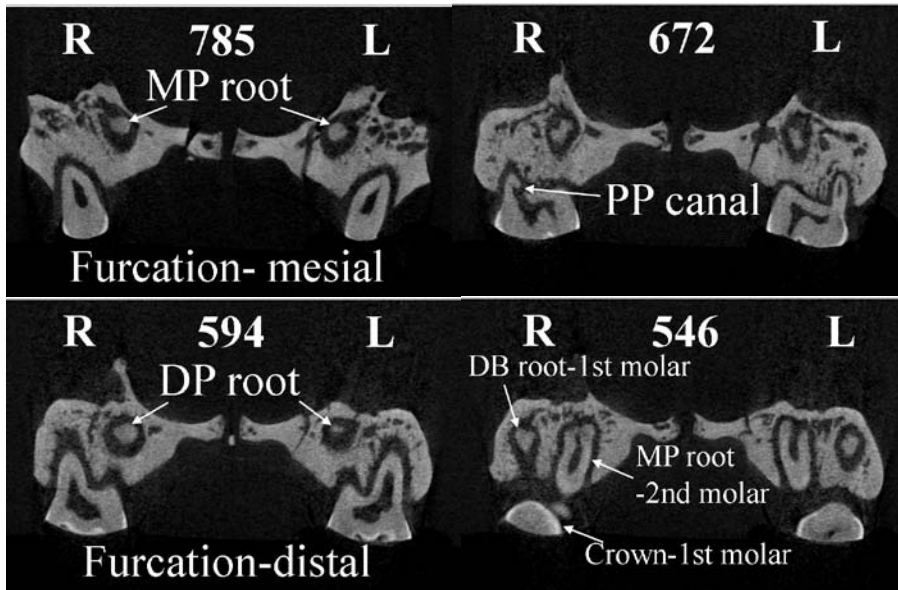
Figure 17. Micro-CT coronal images from an experimental sham rat to illustrate coronal dental anatomy of the upper 1st molars. MP: Mesiopalatal, PP: Pulpal-periodontal, DB: Distobuccal, DP: Distopalatal.

'829', representing the mesial end, corresponded with most mesial image of the right mesiobuccal root. This would have been the starting landmark for section counting, with the purpose, at 10µm thick sections, to select the 100th to 200th sections. The furcation region, regarded as the zone between 2 or more roots, was present between Z values of 785 to 594. The tomogram Z=672 suggests the natural occurrence of a pulp-periodontal canal, on the right molar within the furcation region. 546', representing the distal end, corresponded with a diminishing appearance of the crowns of the upper right and left first molars. The mesial inclination of the upper first molar roots was apparent, with the mesiobuccal root structure of the upper 1st molar teeth appearing first before the crown. At each tomogram slice, the right and left first molars were almost mirror images of each other. This was possible as the Skyscan 1072 allowed for fine 3D positioning of the specimen block.

These images validated the use of this study's methodology (section 8.7) in obtaining the interradicular furcation. By improving the author's understanding of the rat's coronal dental anatomy, it also facilitated a thorough definition of measurement protocols of sections within the representative furcation for quantitative analysis.

9.4 <u>Slides</u>

Coronal sections which were at a markedly different angle than the optimal 90 degrees to the occlusal plane resulted in crown sizes out of proportion with the root size or large relative differences between the left and right molars. These sections were generally few, with regions on the slide outside the representative furcation excluded from quantitative or semiquantitative analysis.

Bone and root resorption, pulpal changes, bone formation and repair of resorption lacunae will be discussed, among the histomorphological changes. The bone labeling patterns and types, as seen in the unstained sections, will also be examined.

9.4.1   General morphological observations

Over time, there was a cumulative decrease in the size of the pulp chamber on the right molar of the treatment rats, as a result of the deposition of mineralized tissue along the walls of the pulp chamber. The difference in size between the left and right first molar pulp chambers was particularly noticeable in the Group 4 treatment rats.

Ankylosis, as seen in this study, was morphologically defined as the physical union between the alveolar bone and furcal root surface that extended across the entire width of the PDL space. Of the 28 rats, there were 3 experimental animals which developed

ankylosis on their upper right first molars (Table 1). Ankylosis was not seen in any of the sham rats or in any of the control molars of the treated rats.

Table 1. Distribution of ankylosis in experimental rats

Time Period	Number of animals with ankylosis in furcation	Rat ID
7 days	0	-
14 days	2	3,7
21 days	1*	2
28 days	0	-

*3 additional rats (rat ID 1, 4 and 5) had morphological features of pronounced mineralized tissue deposition on the furcal root surface but no definite ankylotic bridge.

In the morphological analysis, the unstained sections were all compared with their corresponding adjacent VK/H&E and H&E sections to check for consistency and verification of histological features.

9.4.2   Day 7

9.4.2.1   H&E and VK/H&E sections

Resorption was less common in the left side molars (control) of the treated rats, which generally displayed a smooth furcal root surface.

Small resorption lacunae of superficial depth were noted on the furcal root surface of the right side (treatment) molars. In certain cases, the presence of multinucleated cells within the resorption lacunae were noted, suggesting active resorption. The adjacent alveolar bone surface was also more irregular than the control side, with resorption lacunae more prevalent (Fig 19). The osteocytes surface lacunae of the alveolar bone in the furcation contained pyknotic nuclei or were often empty.

Within the PDL a reduced cellularity, compared with the left molars, was seen.

Numerous small blood vessels were noted within the pulp chamber of the right molars.

The pulp chamber was much less cellular than the left molars, and the odontoblast layer

of cells was generally absent (Figs 18, 20).

Figure 18. Increased vascularity within the pulp chamber was a common finding in the treated molars. BV: Blood vessels, PP: Pulpal-periodontal canal.
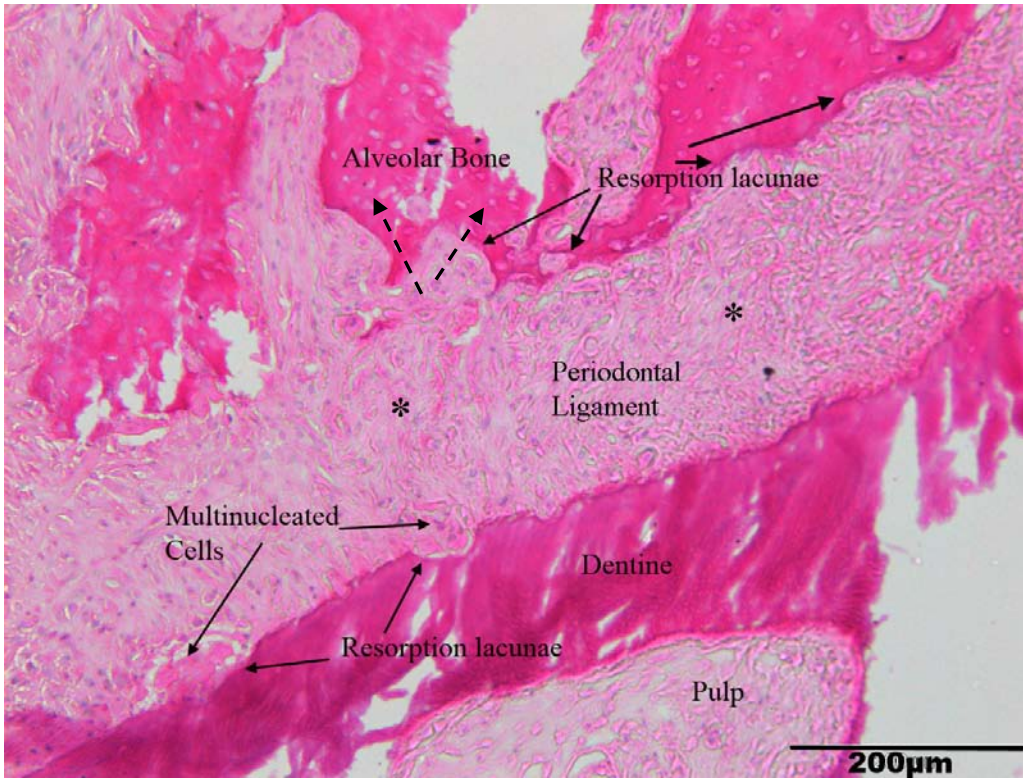Day 7, Rat 2. Right molar. VK/H&E stain. 10x magnification

Figure 19. Extensive surface bone and root resorption with a decreased cellularity (asterisks) in the periodontal ligament compared with the control molars. Avital alveolar bone suggested by the absence of osteocytes in lacunae (dotted arrows).
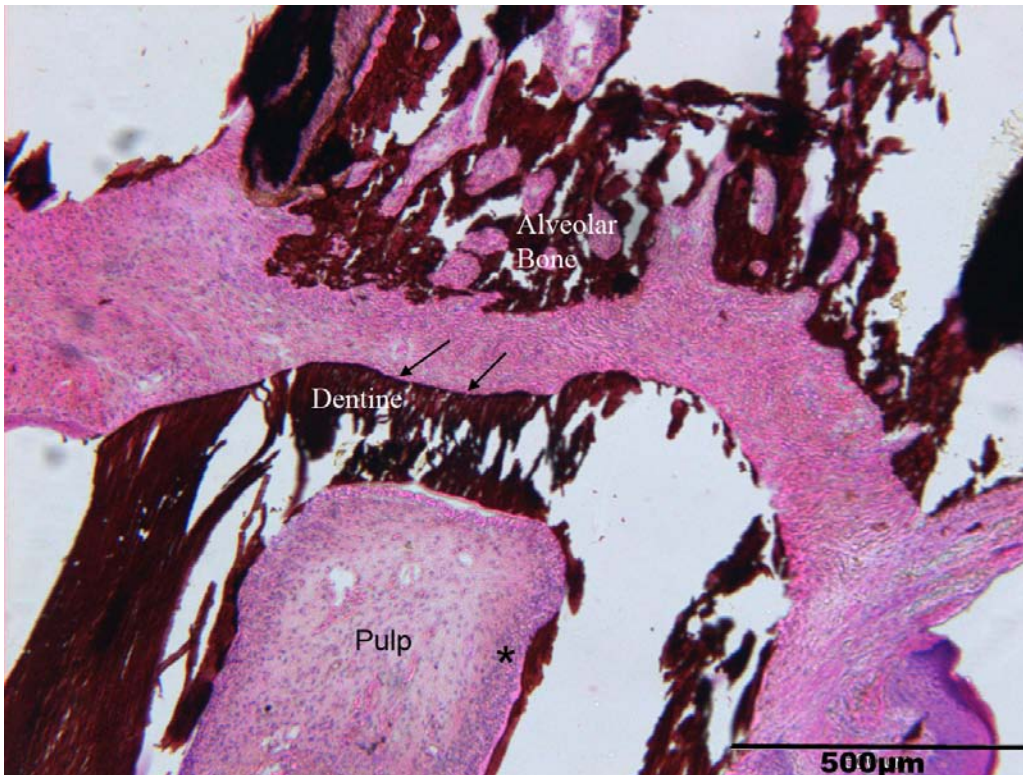Day 7, Rat 5, Right molar. H& E stain. 20x magnification

Figure 20. Markedly less resorption along the root surface (arrows). Asterisk shows a well defined continuous zone around the pulpal walls resembling odontoblasts. These features were common to all control molars in treated and sham rats.
Day 7, Rat 7. Left molar. VK/H&E stain. 10x magnification

9.4.2.2 Unstained sections

Table 2. Distribution of labels among rats in Group 1 (7 days)

Number of labels	Label Type	Number of rats	Rat ID
2	Calcein and Alizarin Red	0	
1	Calcein	7 (6 + sham)	2, 3, 4, 5, 6*, 7, sham
1	Alizarin Red	0	

* Rat 6 had a cumulative total of 5 minutes of dry ice application (see section 9.2)

All the rats within this group had only 1 label present when viewed under fluorescent light. (Table 2) The sham rats were rat 1 in Groups 1 and 2 and rat 7 in Groups 3 and 4. Within the right molars of the treated rats, generalized pitting was occasionally noted on the furcal root surface, characterized by small resorption lacunae when the adjacent stained sections were viewed (Fig 21). This surface feature was not present on the left molars of all the treated rats.

The distance of the calcein labels to their corresponding mineralized tissue surfaces was greatest along the alveolar bone surface of both the left and right molars. In some rats, a faint continuous line of calcein label was noted lining the walls of the pulp chamber of the left and right molars. Calcein labels were rarely present along the root surface of the right molars, particularly where resorption was present (Fig 22).

Similar morphological appearances were noted between the untreated left molars of the treatment rats and the sham control rats (Fig 23).
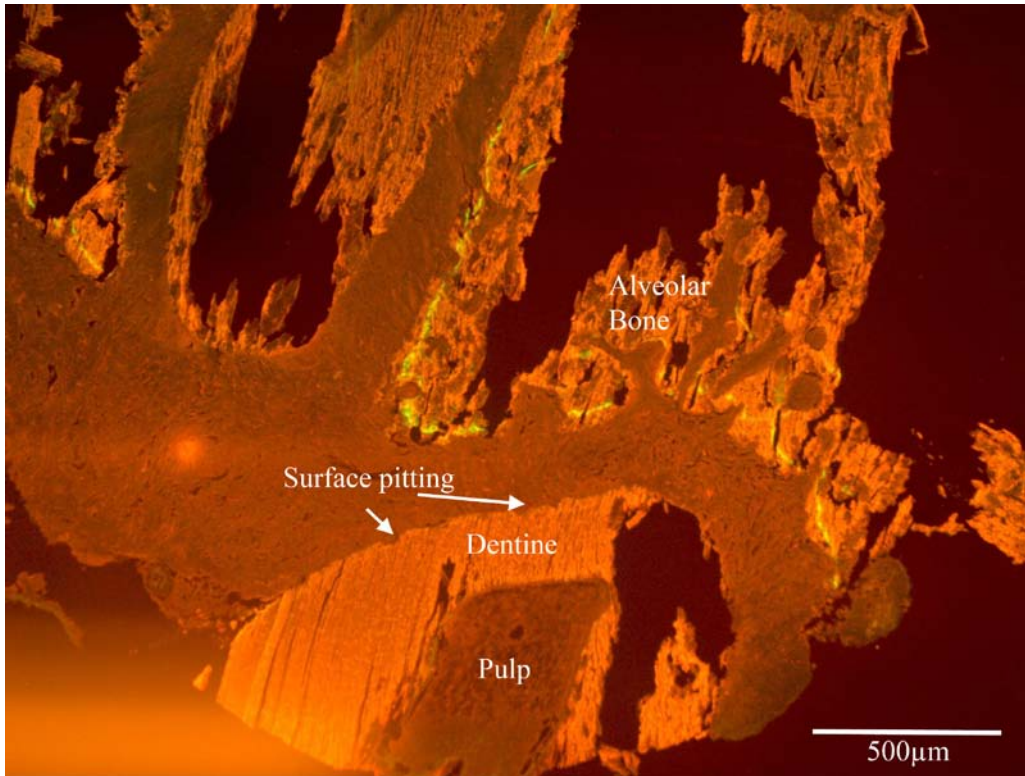
Figure 21. Surface pitting on the root surface with an absence of active mineralization.
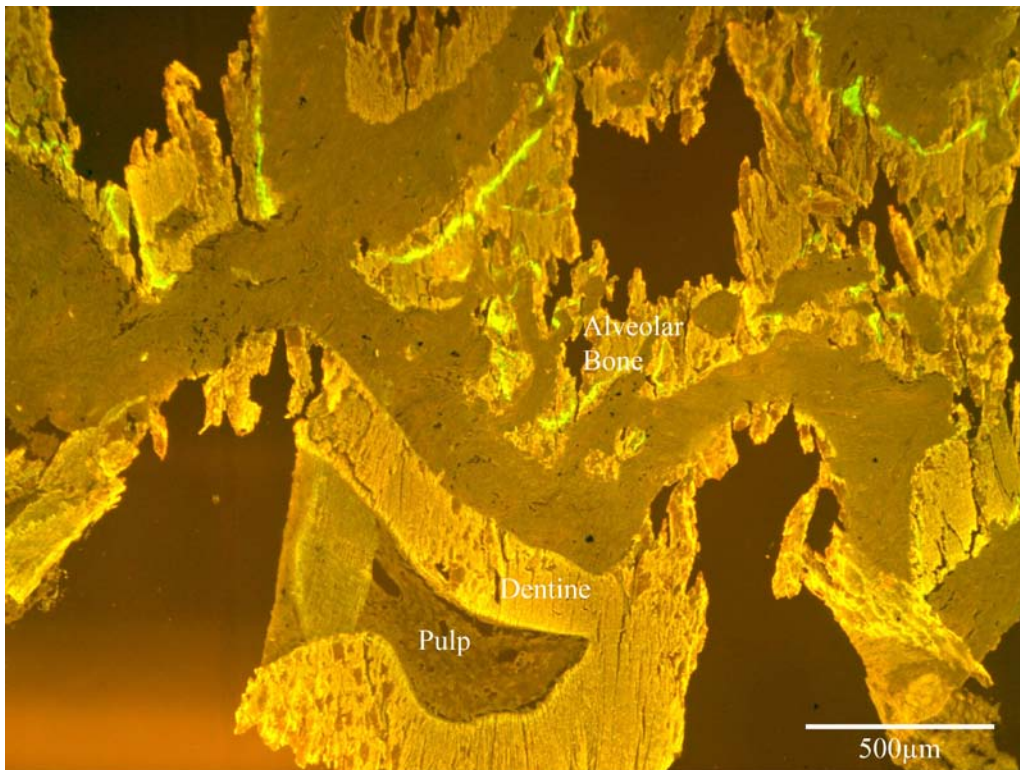Day 7, Rat 5. Right molar. 5x magnification. Calcein label.

Figure 22. Distance of the label to its corresponding mineralized tissue surface was largest in alveolar bone, much less along the pulpal floor and least along the root surface. This suggested the alveolar bone was a much more active formative tissue than the pulpal or root surfaces.
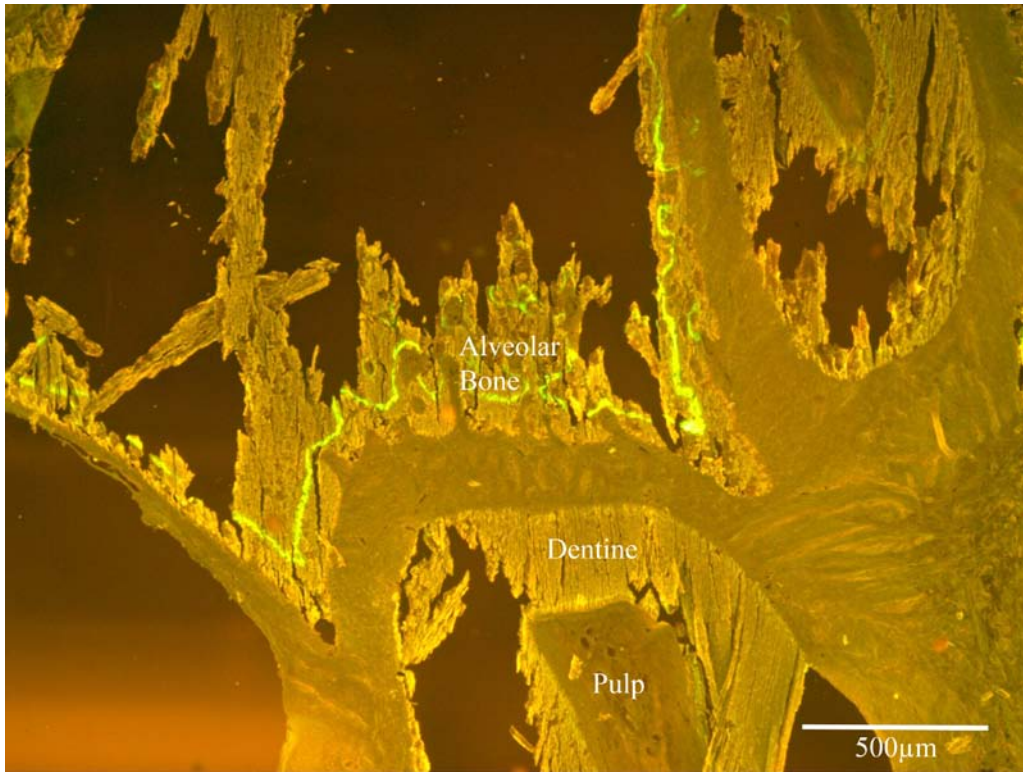Day 7, Rat 3. Right molar. 5x magnification. Calcein label.

Figure 23. Similar rank order of appositional activity (as in Fig 22) also seen in controls.
Day 7, Rat 3. Left molar. 5x magnification. Calcein label.

9.4.3 Day 14

9.4.3.1 H&E and VK/H&E sections

Root resorption was observed along the furcal root surface in the frozen molars.

However, signs of rapid repair of the resorption lacunae were also seen, with cellular

cementum-like material observed along the root surface. (Figs 24, 27, 30)

A definite ankylosis was seen in two treatment rats, Rat 3 and Rat 7 (Figs 29, 31). When

present, fusion between the bone and root was only present in a few sections, suggestive

of a focal nature, with finger-like whorls of mineralized tissue extending from both the

bone and root surface into the PDL. The bone and root surfaces adjacent to these

extensions were irregular and characteristic of resorption. A layer of unmineralized

matrix was seen around the area of ankylosis and along its immediate connecting bone

105

and root surfaces (Fig 29). Blood vessels within the PDL were seen in close proximity to the ankylotic tissue (Fig 30).

There was a haphazard arrangement of the PDL fibres which did not appear to display its uniform directional orientation between the root and bone surfaces (Fig 27). Compared with the treated rats at day 7, an increased cellularity within the PDL was observed. Cells lining the bone surface were often cuboidal or columnar, resembling active osteoblast-like cells. Resorption along the bone surface did not seem as prevalent as seen during day 7. Nuclei were often seen in the lacunae of the alveolar bone.

Similar sized plump cells lining the root surface appeared concentrated around areas of cellular cementum-like tissue and within the resorption lacunae (Fig 27). Occasionally, discrete mineralized nodules were noted in the PDL space (Fig 28).

Within the pulp, a zone of odontoblast-like cells was seen only beneath areas of pronounced unmineralized predentinal matrix. Where bone-like tissue was seen in the pulp, this layer of cells was absent. However, a concentration of hematoxyphilic cells lined the surfaces of this tissue and the adjacent blood vessels. (Figs 25, 26)

These observations suggested that where ankylosis was present a highly active repair process was underway within the PDL, along the bone and root surfaces, and within the pulp.
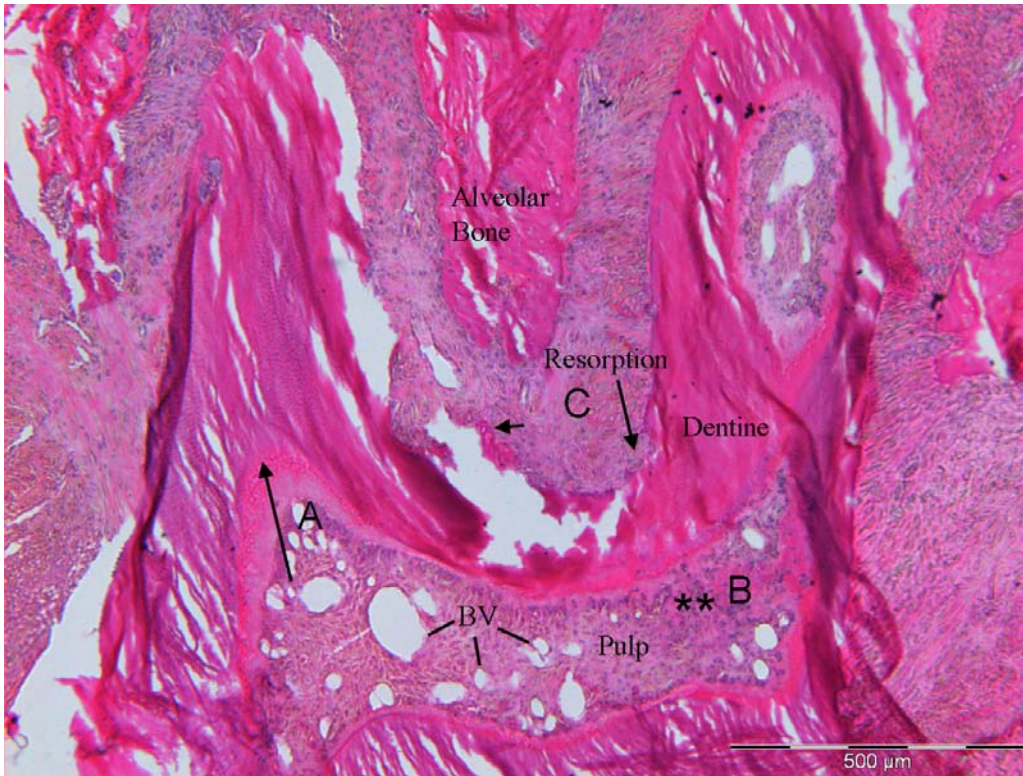
Figure 24. Root resorption with repair cellular cementum-like tissue formation on the root surface, concurrent with marked localized cellular and vascular changes in the pulp, including bone-like tissue (**). Higher power views of regions A, B and C are shown in figures 25,26 and 27.
Day 14, Rat 3, Right molar. H&E stain, 10x magnification. Small arrow: the cellular cementum-like tissue on root surface. Long arrow: amorphous mineralized tissue resembling tertiary dentine. BV: Blood vessels

Figure 25. A discontinuous layer of of odontoblast-like cells (arrows) lying deep to a wide layer of unmineralized predentinal matrix (asterisk)
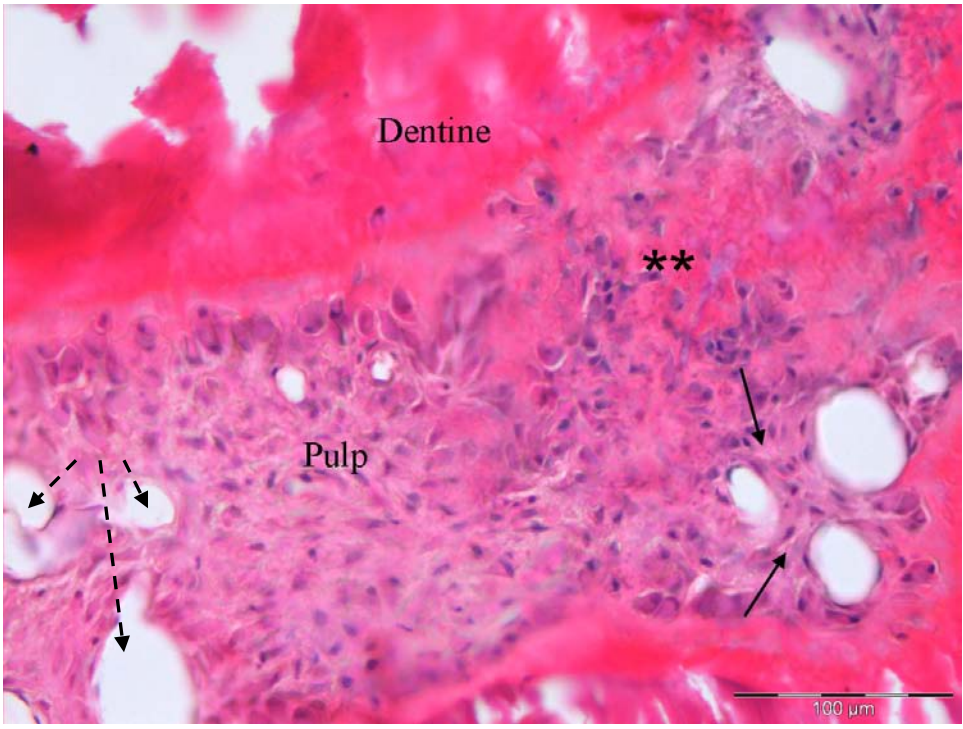Higher power view of Region A in pulp chamber in Fig 24, 40x magnification

Figure 26. Bone-like tissue(**) in pulp chamber surrounded by hematoxyphilic cells. The vascular pericytes close to this bone like tissue are a rim of hematoxyphilic cells (unbroken arrows) which is absent around the blood vessels (broken arrows) in the left of this diagram, distant from the bone-like tissue.

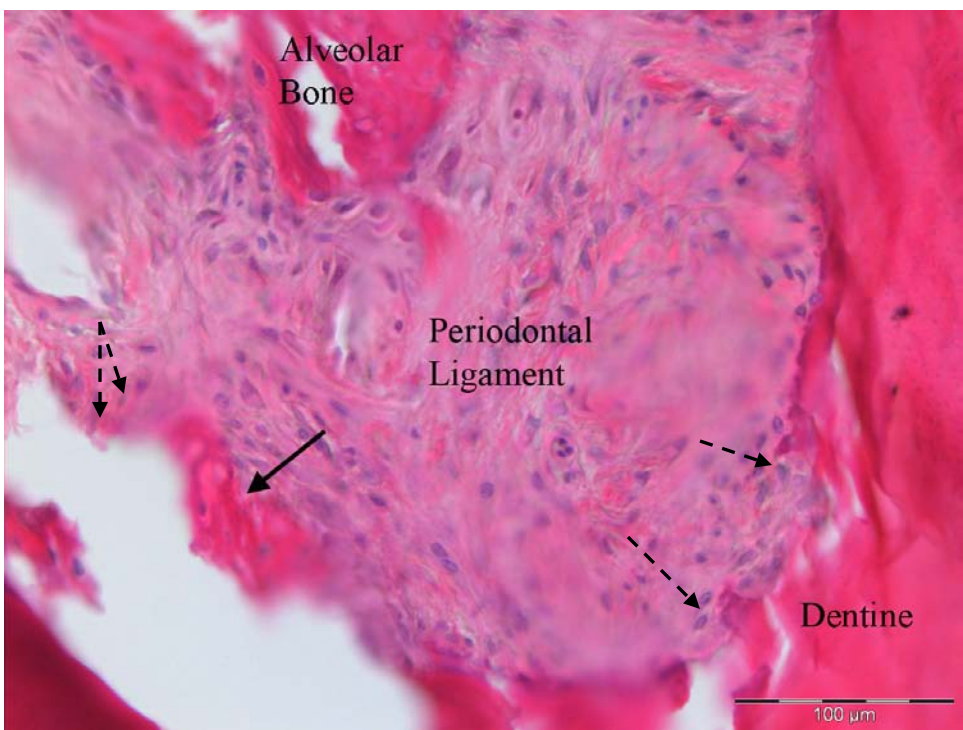Higher power view of Region B in pulp chamber in Fig 24, 40x magnification

Figure 27. Signs of rapid repair of resorption along the bone and root surface 14days after thermal insult with haphazard arrangement of periodontal ligament collagen fibres. Unbroken arrow denotes cellular cementum-like material. An increased presence of mononuclear cuboidal cells (broken arrows) lining the root surface compared with Day 7.

Higher power view of Region C in periodontal ligament in Fig 24, 40x magnification
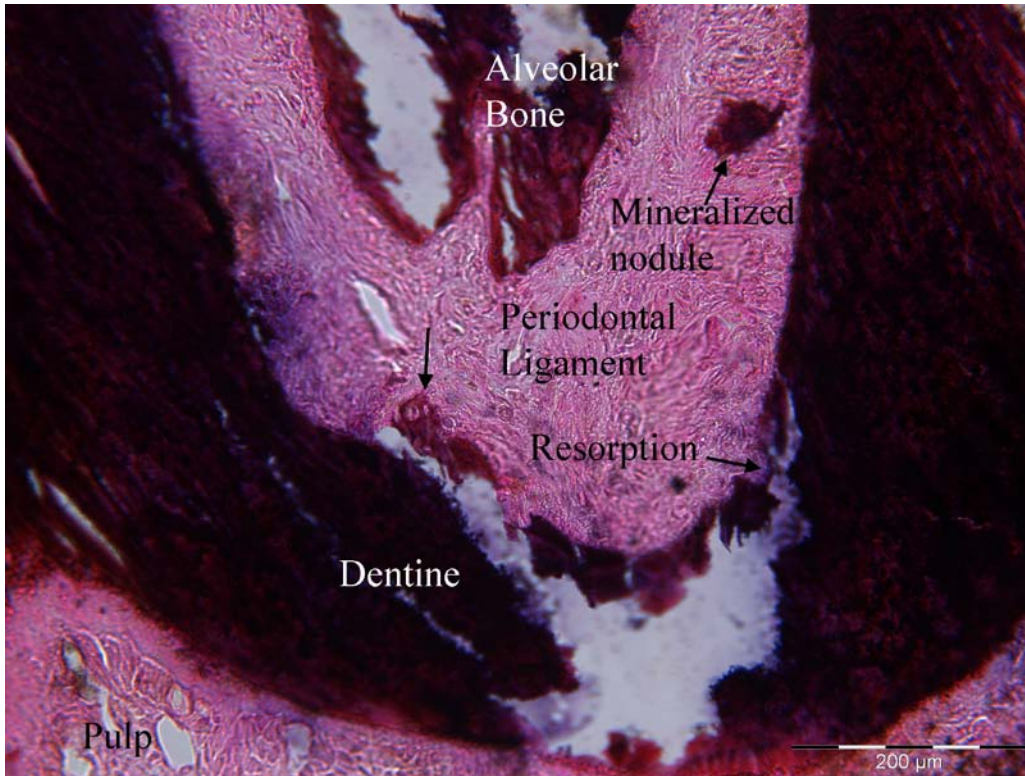
Figure 28. Unattached mineralized nodule within the periodontal ligament space of the same rat. Unlabeled arrow denotes cellular cementum-like tissue on root surface.
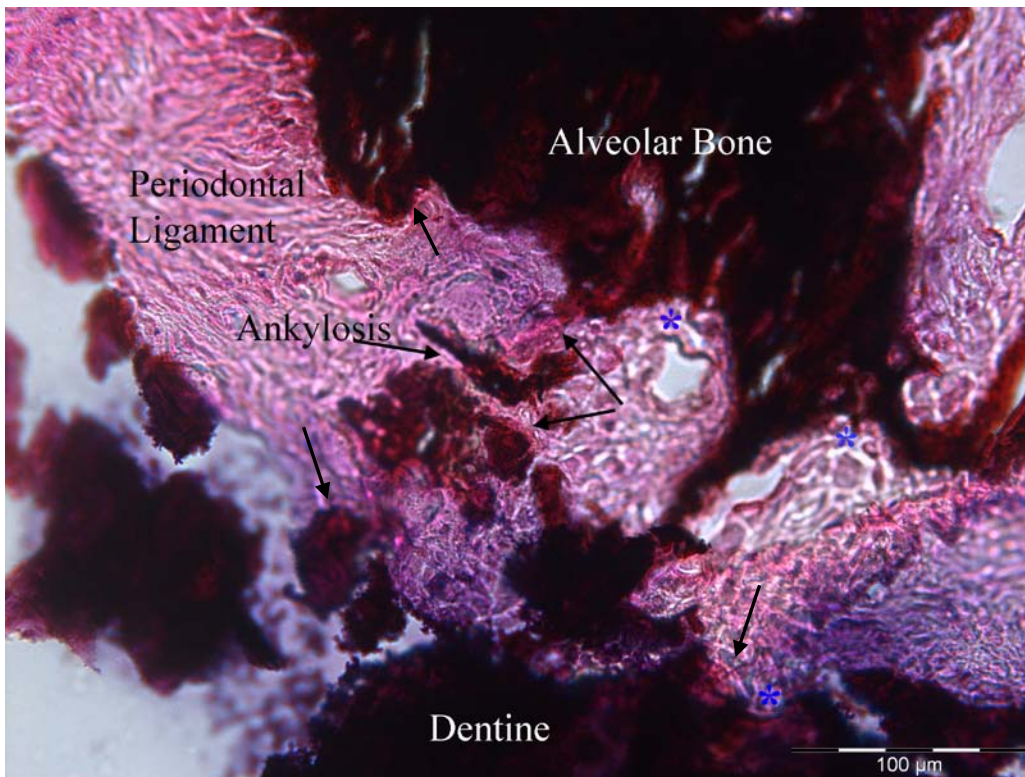VK/H&E stain of adjacent section to Fig 27, 20x magnification.

Figure 29. Deposits of unmineralized matrix along the bone, root surfaces and in the body of the ankylotic region (arrows). Ankylotic extensions occur adjacent to irregular surfaces characteristic of resorption along the bone and root surface (asterisks)
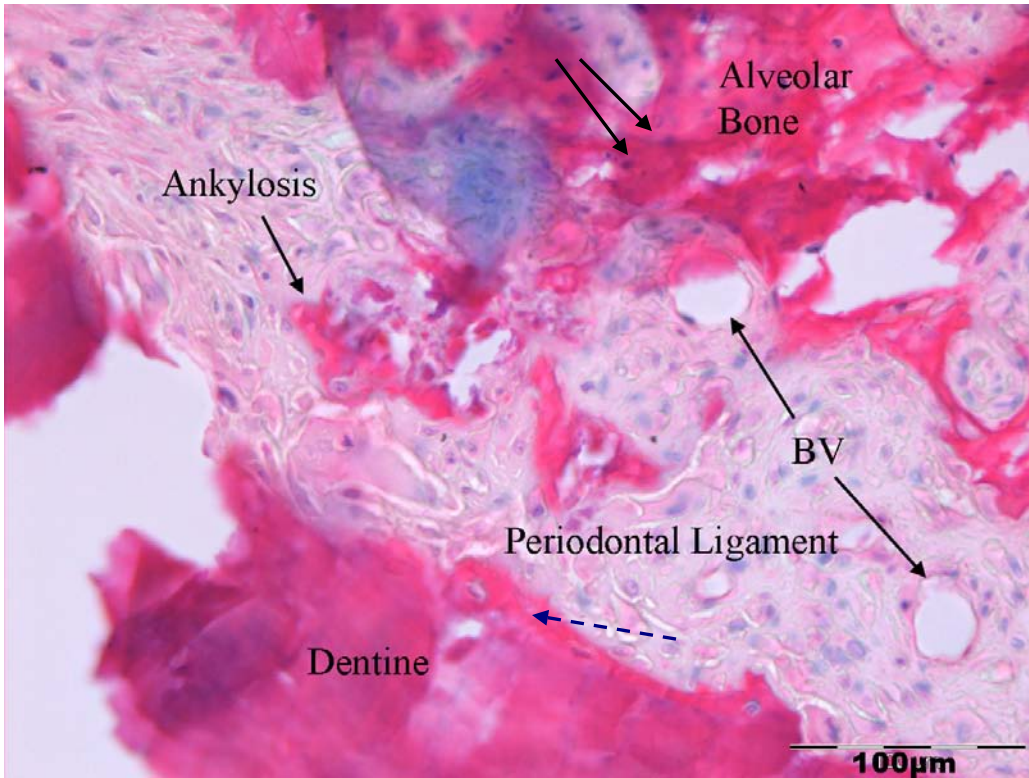Day 14, Rat 7. Right molar. VK/H&E stain. 40x magnification

Figure 30. Ankylosis with increased cellularity and vascularity in the periodontal ligament. Cellular cementum-like tissue (broken arrow) on the root surface. Alveolar bone with osteocytes (unlabeled arrows), some of which are in a different plane to the ankylotic tissue.
Higher power view of adjacent section. H&E stain, 40x magnification. BV: Blood vessels

9.4.3.2 Unstained sections

Table 3. Distribution of labels among rats in Group 2 (14 days)

Number of labels	Label Type	Number of rats	Rat ID
2	Calcein and Alizarin Red	2 (1 + sham)	3, sham
1	Calcein	4	2, 4, 6, 7
1	Alizarin Red	1	5

There was a wide variation in the appearance of labels in this group (Table 3). Within the calcein label group, the labels varied from long continuous lines to broken and interrupted lines. This labeling pattern tended to be consistent through the entire range of sections within each rat.

In the two rats where ankylosis was noted, there were differences in the label uptake (Figs 31,32,33).

The first rat with ankylosis (rat 3) had marked mineralized tissue apposition along the root surface in most sections (Fig 31). Along the root surface, mineralization tended to occur in an outward direction from the the root surface towards the PDL, similar to the pattern seen during cementum regeneration [120], with the calcein label deep to alizarin red. The labeling pattern ranged from a focal region of calcein and alizarin red labels to a much more extensive width bucco-palatally, which extended across both smooth and irregular root surfaces. This suggested apposition had occurred along both unresorbed root areas and as part of the repair of existing resorption lacunae. The ankylotic region was characterized by a focal finger-like extension of increased and rapid mineral apposition along the bone and root surfaces, as seen by the concentration of alizarin red and absence of calcein.

In the second rat with ankylosis (rat 7), there was an absence of labeling lines along the

root surface and the walls of the pulp chamber (Figs 32,33). However, prominent finger-

like extensions of mineralized tissue which projected from the root surface suggested

recent formation, as these were not present in the left control molars or in the 'Day 7'

rats.

All the other treatment rats in this group displayed minimal or no labeling activity on the

furcation root surface.

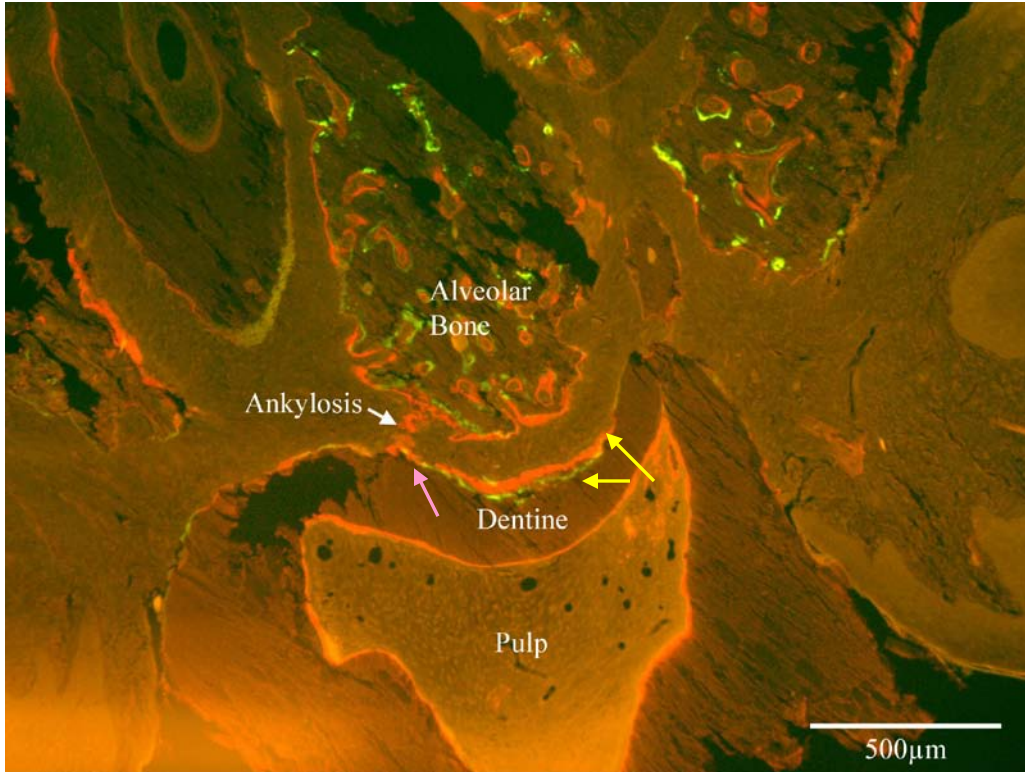**Figure 31. Focal type of ankylosis with rapid apposition across the periodontal ligament space. characterized by a concentration of alizarin red (white arrow). Mineralization along root surface has occurred across both smooth (pink arrow) and irregular (yellow arrows) surfaces characteristic of previous resorption.**
Day 14, Rat 3. Right molar. Unstained. 5x magnification. Calcein and alizarin red labels.
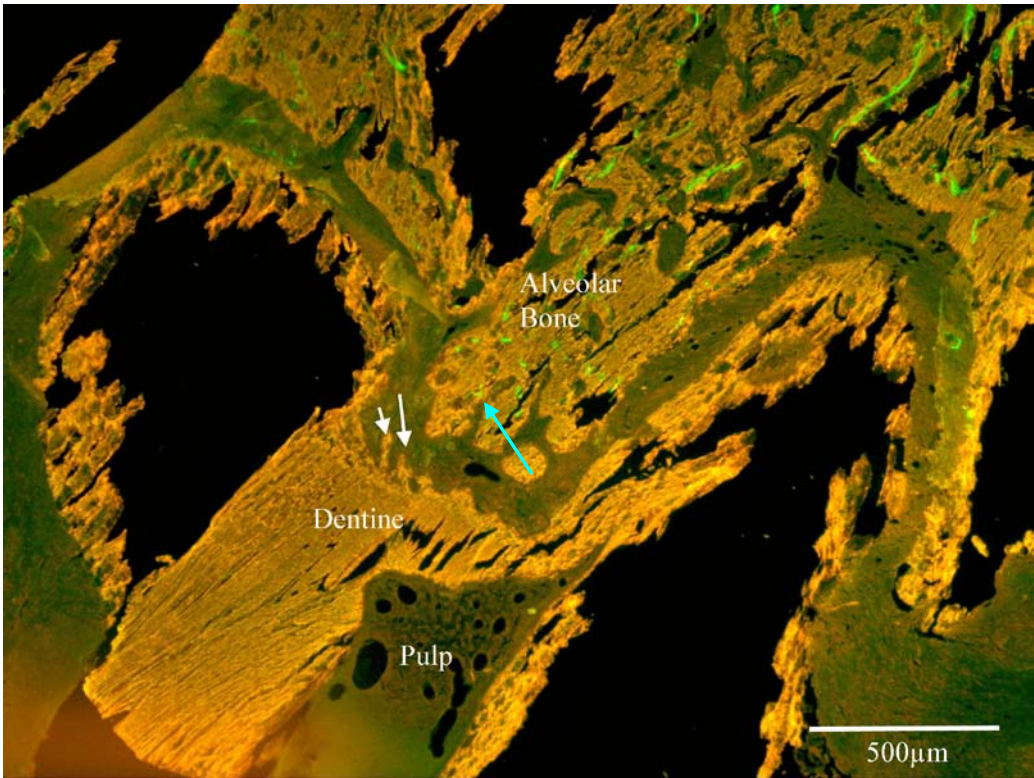
Figure 32. Finger like projections from the root surface (unlabeled arrows) with an absence of label uptake along the root surface. Labels in alveolar bone (blue arrow) are short and irregular.
Day 14, Rat 7. Right molar. Unstained. 5x magnification. Calcein label. Mesial section of furcation.
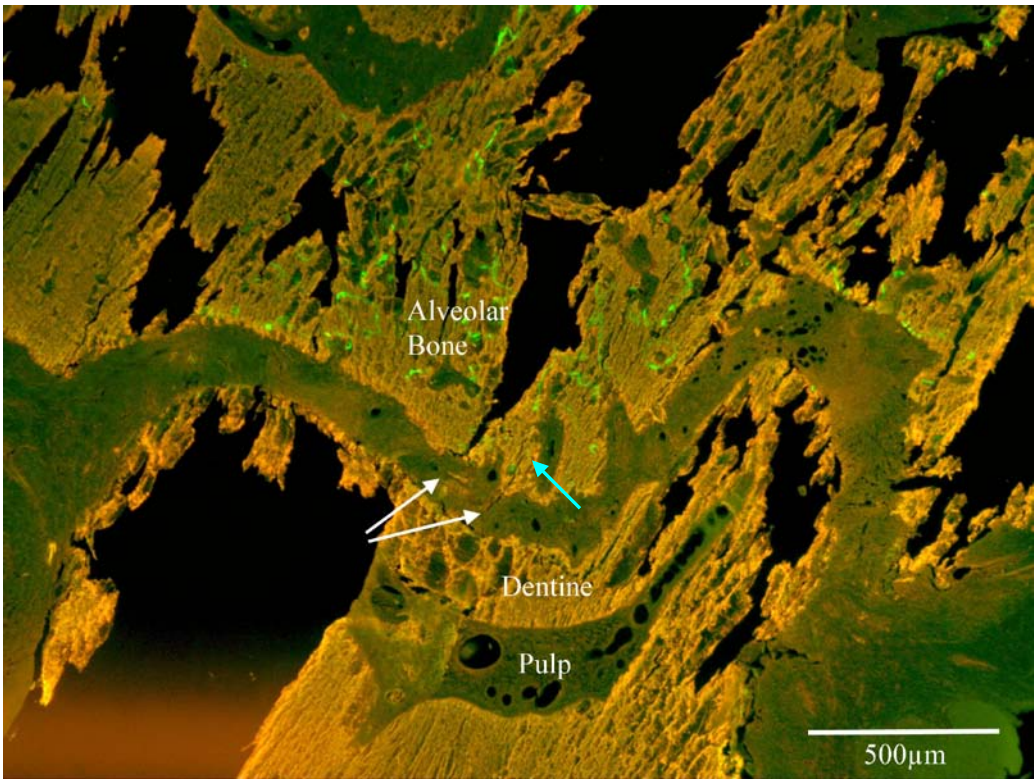
Figure 33. Ankylosis but no label uptake. White arrows denote the lateral outline of the ankylosis seen in the adjacent VK/H&E section in Fig 29. Labels in alveolar bone (blue arrow) are short and irregular.
Rat 7. Unstained. 5x magnification. Calcein label. Distal section of furcation.

113

Similar appearances were noted between the molars of the sham rats and the control

molars in the treated rats. The distance between the calcein and alizarin red labels was

greatest in the alveolar bone and much less along the pulp chamber walls. Along the root

surface, no distinction could be made between the two labels. The furcal root surface was

smooth and finger-like extensions were absent from the root surface. The alveolar bone

surfaces were more irregular but this appeared to be characteristic of the tissue, with a

normally active appositional bone surface that undergoes a high rate of turnover. (Fig 34)
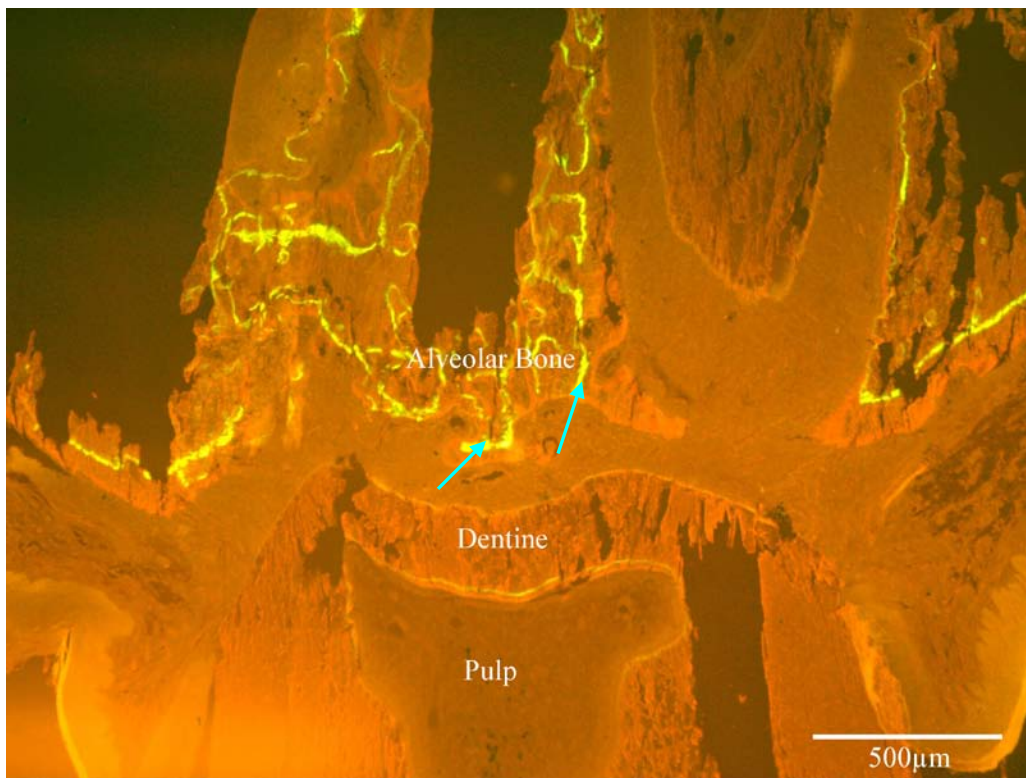
Figure 34. Sham control rat. Mineral apposition greatest along alveolar bone surface with an absence of mineralization along the root surface. Labels in the alveolar bone (blue arrows) are longer, more regular and of a more uniform orientation than seen in the rats with ankylosis (Figs 31, 32, 33) Day 14. Left molar. Unstained. 5x magnification. Calcein and alizarin red labels.

9.4.4 Day 21

9.4.4.1 H&E and VK/H&E sections

A definite ankylosis was seen in 1 treatment rat (Table 1- page 100). Some common

features were also noted in the pattern of ankylosis as seen in Day 14 (Figs 29 and 35).

Finger-like extensions connected the focal ankylotic region to the adjacent bone and root surfaces. A layer of unmineralized matrix lined the peripheral surfaces of the ankylotic region and between its bone and root connection. Cellular cementum-like material noted along the root surface (Fig 36) suggested a repair response had occurred, possibly to the presumed root resorption seen in the earlier time periods.

Three treated rats with no definite ankylosis had large amounts of cellular cementum-like deposits on the root surface (Rat 1,4 and 5). Finger-like extensions extended from the surface of the alveolar bone (Fig 37). Mineralized bone-like tissue was occasionally noted in the central part of the PDL and in the pulp.

In the other two treatment rats (rat 3 and 6), no cellular cementum-like material was observed along the root surface (Fig 39). Instead, an irregular root surface, characteristic of resorption was present. Signs of repair were present in the pulp chamber with regular amorphous, mineral deposits resembling a layer of tertiary dentine along the walls of the pulp chamber with a cellular layer resembling odontoblasts, deep to an unmineralized pre-dentine layer (Fig 38).

In all the treated rats, an irregular root surface characteristic of resorption was more prevalent on the right molars than the left molars. The sham rats displayed no reactive cellular hard tissue deposits on the root surface or the pulpal walls.
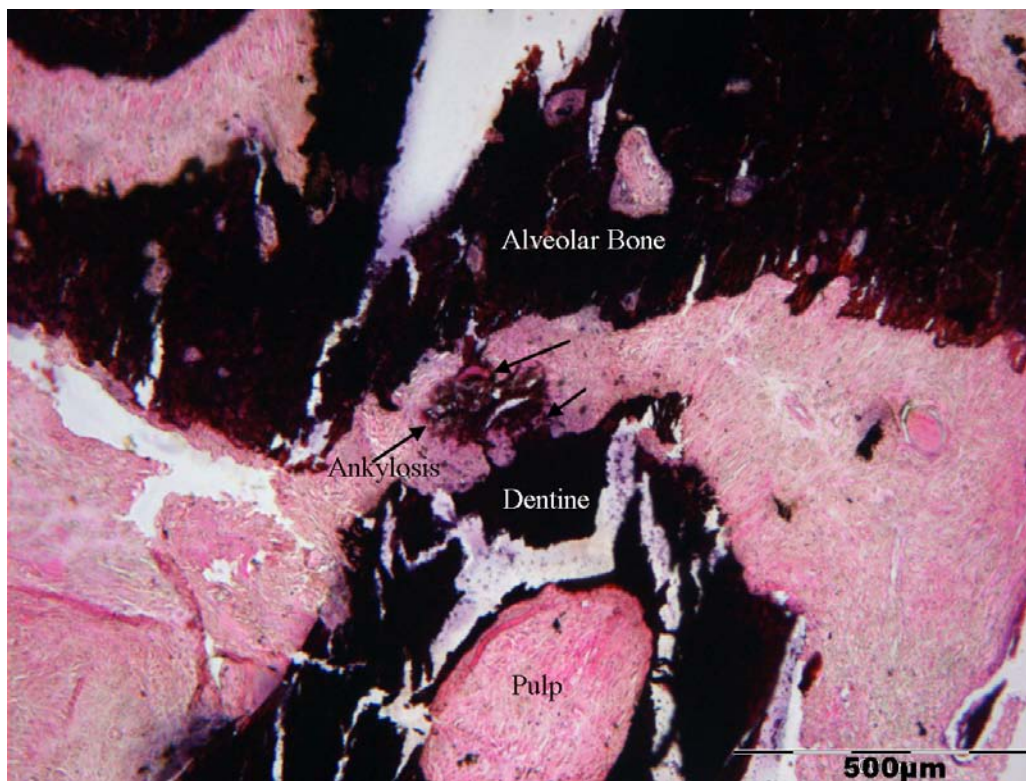
Figure 35. Ankylosis with deposits of unmineralized matrix (unlabeled arrows) along its peripheries.
Day 21, Rat 2. Right molar. VK/H&E stain. 10x magnification.

Figure 36. Cellular cementum-like material (arrows) on the root surface.
Day 21, Rat 2. Right molar. H&E stain. Non-adjacent distal section. 20x magnification.
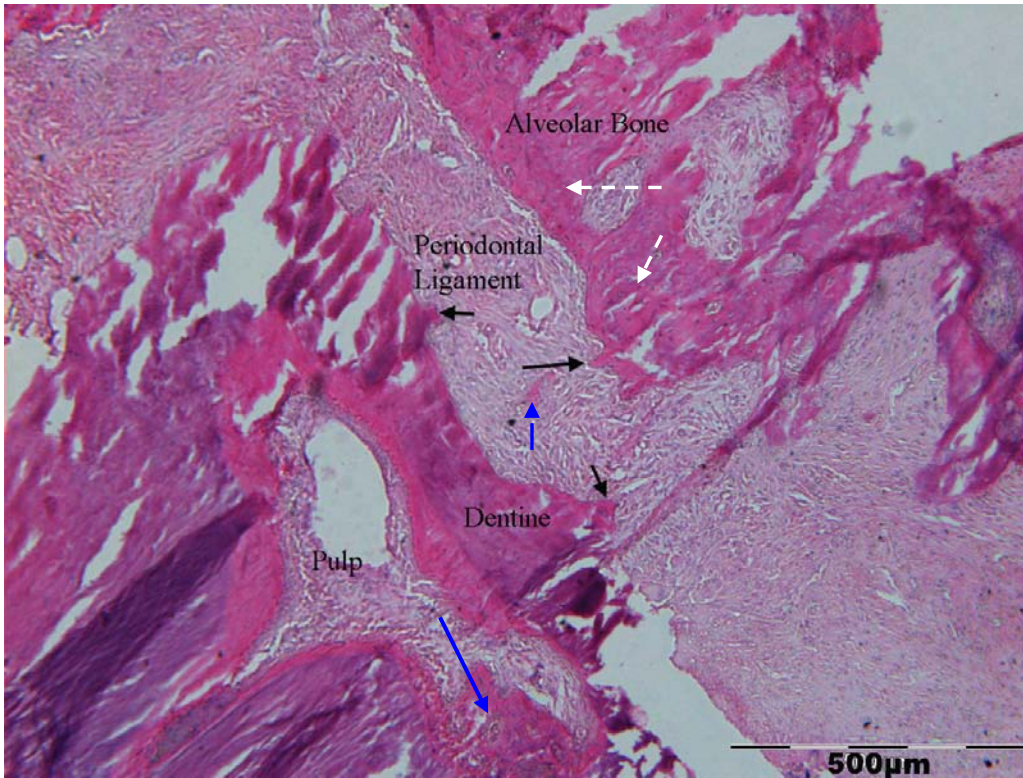
Figure 37. Rat 4- No ankylosis but irregular extensions from bone and root surface (black arrows) and bone –like tissue (blue arrows) within the middle of the periodontal ligament and along the walls of the pulp. Broken arrows: reversal line in alveolar bone
Day 21, Right molar. H&E stain. 10x magnification.
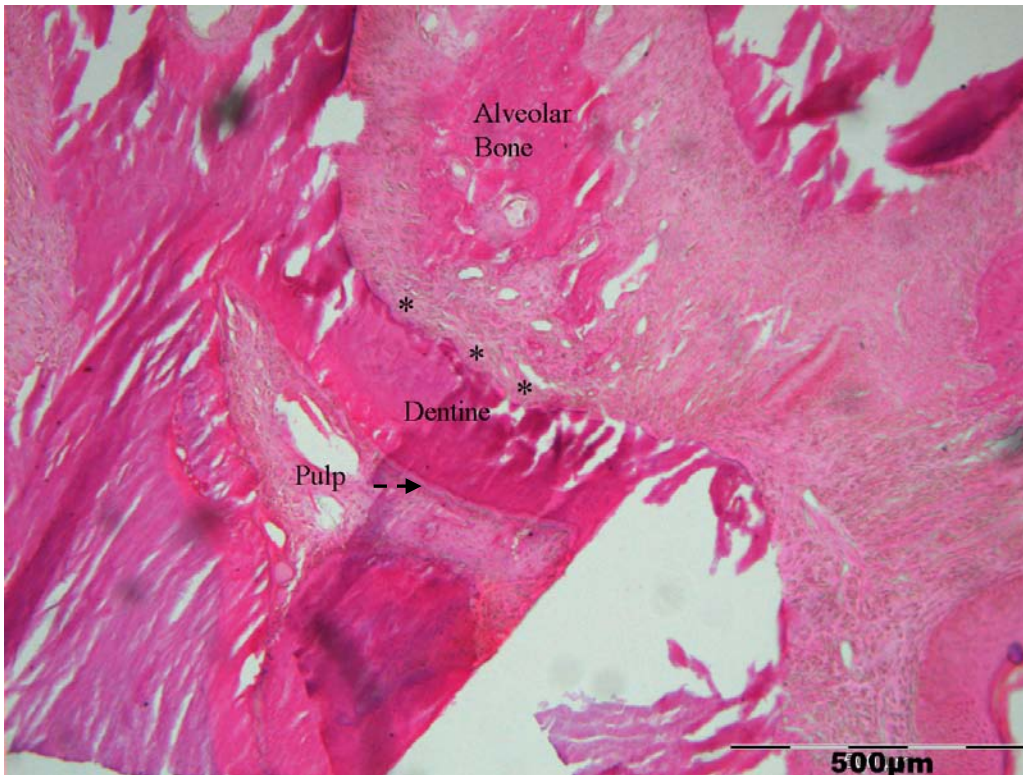
Figure 38. An irregular root surface (asterisks) characteristic of resorption, and a rim of odontoblast-like cells, when seen under higher power, lining the walls of the pulp (broken arrow).
Day 21, Rat 3. Right molar. H&E stain. 10x magnification.

117
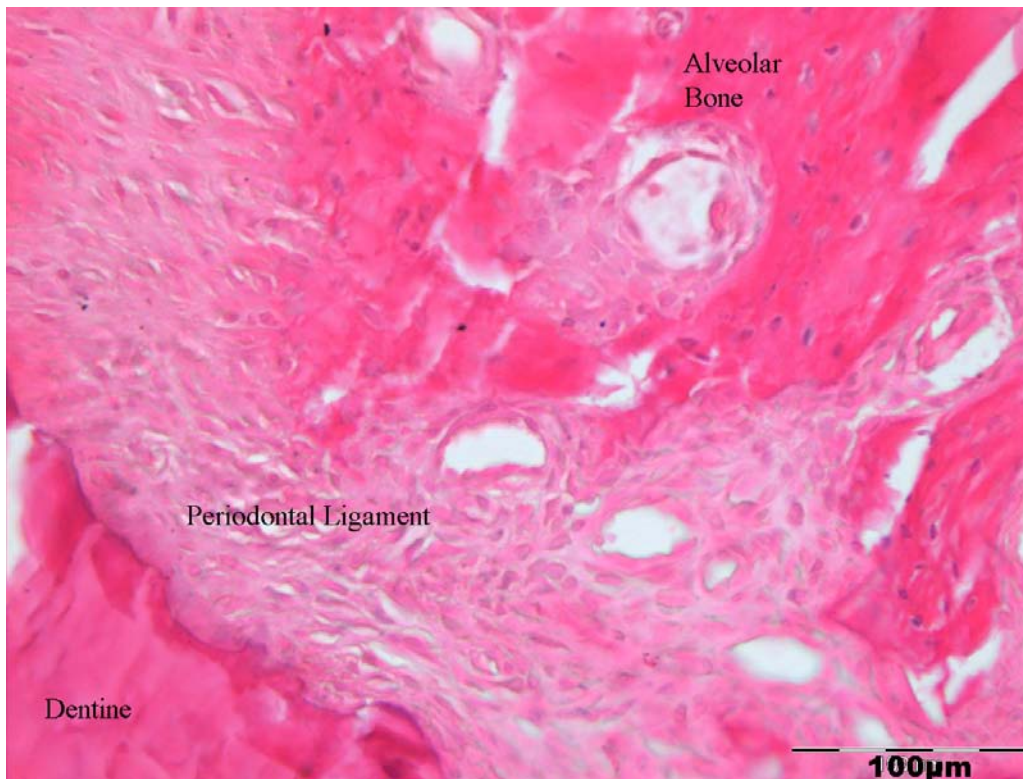
Figure 39. Cellular-like cementum absent from root surface.
Higher power view of previous section. 40x magnification.

9.4.4.2 Unstained sections

Table 4. Distribution of labels among rats in Group 3 (21 days)

Number of labels	Label Type	Number of rats	Rat ID
2	Calcein and Alizarin Red	2	3, 5
1	Calcein	5 (4 + sham)	1, 2, 4, 6, sham
1	Alizarin Red	0	

As with the rats in Group 2, there was a variation in the appearance of the calcein labels which ranged from short and interrupted, to longer continuous lines (Figs 40,41). (Table 4)

In the rat with ankylosis, only calcein labels were present. These labels were concentrated along the peripheries of the ankylotic body, and the immediately adjacent bone and root

118

surfaces on either side. Along the root, mineral apposition was present along both smooth and irregular surfaces (Fig 40). This suggested that the ankylosis may have been a result of an overexuberant mineralized tissue apposition, which may have occurred initially as a part of a repair response to resorption along the root surface. The absence of the alizarin red label is postulated to be due to a combination of factors, elaborated in Discussion (Section 10.2).

In the rats with cellular cementum-like tissue on the root surfaces (when the stained sections of these rats were viewed with transmitted light) and no ankylosis, mineralization of discrete nodules within the middle of the PDL was occasionally seen (Fig 41). Recent mineralization was present along the root surface in focal regions which seemed to correspond with cellular cementum-like tissue on the stained sections. In this group of rats, the labeling lines within the alveolar bone appeared shorter, more discontinuous and of a random orientation compared to the left control side and sham rats. (Figs 41,42,44).

In the treated rats with no cellular reactive hard tissue root deposits, root resorption was suggested by the absence of prominent labels along an irregular root surface. No definite ankylosis was observed. Recent mineralization of apparently 'separate' nodules within the periodontal ligament space was seen. However, this may have been related to the plane of section, with similar morphological appearances noted in the left control molars (Figs 43,44).

Smooth furcal root contours with an absence of scalloping and minimal appositional

activity along the pulp and root surfaces were noted in the left control molars of the

treated rats (Fig 44) and the right and left molars of the sham rat.
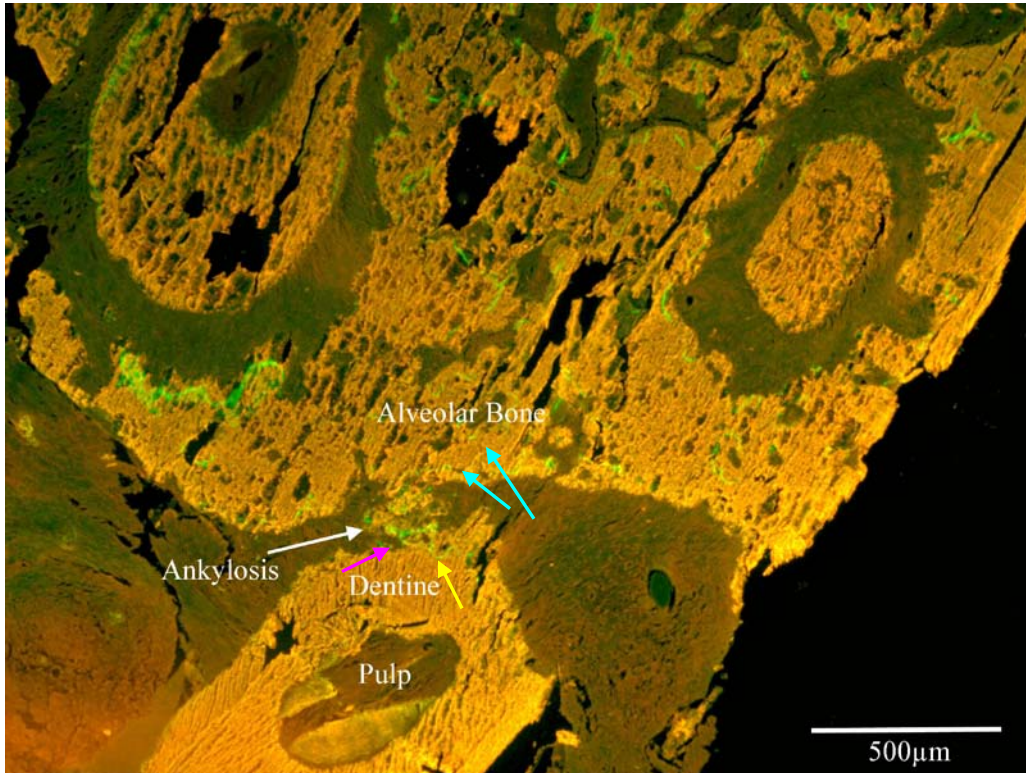
Figure 40. Focal region of ankylosis. Active mineral apposition present on the surface of the ankylotic body and along its immediately connecting bone and root surfaces. Apposition along the root has occurred across an irregular root surface (yellow arrow) which is characteristic of previous resorption, and along a smooth surface (pink arrow). Labels in alveolar bone (blue arrows) are short and irregular.
Day 21, Rat 2. Right molar. Unstained. 5x magnification. Calcein label.
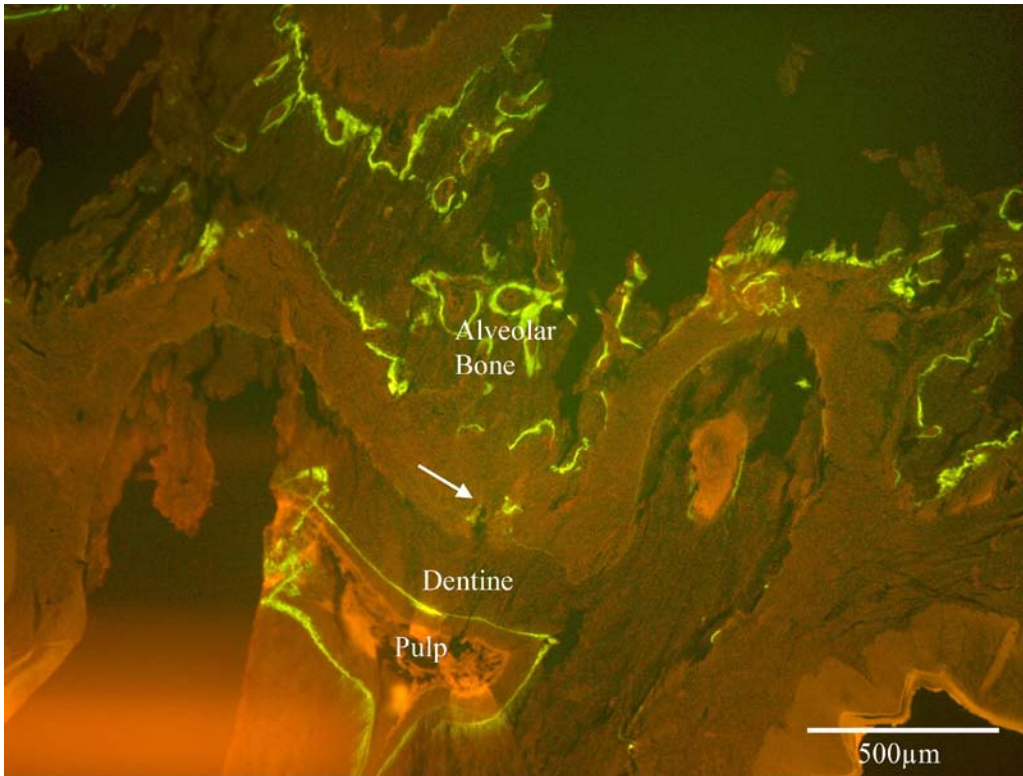
Figure 41. Mineralization (arrow) within the middle of the periodontal ligament space.
Day 21, Rat 1. Right molar. Unstained. 5x magnification. Calcein label.
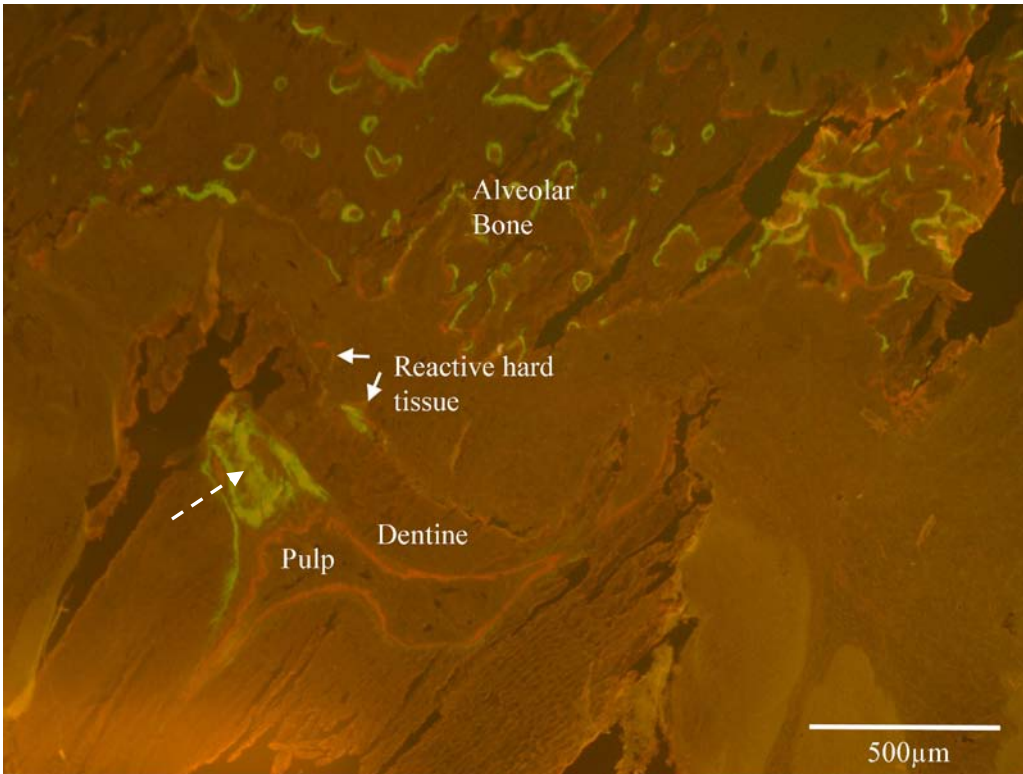
Figure 42. Mineralization of reactive hard tissue which corresponded with cellular-like cementum tissue when stained sections were viewed under transmitted light. Prominent mineral apposition present within the pulp (broken arrow) which may also be a feature of the plane of section.
Day 21, Rat 5. Right molar. Unstained. 5x magnification. Calcein and alizarin red labels.

121
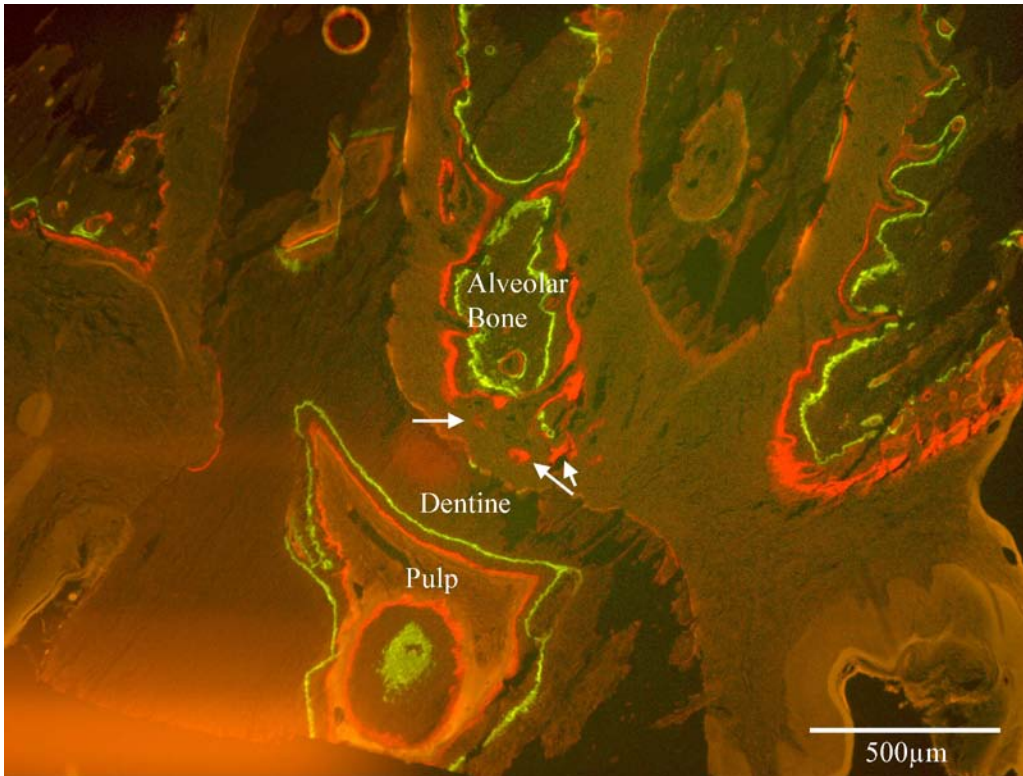
Figure 43. An irregular root surface characteristic of resorption and mineralization of alveolar bone nodular extensions (arrows) within the middle of the periodontal ligament space.
Day 21, Rat 3. Right molar. Unstained. 5x magnification. Calcein and alizarin red labels.
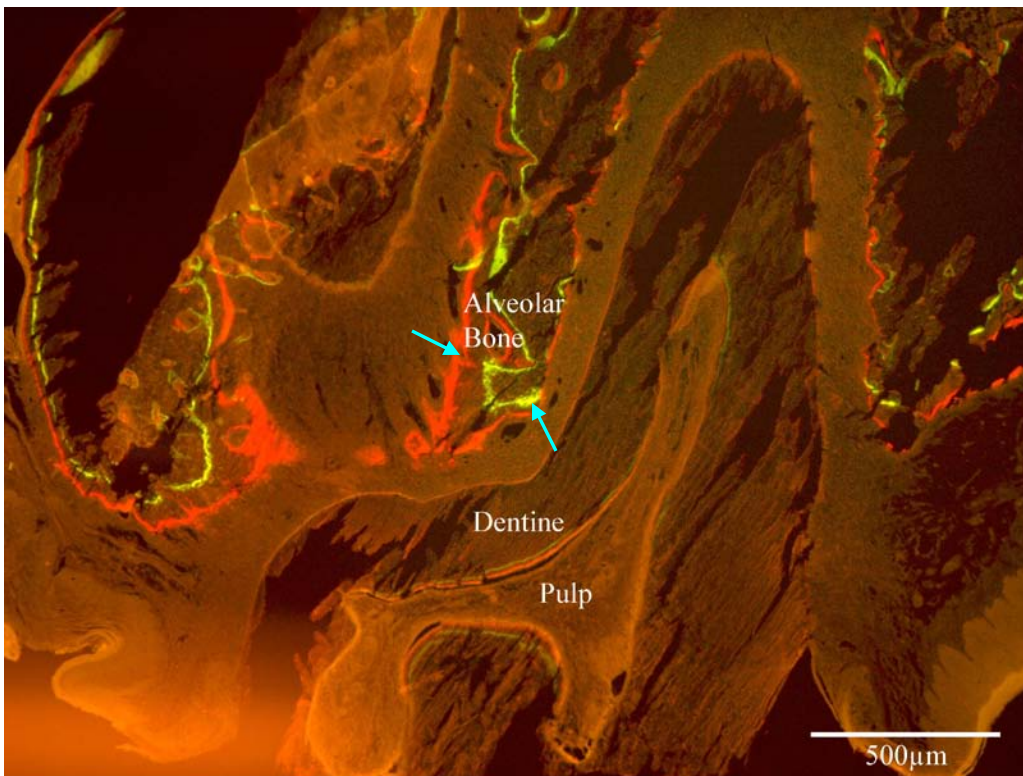
Figure 44. Minimal appositional activity along the root and pulpal surface in control left molar. Labels in alveolar bone (blue arrows) are longer, more regular and of a more uniform orientation than seen in the treated rat with ankylosis (Fig 40).
Day 21, Rat 3, Unstained. 5x magnification. Calcein and alizarin red labels.

9.4.5 Day 28

9.4.5.1 H&E and VK/H&E sections

No ankylosis was present in any of the treatment rats. (Figs 45, 47)

An increased cellular density was present in the PDL space compared to the earlier time periods. These cells appeared to be spindle-shaped cells resembling fibroblasts. There was a more organized arrangement of the PDL fibres and numerous cuboidal cells resembling cementoblasts were seen lining the root surface. Various stages of repair of resorption lacunae were seen along the root surface, with cellular cementum-like tissue present, though extensive deposits and finger-like extensions were absent (Fig 46). A scalloped root surface with an absence of repair deposits was occasionally seen (Fig 48). Along the alveolar bone surface, a combination of cuboidal and flattened cells were seen, morphologically resembling osteoblasts and bone lining cells. Osteocytes were present in the lacuna of the alveolar bone. (Figs 46, 48)

Extensive mineral deposits were noted along the walls of the pulp chamber in all the 6 treatment rats, in which dentinal tubules were seen sporadically (Fig 46). The vascular reactive response to the initial thermal insult was less, as fewer blood vessels were noted in the pulp chamber compared with the preceding three time periods, although this may be partly due to the smaller size of the pulp chamber seen in the treated rats (Figs 45, 47). A well defined, organized layer of cuboidal and columnar cells resembling odontoblasts, from which dentinal tubules seemed to originate, were seen within a cellular pulp chamber. These features suggested signs of pulpal repair after the initial freezing insult.

Similar observations were noted between the controls and the right and left molars of the

sham rat. There was generally a smooth furcal root surface with an outermost layer of

acellular cementum, a cellular pulp and a well defined odontoblast layer. Resorptive

surfaces were not commonly present on the alveolar bone surface. Cellular density

appeared evenly distributed in the PDL, with a rim of cells lining the alveolar bone and

root surfaces. (Figs 49, 50)
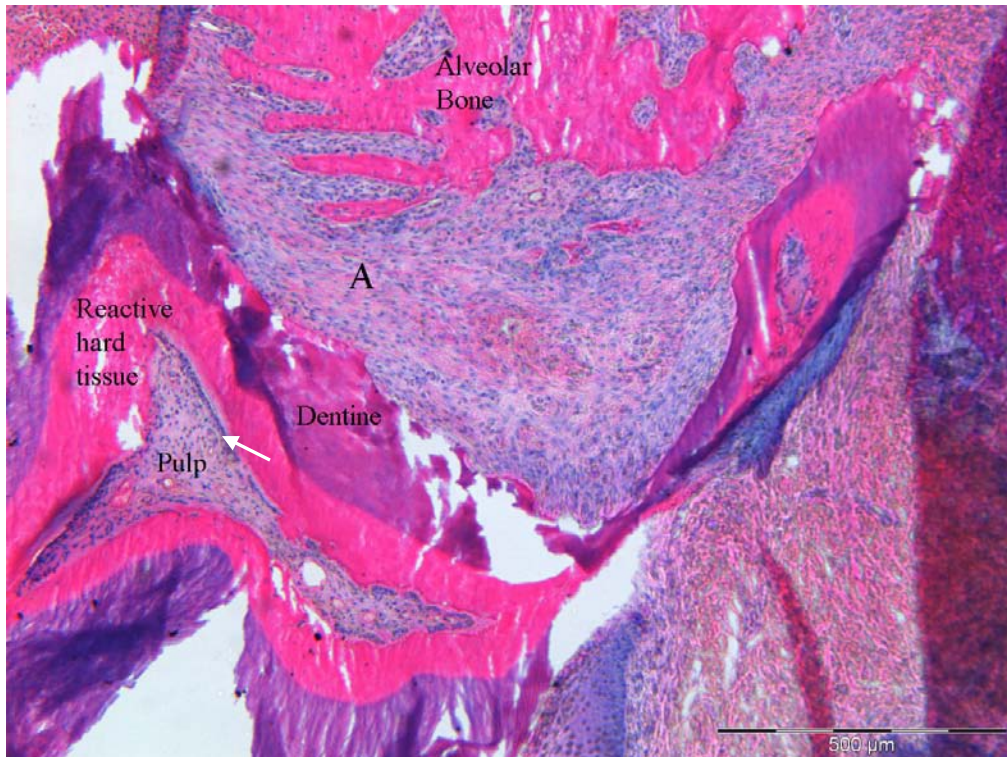
Figure 45. Fewer blood vessels in the pulp compared with earlier time periods (Figs 18 and 24), lined by a rim of odontoblast-like cells (white arrow), which lie beneath a wide zone of reactive hard tissue. Oblique coronal section. Day 28, Rat 5. Right molar. H&E stain. 10x magnification.
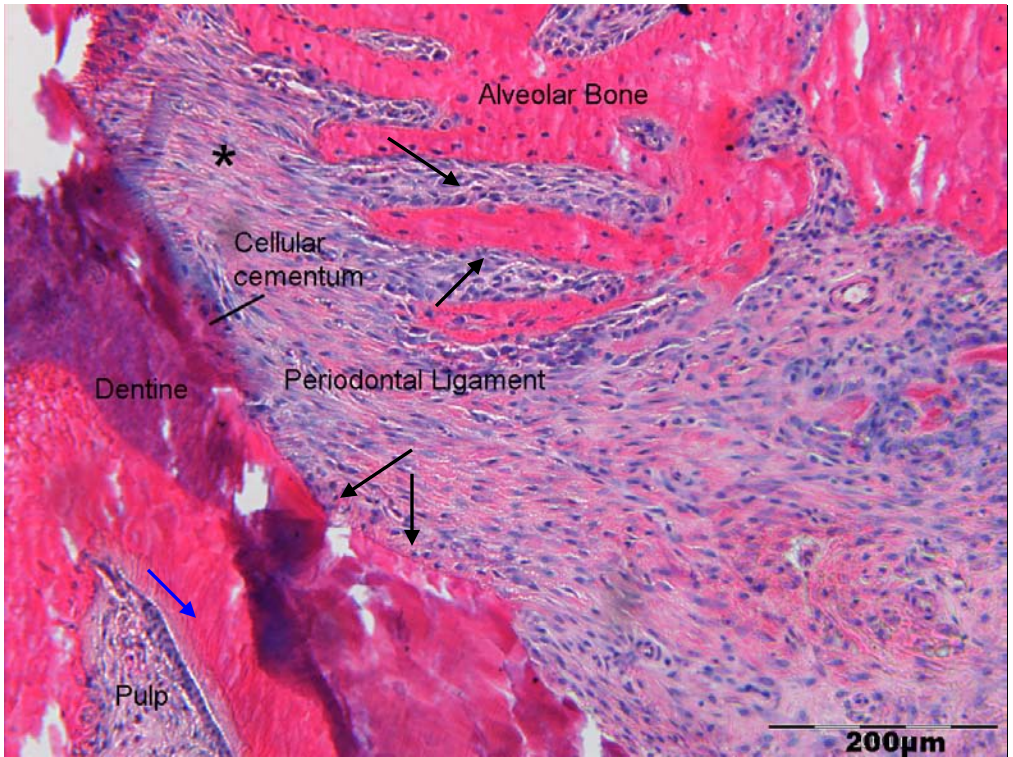
Figure 46. An organized, cellular periodontal ligament, with a rim of cells lining the root and bone surfaces (black arrows). Repair of resorption lacunae with cellular cementum-like tissue is seen along the root surface. Regular, oriented collagen fibres (asterisk) between the root and bone surfaces, interspersed with spindle shaped cells, and a cellular alveolar bone. The presence of dentinal tubules (blue arrow) connected to a rim of odontoblast-like cells suggests the reactive hard tissue to be tertiary dentine.
Higher power view of region A in previous section. 20x magnification.
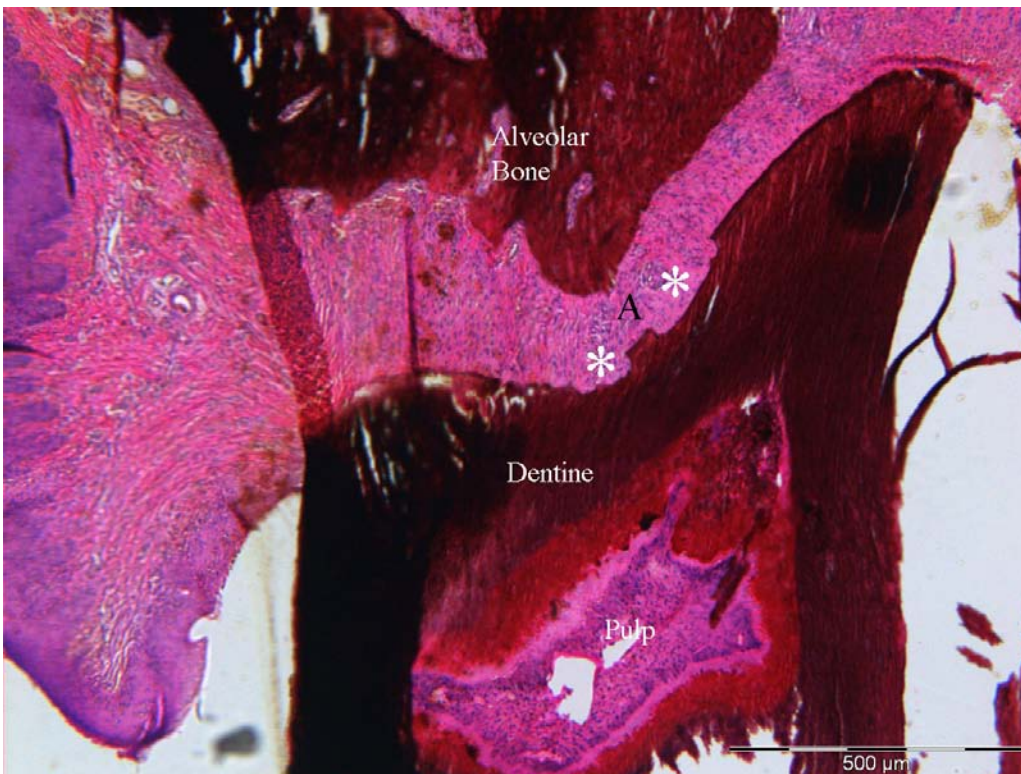
Figure 47. A cellular pulp with an irregular root surface (asterisks) characteristic of resorption.
Day 28, Rat 6. Right molar. VK/H&E stain. 10x magnification.
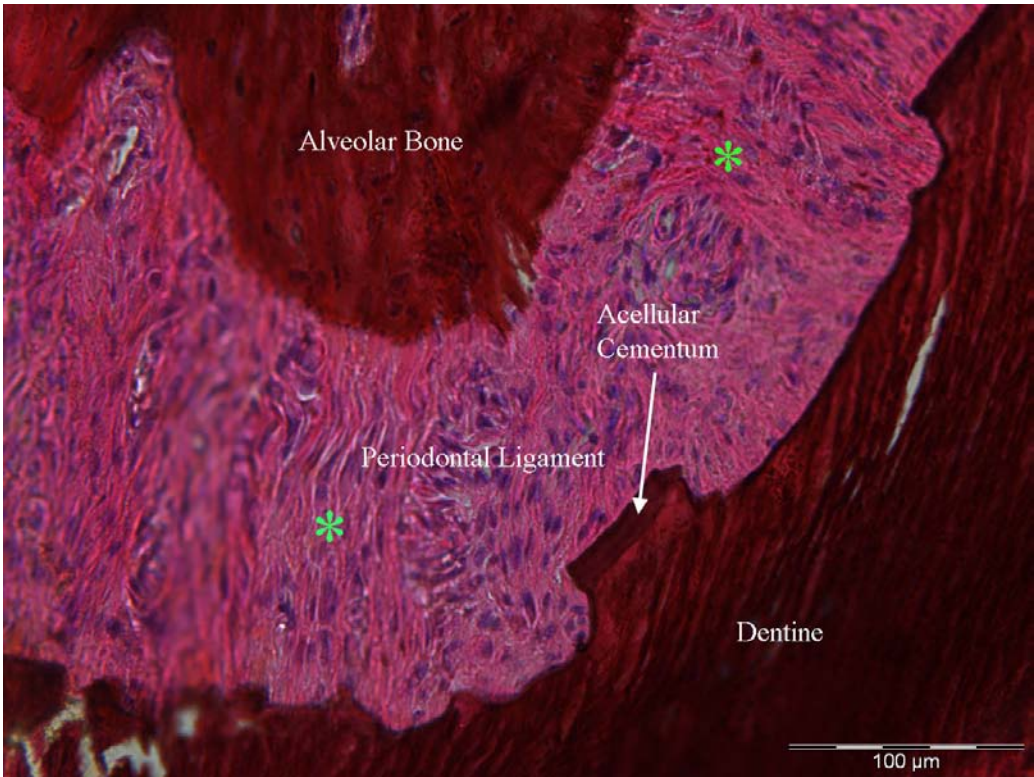
Figure 48. Absence of cellular-like cementum on root surface with organized arrangement of collagen fibres (green asterisks) in the periodontal ligament.
Higher power view region A in previous section. 40x magnification.
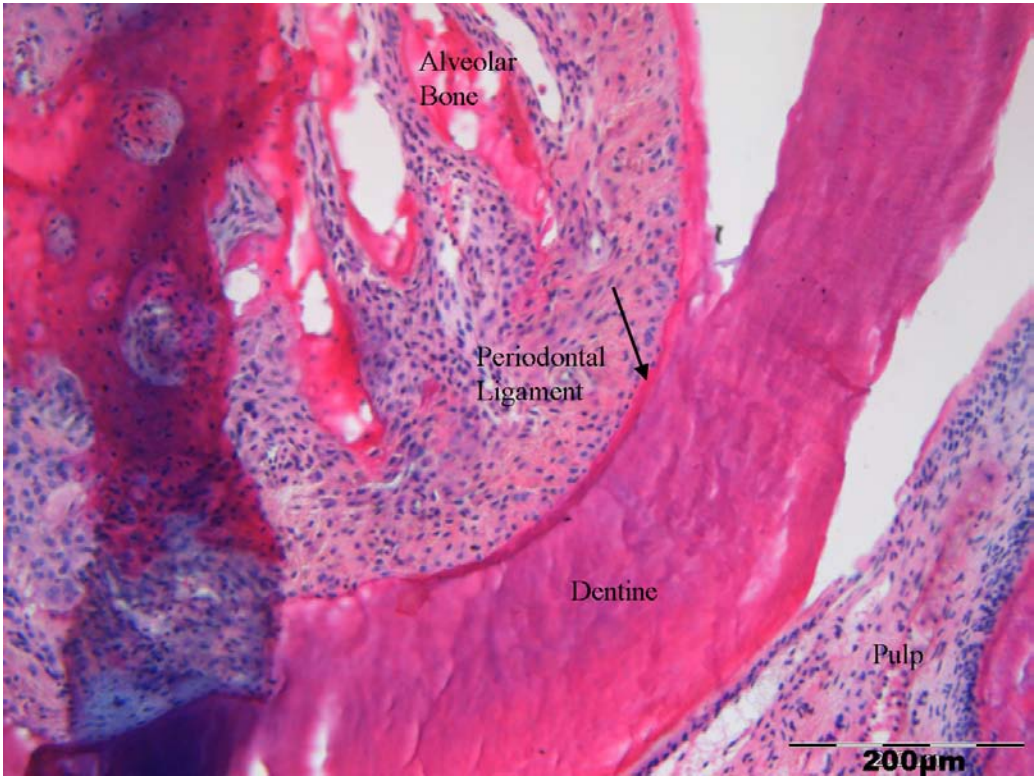
Figure 49. A cellular periodontal ligament with a layer of acellular cementum (arrow) lining the root surface of the control molar
Day 28, Rat 5. Left molar. H&E stain. 20x magnification

126
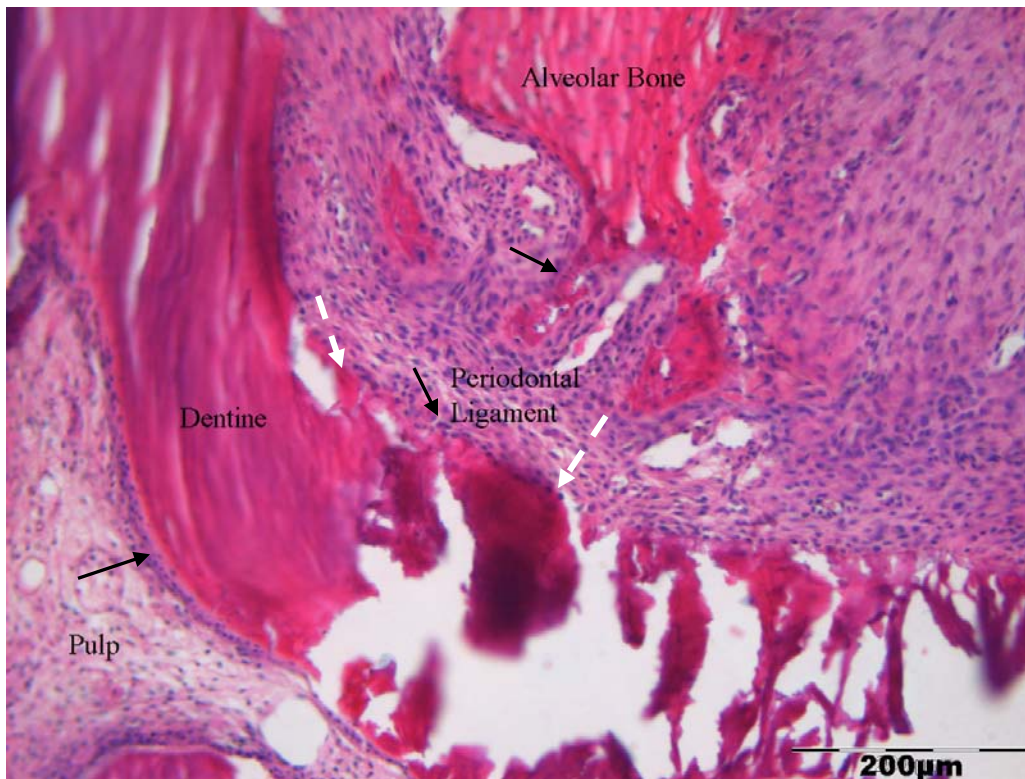
Figure 50. Smooth root surface (white arrows) suggestive of an absence of resorption, and a lining of cells along the the bone, root and pulpal surfaces (black arrows)
Day 28, Sham rat. Right molar. H&E stain. 20x magnification

9.4.5.2   Unstained sections.

Table 5. Distribution of labels among rats in Group 4 (28 days)

Number of labels	Label Type	Number of rats	Rat ID
2	Calcein and Alizarin Red	3 (2 + sham)	5, 6, sham
1	Calcein	4	1, 2, 3, 4
1	Alizarin Red	0	

The pattern of labels within the sections were divided into 2 groups: a single calcein label or the double labels of calcein and alizarin red (Table 5). There were no focal concentrations of labeling lines along the furcal root surface in any of the treatment rats, with none or a thin lining of labels present. Compared with the three earlier time periods, the root surfaces were less irregular (Fig 51), suggestive of a repair process of earlier

127

occurring resorption. Less resorption may have also been present during the early periods compared with Groups 1, 2 and 3. These repair processes were also observed concurrently in the pulp with greater mineral apposition noted along the walls of the pulp chamber compared with controls (Figs 51,52). Occasionally, prominent irregular surfaces were seen along the root which did not accumulate label (Fig 52). When the adjacent stained section was viewed, no multinucleated cells were seen in the depths of this resorptive surface (Fig 48). This suggested an absence of mineralization or active resorption and possibly a reversal stage.

Similar morphological observations were noted in the left and right molars of the sham rats. As with the sham rats in Groups 1, 2 and 3, mineral apposition was greatest along the alveolar bone surface. Mineral apposition was least along the furcal root surface where the presence of two labels could not be distinguished (Fig 53).
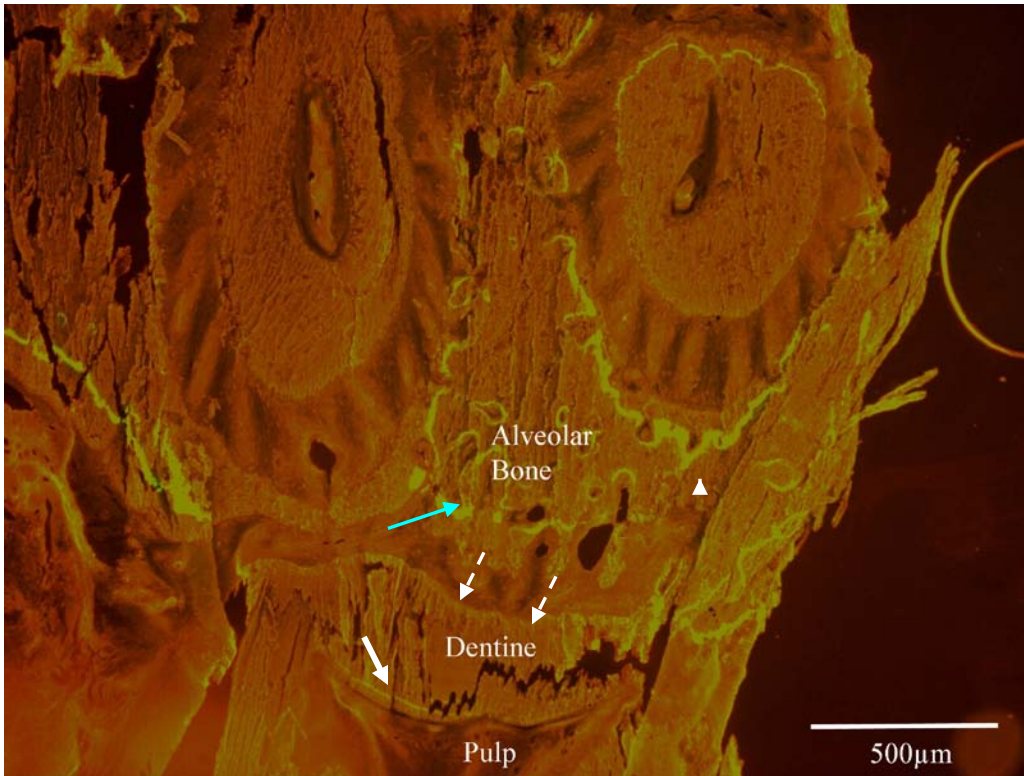
Figure 51. Less irregular root surface (broken arrows) compared with Days 7, 14 and 21, with mineral apposition in the pulp (unbroken arrow). Regular, continuous label along bone surface (blue arrow)
Day 28, Rat 4. Right molar. Unstained. 5x magnification. Calcein label.
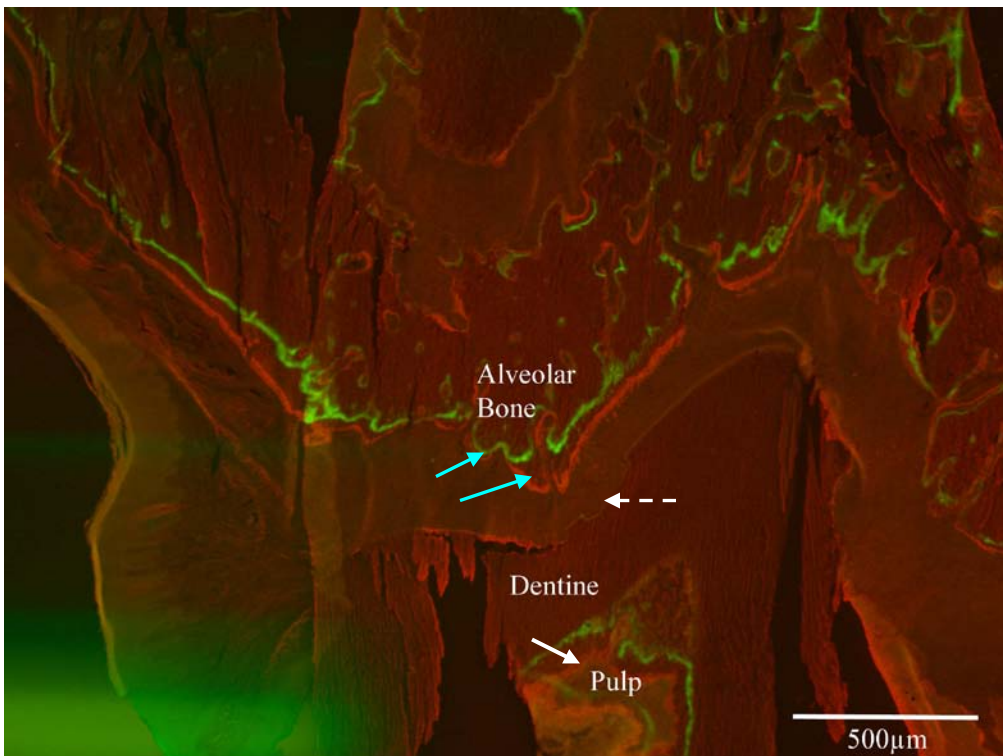
Figure 52. An irregular root surface characteristic of resorption lacunae (broken arrow) along the root surface which did not accumulate label. This was accompanied by recent extensive mineral apposition in the pulp (unbroken arrow). Regular continuous labels in alveolar bone (blue arrows)
Day 28, Rat 6. Right molar. Unstained. 5x magnification. Calcein label and alizarin red label.
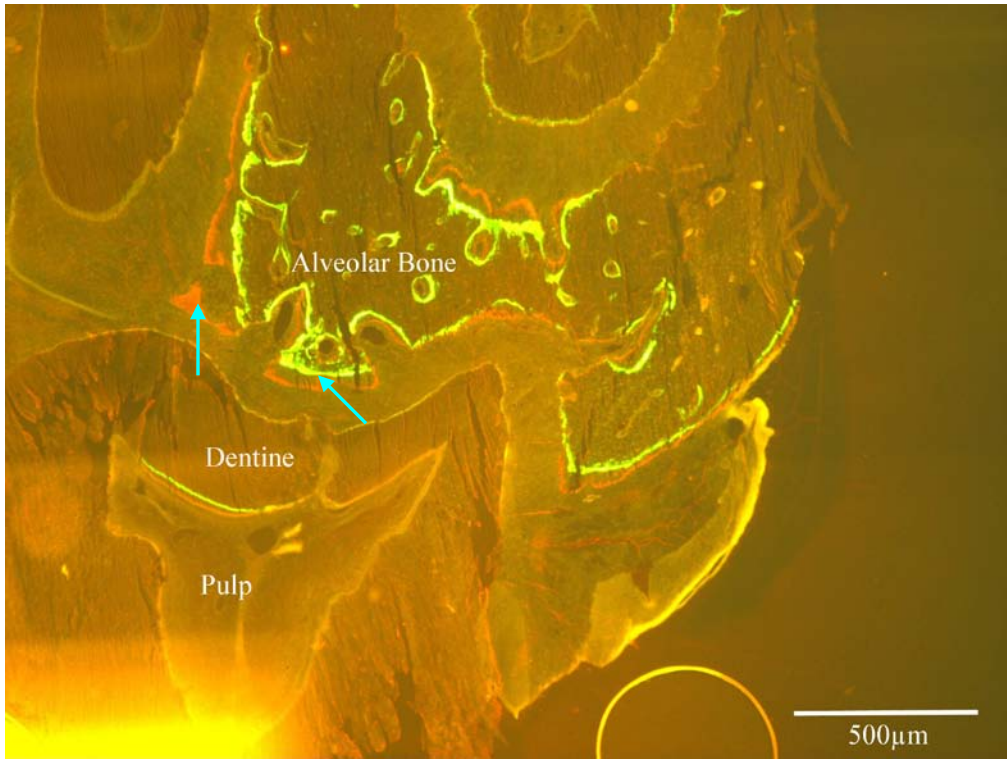
Figure 53. Largest mineral apposition within the alveolar bone. Similar rank order of appositional activity amongst bone, pulp and root surfaces with two labels, as with one label in Fig 22. Similiar pattern of labels within the alveolar bone in treated and sham rats (blue arrows in Figs 51,52,53): labels are regular, continuous and approximate the bone surface.
Day 28, Sham rat. Right molar. Unstained. 5x magnification. Calcein label and alizarin red label.

9.4.6 Polarized light

3 categories of sections were chosen in a pilot trial to further elucidate the variation in the morphological appearance of the labeling line/lines within the unstained sections of the experimental rats. Selected unstained sections were categorized as follows:

1. Sections where ankylosis was present (Fig 54A).

2. Sections from the right molars of treatment rats where no ankylosis was observed (Fig 54B).

3. Sections from a sham rat where no ankylosis was expected (Fig 54C).

These sections were viewed under polarized light, using the Leica DM600B microscope. In all instances, the bone which formed in the cervical interradicular region had collagen fibres with a random orientation, characteristic of woven bone. In rare cases, further from the interradicular crest in the apical region, outside the 1000µm x 1000µm region of interest, the collagen fibres adopted an orderly orientation, characteristic of lamellar bone.

Within the region of interest, as no morphological differences could be distinguished between the collagen fibres in bone under polarized light across the three categories, further analysis of the unstained sections from the experimental rats under polarized light was not undertaken.

Alveolar
Bone

*

→

Periodontal
Ligament

*

Dentine

Pulp

200μm

A

Alveolar Bone

*

200μm

*

Periodontal Ligament

Dentine

Pulp

B
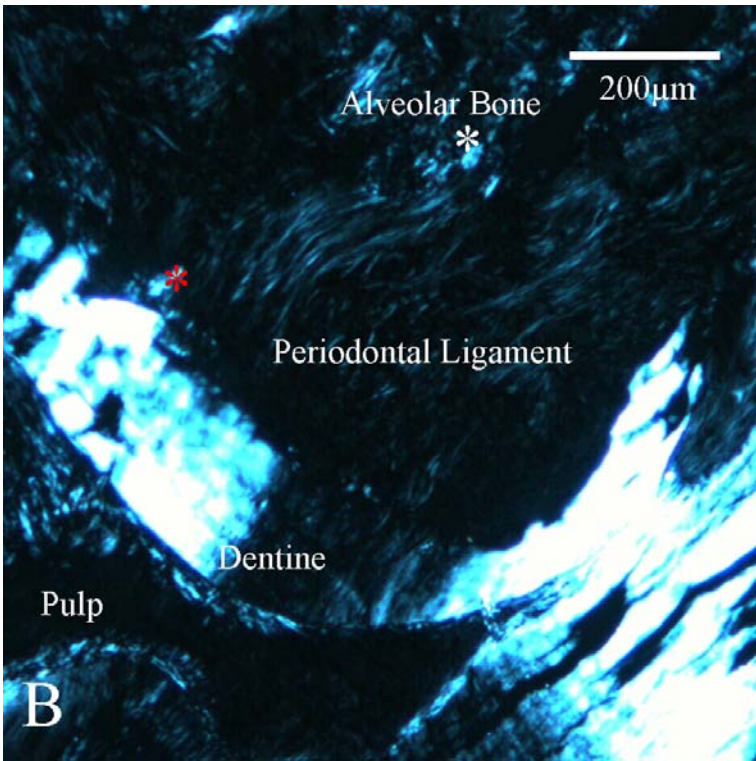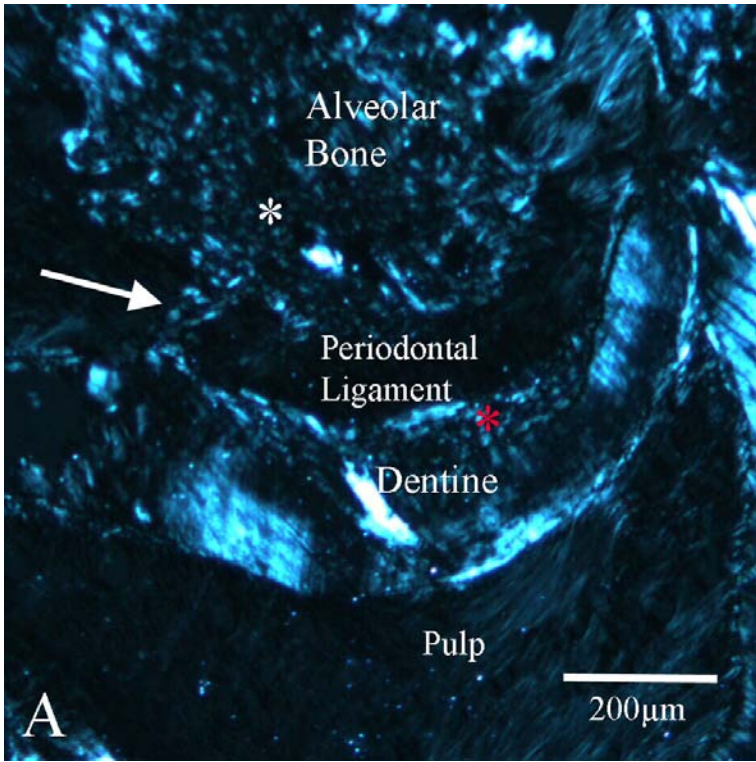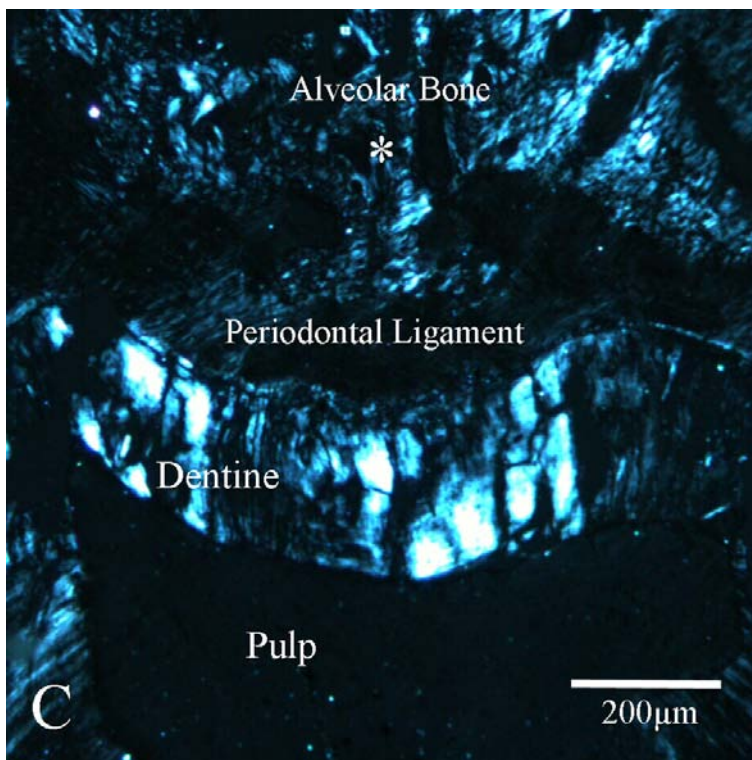
Figure 54. 1000μm x 1000μm region of interest. No differences in the pattern of polarization across the 3 categories: within the ankylotic body (arrow, Fig A), alveolar bone (white asterisks, Figs A, B, C), and mineralized tissue on root surface in treated rats (red asterisks, Figs A, B)
A. Day 14, Rat 3. Right molar. Unstained.
B. Day 21, Rat 5. Right molar. Unstained.
C. Day 14, Sham rat. Left molar. Unstained.

9.5 Statistical Analysis

Significance was set at the $p<0.05$ level, with significant outcomes printed in bold. Rat number 6 in Group 1 was excluded in the statistical analysis as it had a cumulative total of 5 minutes freezing time. (Section 9.2, page 98)

9.5.1 Mineral Apposition rates (MAR)

Logarithmic MAR values were used to obtain a more normally distributed outcome for fitting linear models as the values of MAR were positively skewed (Appendix 12.3.1 and 12.3.2).

The adjustment for the multivariate analysis required a modification to the process to reflect the MAR dataset. Adjusted means in the derivation of mean MAR were set to consider the differences in proportion of label types seen among the total rat pool, and the proportion of treatment and sham rats in each of the 4 groups (Table 6).

Table 6. Results of multivariate analysis of the MAR data from all rats[+]

Variable	p-value
Label Type	**0.0017**
Time	**0.0042**
Location	**<0.0001**
Side	**0.0333**
Group	0.6031
Aspect	0.8473
Side*Location	**0.0008**
Group*Side	**0.0035**
Time*Side	**<0.0001**
Time*Location	**0.0019**
Time*Side*Location	**0.0319**

[+] Excluding Rat number 6 in group 1

The 'buccal or palatal surfaces' was not a significant predictor of MAR. There were also no significant interactions between buccal/palatal and side (p=0.6735) or buccal/palatal and group (p=0.753). Within the treatment rats, there were significant differences (p<0.0001) in MAR between the control and treatment side.

As expected, no significant differences (p=0.7477) were seen in MAR between the left and right side of the sham rats. There were also no significant differences between the control side of the treatment rats and the right side (p=0.5353) or left side (p=0.3719) of

the sham rats. This suggests that any stress induced from a 20 minute continuous dry ice application in the treatment rats has no effect on mineral apposition on the bone, root and pulpal surfaces in the control side.

MAR was significantly (p=0.0295) influenced by a combination of 3 variables: time (days 7, 14, 21 or 28 at rat sacrifice), side (left or right) and location (bone or root or pulp). The full list of mean MAR values and p values for each of these time intervals, side and locations is listed in Appendix 12.3.4. A summary of certain aspects of this is presented below in the following graphical representations:

9.5.1.1   Bone

Graph 1. Mean MAR (and SE) on bone surfaces for left and right first molars

Bone- mineral apposition rate
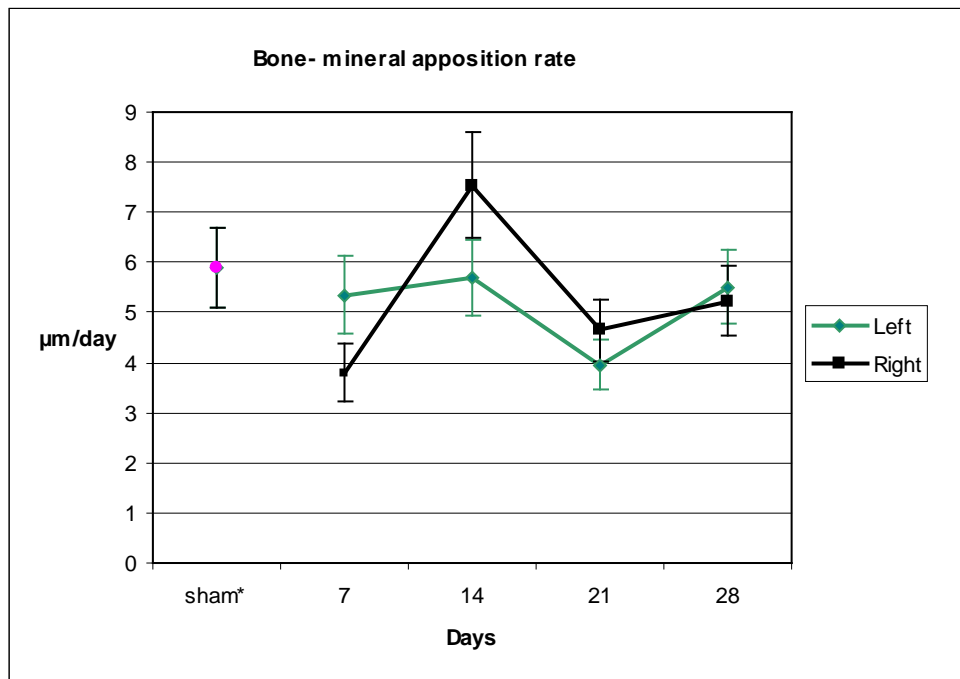
Table 7. Dataset for mean MAR$_{bone}$ on left and right first molars

Days	Left	SE	Right	SE	p values
sham*	5.90	0.80	5.90	0.80	-
7	5.34	0.78	3.79	0.58	0.055
14	5.70	0.77	7.54	1.05	0.082
21	3.96	0.50	4.64	0.61	0.30
28	5.50	0.74	5.22	0.70	0.74

* Averages of right and left sides for sham rats across days 7, 14, 21 and 28

The MAR$_{bone}$ for the sham rats across days 7, 14, 21 and 28 were pooled and averaged for comparative purposes.

When the left and right treatment molars were compared, no significant differences in MAR$_{bone}$ across days 7, 14, 21 and 28 were noted. However, within the right molars, there was a significant increase (p=0.0018) in MAR$_{bone}$ between days 7 and 14, but this was followed by a significant decline (p=0.013) between days 14 and 21 (Graph 1 and Table 7). No significant differences were noted within the left molar across days 7, 14, 21 and 28.

9.5.1.2 Root

Graph 2. Mean MAR (and SE) on root surfaces for left and right first molars

Root- mineral apposition rate
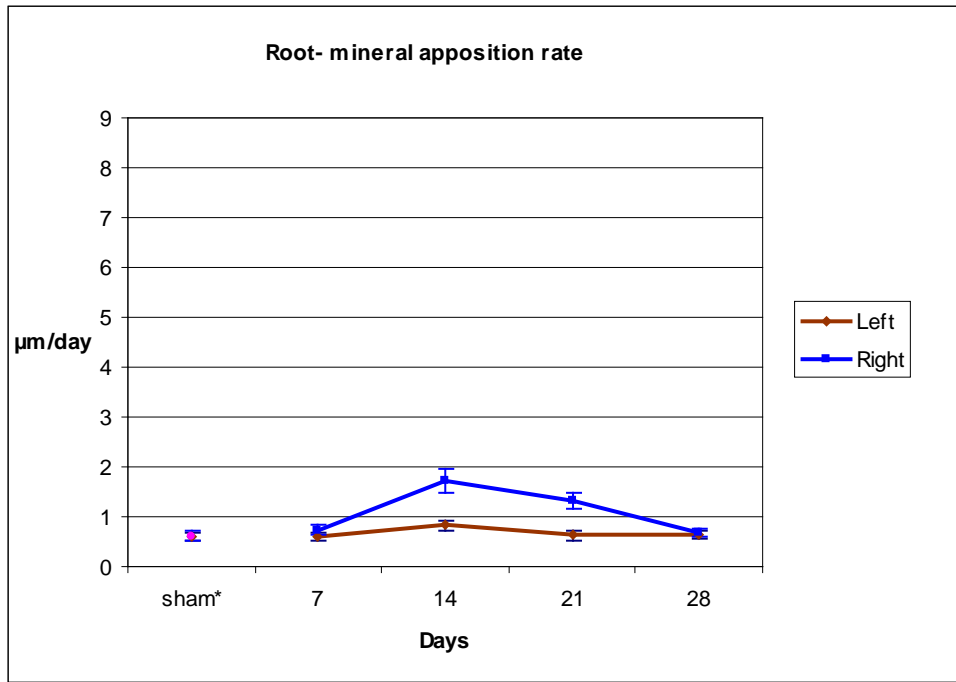
Table 8. Dataset for mean MAR_{root} on left and right first molars

Days	Left	SE	Right	SE	p values
sham*	0.62	0.084	0.62	0.084	-
7	0.60	0.082	0.74	0.10	0.19
14	0.83	0.11	1.74	0.24	**<0.0001**
21	0.63	0.094	1.32	0.17	**<0.0001**
28	0.64	0.082	0.68	0.095	0.70

* Averages of right and left sides for sham rats across days 7, 14, 21 and 28

The MAR_{root} for the sham rats across days 7, 14, 21 and 28 were pooled and averaged for comparative purposes.

There were significant differences ($p<0.0001$) between the left and right molars in MAR_{root} at days 14 and 21. (Graph 2 and Table 8) For the right molar, between days 7 and 14, there was a significant increase ($p<0.0001$) in $MAR_{root,}$ followed by a significant decline ($p=0.0006$) between days 21 and 28.

No significant differences were noted within the left molar across days 7, 14, 21 and 28.

9.5.1.3 *Pulp*

Graph 3. Mean MAR (and SE) on pulpal surfaces for left and right first molars

Pulp- mineral apposition rate
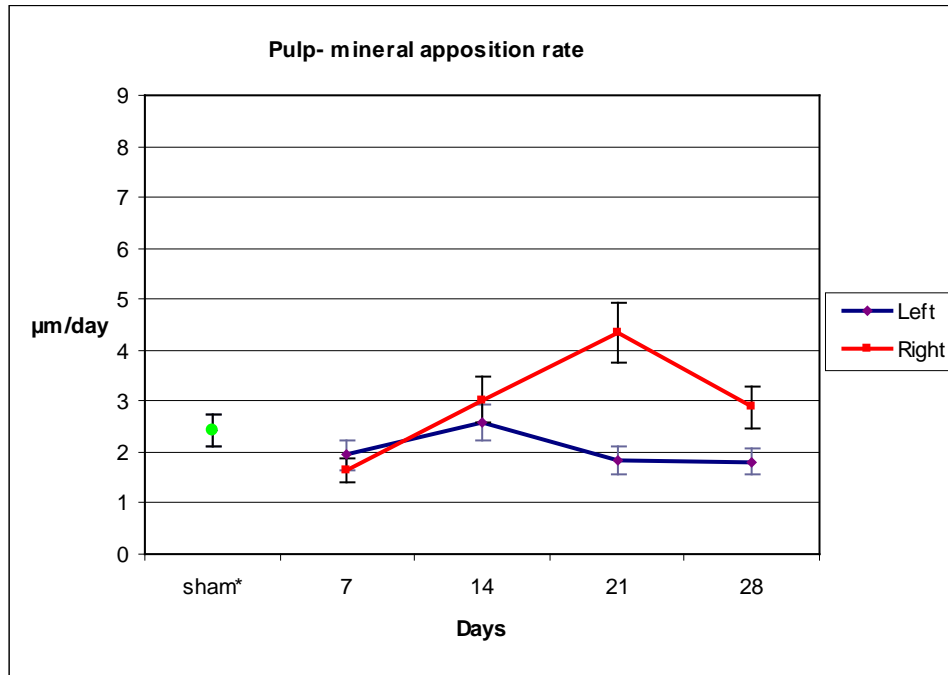
Table 9. Dataset for mean MAR$_{pulp}$ on left and right first molars

Days	Left	SE	Right	SE	p values
sham*	2.42	0.32	2.42	0.32	-
7	1.94	0.28	1.64	0.24	0.33
14	2.58	0.35	3.03	0.44	0.34
21	1.84	0.27	4.35	0.59	**<0.0001**
28	1.81	0.25	2.88	0.42	**0.0061**

* Averages of right and left sides for sham rats across days 7, 14, 21 and 28

The MAR$_{pulp}$ for the sham rats across days 7, 14, 21 and 28 were pooled and averaged for comparative purposes.

There were significant differences between the left and right molars in MAR$_{pulp}$ at day 21 (p<0.0001) and day 28 (p=0.0073). For the right molar, there was a significant increase (p=0.0039) in MAR$_{pulp}$ between days 7 and 14, followed by a significant decrease (p= 0.042) between days 21 and 28. No significant differences were noted within the left molar across days 7, 14, 21 and 28. (Graph 3 and Table 9)

9.5.2   MAR and label types

Differences in MAR outcomes among the label types within the 28 experimental animals were examined further. As the 'label type' was a significant predictor of MAR (p=0.0012), back-transformed adjusted mean MAR values were also obtained for the 3 different label types. (Tables 10 & 11)

Table 10. Differences of adjusted means for 3 label types.

Label types	Label types	p- value
Calcein and Alizarin Red	Calcein	0.15
Calcein	Alizarin Red	**0.0004**
Alizarin Red	Calcein and Alizarin Red	**0.0048**

Table 11. Mean MAR for the 3 different label types

Label types	Mean MAR	Standard Error
Calcein and Alizarin Red	2.01	0.17
Calcein	2.34	0.12
Alizarin Red	1.01	0.22

In the presence of only 1 label, 'mineral apposition rates', in strict terms, as defined by Parfitt [100, 111] are not able to be quantified. This is because labels are deposited during the mineralization of the organic matrix, and in the absence of a second label, it was not possible to quantify the time duration between the administration of the first label and the mineralized tissue surface.

However, the results above are consistent with the time lapse between label (or inter-label) administration and rat sacrifice (Tables 10,11, and Fig 3 on page 72). This time

139

lapse would have been 8 days for the 'calcein and alizarin red label' rats, 10 days for the 'calcein label' rats and 2 days for the 'alizarin red label' rats. By using a time factor of 8 days for all rats, it resulted in the above rank order for Mean MAR values (Table 11).

No significant differences were noted in MAR between the sections with 'calcein and alizarin red' and 'calcein' labels (p=0.1624). These 2 label types comprised almost the entire rat pool (27 out of the 28 experimental animals). As the adjusted means for mean MAR were set to consider the differences in proportion of label types as part of the multivariate analysis, it was considered appropriate to maintain the formulae used to derive MAR (see section 8.11.1.1.4- *Measurement parameters)* across the entire rat pool.

9.5.3 Periodontal ligament width

As the histogram data for PDL width was approximately normally distributed, mean PDL width was the outcome assessed for statistical testing. (Appendix 12.3.3)

Table 12. Results of multivariate analysis of PDL width from all rats

Variable	p-value
Time	0.23
Group	0.80
Side	**<0.014**
Time*Side	0.30
Group*Side	**0.036**

There were no significant (p=0.30) differences in PDL width across days 7, 14, 21 and 28 (Table 12).

Significant (p=0.036) differences were noted in PDL width between the sham and treatment rats, when the right and left sides were compared. Within the treatment rats, the

right PDL width was significantly larger (p<0.0001) than the left PDL width. As

expected, there were no significant differences (p=0.86) between the

left and right side of the sham rat. There were no significant differences between the

control side of the treatment rats and the right side (p=0.29) or left side (p=0.34) of the

sham rat.

This suggests that any stress induced from a 20 minute continuous dry ice application in

the treatment rats has no effect on PDL width in the control side.

Graph 4. Mean PDL width for left and right first molars
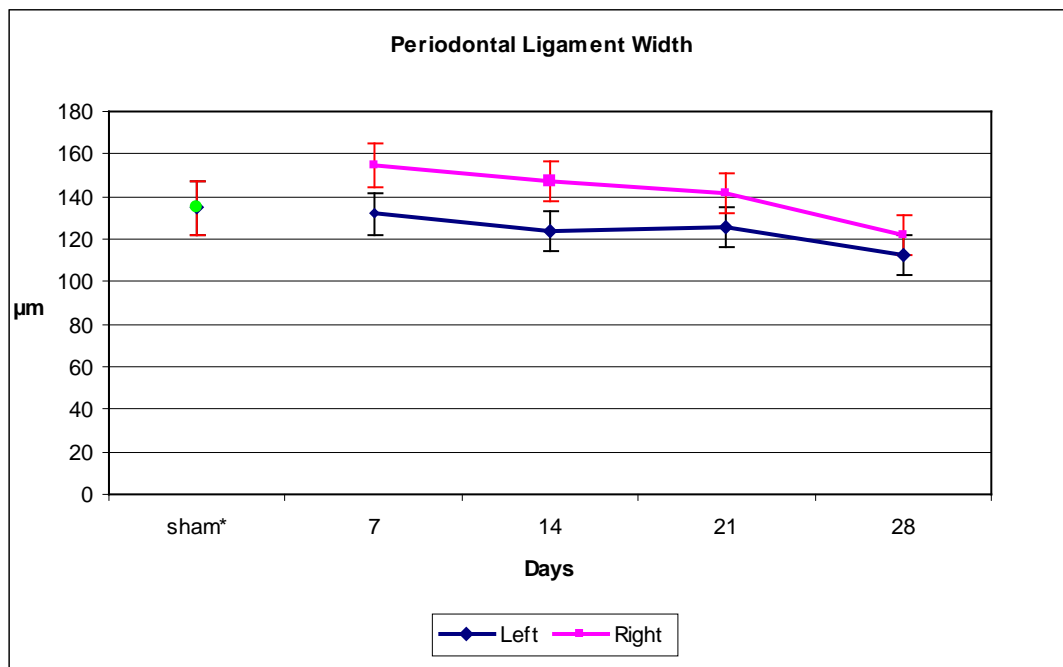
Table 13. Dataset for mean PDL width

Days	Left	SE	Right	SE
sham*	134.62	12.36	134.62	12.36
7	131.72	10.11	154.65	10.11
14	123.35	9.36	147.59	9.36
21	125.92	9.36	141.35	9.47
28	112.80	9.36	121.64	9.36

* Averages of right and left sides for sham rats across days 7,14,21 and 28

The PDL width for the sham rats across days 7, 14, 21 and 28 were pooled and averaged

for comparative purposes (Graph 4 and Table 13). Areas of ankylosis were excluded from

the PDL width derivations. Across days 7, 14, 21 and 28, mean PDL width in the right molar was significantly (p<0.0001) larger than the left molar.

Up to day 14, the right molar PDL width diverged from the left molar PDL width. After day 14, there was a downward trend in the PDL width of the right molar, towards approximating the left molar PDL width by day 28. A decline trend was also noted in the left molar PDL width over time. This may have been due to an initial hyperfunction on the left molars, though this was not investigated in this study.

9.5.4

9.5.5 Resorption

9.5.4.1 % resorptive surface ($R_{bone\ or\ root}$)

The results from the negative binomial GEE (generalized estimating equations) model are shown:

Table 14. Variables influencing mean % resorptive surface ($R_{bone\ or\ root}$)

Variable	p-value
Group	0.16
Time	**0.062**
Side	**<0.0001**
Location	**0.0050**
Side*Location	**<0.0001**
Side*Group	0.0916

Side (left or right) and location (within the bone, root or pulp) were significant predictors (p<0.0001) of resorptive surface (Table 14). The time period was also a significant predictor of resorptive surface (p=0.0279). However, the 3 way interaction effect of Time*side*location was not a significant predictor of resorptive surface.

Adjusted mean values for the resorptive surface and corresponding p values at each of the time periods for the bone or root surface, and the left or right side is in Appendix 12.3.5. Outcomes are expressed as a percentage of $T_{bone\ or\ root.}$ (Refer to pg 92)

A summary of certain aspects of this is presented below in the following graphical representations:

9.5.4.1.1   Bone

Graph 5. Mean surface bone resorption (and SE) on left and right first molars
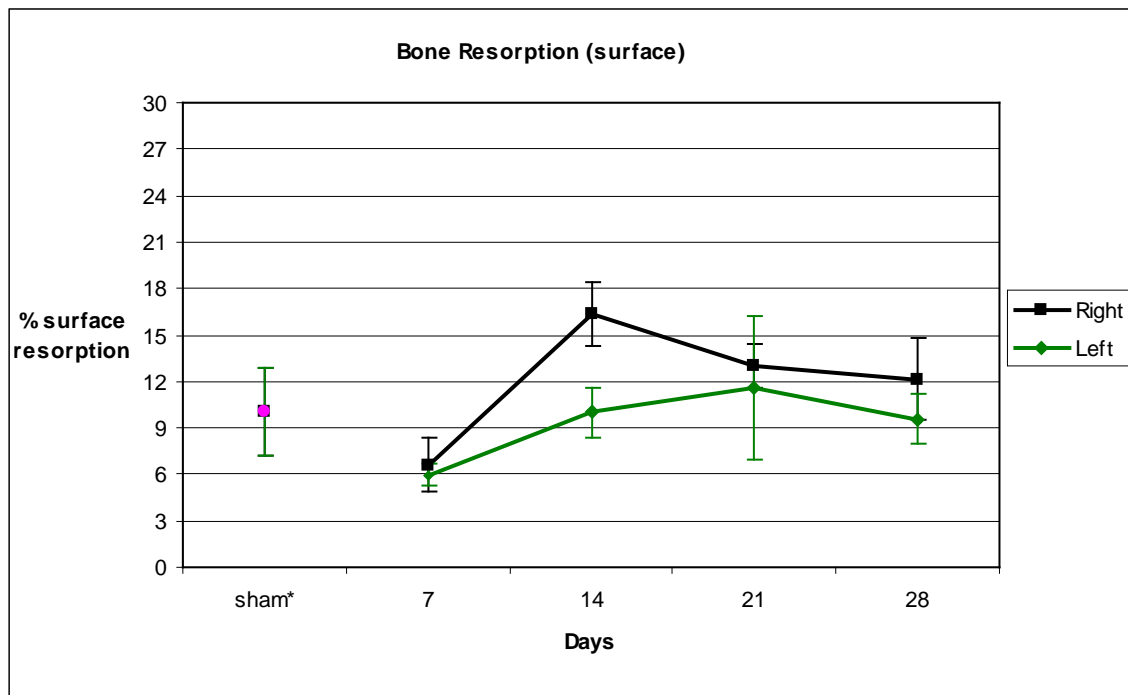
Table 15. Dataset for mean % resorptive surface

Days	Left	SE	Right	SE
sham*	10.02	2.84	10.02	2.84
7	5.95	0.72	6.60	1.74
14	9.98	1.59	16.36	2.03
21	11.60	4.61	12.98	1.42
28	9.56	1.64	12.12	2.65

* Averages of right and left sides for sham rats across days 7, 14, 21 and 28

The % surface bone resorption for the sham rats across days 7, 14, 21 and 28 were pooled and averaged for comparative purposes (Graph 5 and Table 15)

In the treated rats, the % surface bone resorption between left and right molars across days 7, 14, 21 and 28 was on the borderline of significance (p=0.070). Within the right molar, bone resorption peaked at 14 days, followed by a decline to day 28. There were no significant differences (p=0.91) between the sham and the treated rats.

9.5.4.1.2 Root

Graph 6. Mean surface root resorption (and SE) on left and right first molars
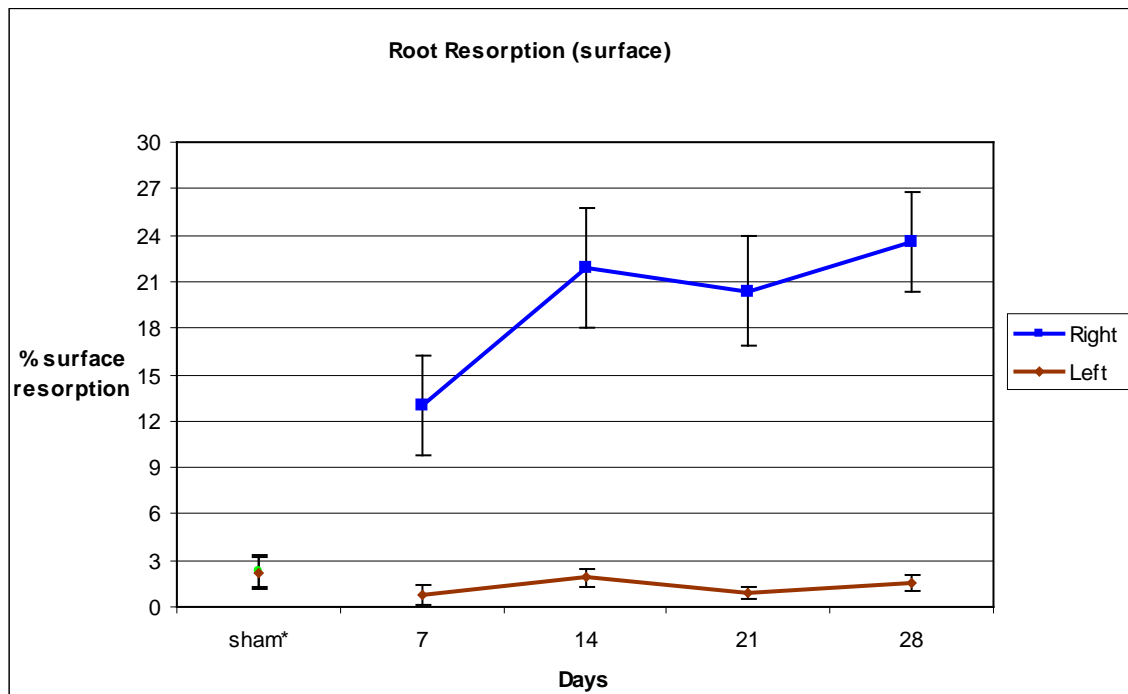
Table 16. Dataset for mean % surface root resorption

Days	Left	SE	Right	SE
sham*	2.31	0.99	2.31	0.99
7	0.74	0.65	12.98	3.25
14	1.90	0.57	21.90	3.81
21	0.91	0.39	20.38	3.57
28	1.58	0.52	23.56	3.16

* Averages of right and left sides for sham rats across days 7, 14, 21 and 28

The % surface root resorption for the sham rats across days 7, 14, 21 and 28 were pooled and averaged for comparative purposes (Graph 6 and Table 16)

In the treated rats, the % surface root resorption was significantly higher (p<0.0001) in the right molars across days 7, 14, 21 and 28. The % surface root resorption in the sham rat was significantly lower (p=0.040) than in the right side of the treated rat.

9.5.4.2   % number of lacunae ($NL_{bone\ or\ root}$)

As the number of resorption lacunae varied with the $T_{bone\ or\ root}$ (see section 8.12.2.1 on page 92), a negative binomial model was applied to the data, with 'number of lacunae' entered as an outcome and log $T_{bone\ or\ root}$ entered as an offset variable. (Table 17)

Table 17. Variables influencing mean % lacunae number

Variable	p-value
Group	0.0661
Time	**0.0441**
Side	**<0.0001**
Location	**0.0010**
Side*Location	**<0.0001**

Side (left or right), location (within the bone, root or pulp) and time (days 7,14, 21 or 28 days) were all significant predictors of the number of lacunae (Table 17). These were also the same significant predictors for resorptive surface. The 3 way interaction effect of Time*Side*Location was not a significant predictor of number of lacunae.

Adjusted mean values for the number of lacunae and corresponding p values at each of days 7, 14, 21 and 28, for the bone or root surface, and the left or right side is in the Appendix 12.3.5.

Outcomes are expressed as a percentage of $T_{bone\ or\ root.}$. A summary of certain aspects of this   is   presented   below   in   the   following   graphical   representations:

9.5.4.2.1 Bone

Graph 7. Mean % lacunae number (and SE) on bone for left and right first molars
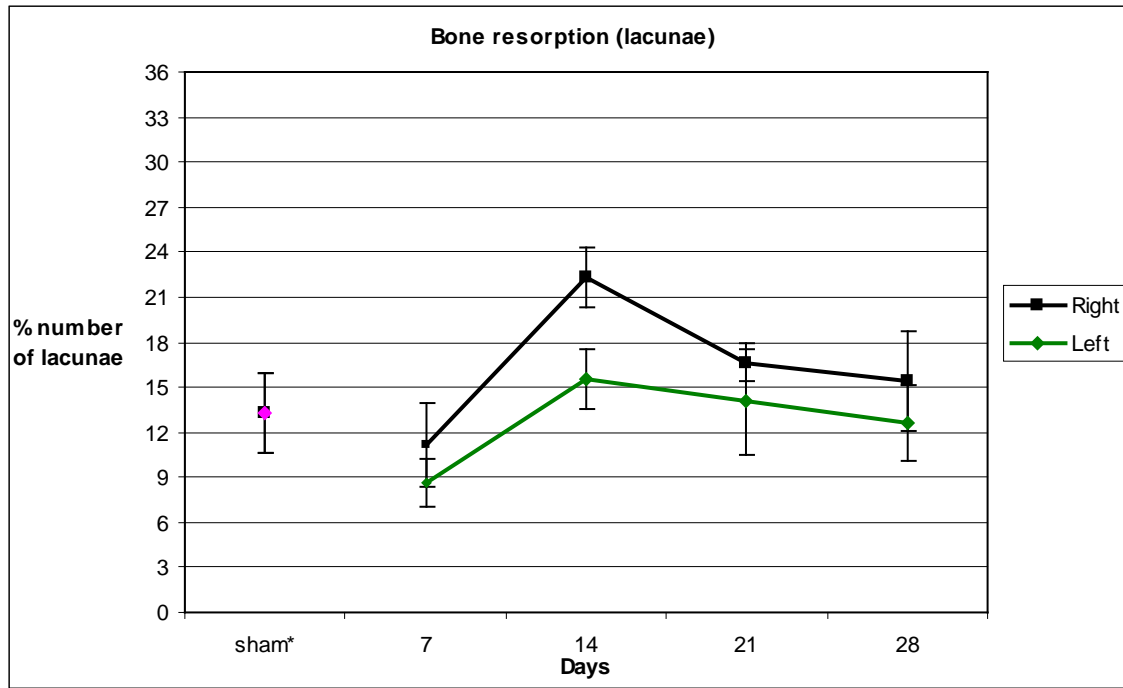
Table 18. Dataset for mean % lacunae number for bone (NL$_{bone}$)

Days	Left	SE	Right	SE
sham*	13.31	2.66	13.31	2.66
7	8.65	1.55	11.12	2.80
14	15.52	2.03	22.26	2.00
21	14.06	3.51	16.65	1.22
28	12.63	2.52	15.41	3.26

* Averages of right and left sides for sham rats across days 7, 14, 21 and 28

The % of bone lacunae for the sham rats across days 7, 14, 21 and 28 were pooled and averaged for comparative purposes (Graph 7 and Table 18)

In the treated rats, the % of bone lacunae was significantly larger (p=0.0241) on the right molar than the left molar across the experimental period at days 7, 14, 21 and 28. As with the % surface bone resorption, for the right molar, % of bone lacunae peaked at 14 days and continued to decline by day 28.

There were no significant differences (p=0.75) between the sham and treated rats.

9.5.4.2.2 Root

Graph 8. Mean % lacunae number (and SE) on root for left and right first molars
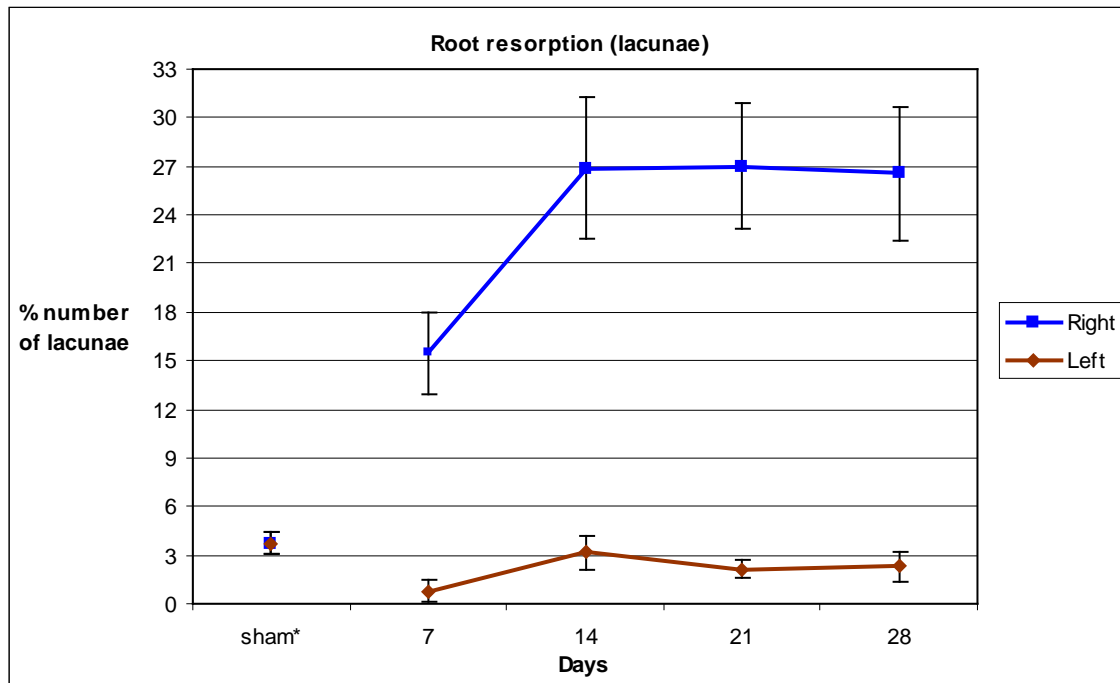
Table 19. Dataset for mean % lacunae number for root (NL$_{root}$)

Days	Left	SE	Right	SE
sham*	3.74	0.70	3.74	0.70
7	0.78	0.69	15.48	2.51
14	3.14	1.04	26.89	4.38
21	2.15	0.58	27.00	3.85
28	2.29	0.88	26.57	4.11

* Averages of right and left sides for sham rats across days 7, 14, 21 and 28

The % of lacunae for the sham rats across days 7, 14, 21 and 28 were pooled and averaged for comparative purposes. (Graph 8 and Table 19)

In the treated rats, the % lacunae number was significantly higher (p<0.0001) in the right molars across days 7, 14, 21 and 28. As with % surface root resorption, resorption on the left molar remained unchanged over time. With the right molar, root resorption significantly increased (p<0.0001) between days 7 and 14, and continued to remain at elevated levels by day 28, showing a mild increase (for % surface root resorption), or continuing to remain steady (for % lacunae number) between days 14 and 28.

The % lacunae number along the right side root surface of the treated rats was significantly higher (p=0.040) than in the sham rats.

9.5.5

9.5.5 Relationship between % surface resorption and % number of lacunae

With % surface resorption on bone or root surfaces as the outcome, the % number of lacunae, $NL_{bone\ or\ root}$ was a significant (p=0.0027) predictor variable. The combination of $NL_{bone\ or\ root}$ and location were also significant variables (p=0.0148). (Table 20)

Table 20. Interaction between R $_{bone\ or\ root}$ and NL$_{bone\ or\ root}$

Variable	p-value
% number of lacunae	**0.0027**
% number of lacunae * location	**0.0148**

With further analysis of the GEE(generalized estimating equations) parameter estimates, this relationship was quantified as for every unit increase in the number of lacunae, the number of resorptive surface units increased by a rate of 1.04 in the root and to a slightly larger extent in bone (1.09). The higher value for the bone surface may be associated with the extensions of resorption lacunae observed, which were generally slightly wider on the bone surface than the root surface.

9.5.6 Error study

Individual limits of agreement were -0.14 ± 0.64 µm/day for MAR_{bone}, -0.03 ± 0.08 µm/day for MAR_{root}, -0.14 ± 0.24 µm/day for MAR_{pulp}. The standard deviations for MAR_{bone} extend over a wider range than reported in other studies [18, 105, 121]. This may have been due to the large proportion of woven bone within the furcation with short continuous labels also being accounted for.

The limits of agreement for PDL width was -4.26 ± 10.36µm, with a 2 standard deviations range from -24.98µm to 16.46µm. The average difference for the '% of resorptive surface' was 6.45, with an upper limit of agreement of 9.67 and lower limit of agreement of -8.38. This negative bias for PDL width and positive bias for resorptive surface measurements may have been partly due to this research being carried out by a single operator and sections not being blinded to the operator during the histomorphometric measurements.

10. DISCUSSION

10.1 Methodology

10.1.1 Sectioning, mounting and staining

A problem in this research study was obtaining and mounting flat, intact sections. Section material loss was first noted during the sectioning process with the microtome. The variables of blade quality, speed, sharpness, and moisture appeared to have minimal influence on the loss of structure.

It was noted in all the torn sections, the specimen was not completely embedded with methylmethacrylate material. This was postulated to be due to the incomplete infiltration of the specimen with the embedding material, as discussed in the 'Processing protocol' below. Manipulation of the already brittle section during the subsequent mounting of sections and staining further increased material loss. Occasionally, folds in sections had to be left in situ to minimize further loss.

Cellular detail was not consistent across the sections. This may be related to the integrity of the sections as all rats received the same processing and staining protocol and the quality of the cellular detail did not appear to be related to the day of sacrifice or the stain type.

Under fluorescent light, folds within the unstained sections usually appeared as a diffuse zone of increased colour intensity. To minimize the analytical problems, a set of measurement protocols had to be developed for quantitative analysis. Areas of the slide where the section was partially missing, torn, stretched or folded, was disregarded. (Section 8.11.1.1.3)

While the use of VK/H&E staining for the undecalcified sections delineated the topography of the bone and root surfaces well, cellular detail within the PDL was occasionally lost due to the processing of sections.

10.1.2   Processing protocol

Further experimentation is needed with the length of the dehydration protocol, especially the role of the acetone stage. Acetone acted as a rapid dehydrant which was miscible with both ethanol and methylmethacrylate. Through a clearing process[122], it removed the water-based graded ethanol solutions from the rat maxilla specimen and allowed infiltration with the methylmethacrylate. This was a necessary stage as ethanol was not miscible with methylmethacrylate. Brown [122] also emphasized the importance of at least 4 changes of acetone, prior to infiltrating with monomer under vacuum.

The protocol used was one which had been successfully used for the rat tibia. It is probable that the rat maxilla had a thicker cortical plate. All specimen blocks were ground to the level of the gingival margin to remove the enamel layer. However, from the pilot 3D CT study on an embedded experimental rat specimen block, it was noted there was still a thin layer of enamel present in the depths of some occlusal fissures and buccal and palatal surfaces of the crown. It was not considered feasible for the specimen blocks to have been ground more apically due to the close proximity of the interradicular furcation. This residual enamel may have adversely affected the infiltration of methylmethacrylate into the specimen as well as causing inconsistent cutting with damage to the specimen due to the enamel density.

As such, it was likely that the specimen blocks were of more variable density that the rat's tibia. A longer period for the clearing and infiltration processes under vacuum may have been beneficial by optimizing each of the above processes.

10.1.3   Orientation- determining the furcation region

The CT images obtained from the Skyscan 1072 (Section 9.2) validated the use of coronal sections to delineate the middle third of the upper first molar as the furcation region.

It was noted that several experimental rats had oblique coronal sections across the left and right molars. This resulted in an exaggerated linear measurement or a distorted crown appearance of the teeth. This may be partly related to the absence of fine controls on the Reichert-Jung microtome to allow precise 3 dimensional positioning of the specimen block on the aluminium stub. Occasionally, porosity on the occlusal surface of the block made visualization of the mesial margins of the upper first molars more difficult.

These two factors may have accounted for sections in some rats not being at the same depth with regard to the mesial margins of the upper first molars.

10.2   Mineralized tissue labels

Of the 28 experimental rats, 20 had one calcein label present, seven had the double labels of calcein and alizarin red and one had alizarin red label present. This type of label patterning did not seem to restrict itself to sham or treatment rats, suggesting the application of dry ice was not a factor in determining this label pattern (Tables 2,3,4,5).

Within the treatment and sham rats, the number and type of labels was consistent between the right and left molars across the bone, root and pulp surfaces. Occasionally, labels were absent from the root surface due to its low appositional activity.

While label escape, increases in mineralization times with corresponding decreases in mineral apposition rates [111], and the presence of resting periods[123] during mineralization of BMU's would account for an increased proportion of single labels to double labels, the proportion of the first and second single labels within the same section would be similar[111]. However, as the resting periods for different BMU's may occur with random frequencies with respect to a given label time and be of different durations[124], this would result in single and double labels of different lengths[110]. Tam[108] showed that interlabel intervals greater than 3 days in rats included rest periods with temporary cessation of matrix synthesis. The above reasons do not account for the complete absence of alizarin red label within all sections in twenty rats.

Frost[77] stated that if biopsy occurred within 24 hours of label administration, label loss may occur due to elution within the fixative. This label storage escape may be a factor as all rats except one had retained the earlier calcein label. However, other labeling studies in the alveolar bone of rats have successfully used a 2 day period after label administration before sacrifice [79]. As with other studies[51, 74], the alveolar bone of rats in this study was an area of active mineral apposition, which would have facilitated the deposition of mineral to cement the 2nd label. If storage escape was the sole factor, all treated rats within each group would have the same number of labels visible under fluorescence which was not the case.

Another factor that may have accounted for the presence of only single labels are geometric projection errors where double labels appear as single labels on obliquely cut sections[77, 124]. The use of a standardized protocol in sectioning (section 8.10) all specimen blocks would have minimized this error. This reason alone does not explain the inconsistency in appearance of labels among the specimen blocks.

As no gross relationships were seen as discussed, it is likely that a combination of all the above factors were present to account for the appearance of single calcein labels where double labels were administered. The one rat with a single alizarin red label present may have been due to inadvertent administration of the initial bone label directly into the intestinal tissues.

There was a distinct contrast in the appearance of the labels in alveolar bone between the treated and control molars, in the cohort of rats which had definite ankylosis (Table 1). In the treated molars with ankylosis, the labels were usually short, irregular and of a reduced density, while they were long and continuous in the control molars. This contrast was most pronounced at day 14, where ankylosis was observed in 2 out of 6 treated rats and was accompanied by a peak in bone resorption and mineralized tissue apposition along the bone surface. However, the label distribution tended to return to a regular shape consistent with the control molars by day 28. This difference in label patterning was not as marked in the cohort of rats with no ankylosis.

The contrast of the labeling lines in these 2 cohorts of rats suggests that in the development of ankylosis, resorptive surfaces within alveolar bone are increased. A more normal appearance of generalized regular bone formation was seen in the rats with

no ankylosis. This pattern of appearance of labeling lines in remodeling and modeling regions of alveolar bone was also observed by Vignery et al[20]. The variation in labeling pattern may also be accounted for by an increased presence of woven bone, characterized by its rapid deposition and low mineral content [19], resulting in 'label escape' [77], with more variable resting periods, in contrast to a more organized pattern of mineralization of lamellar bone.

Ankylosis in the PDL was characterized by a focal region with a marked concentration of labels in situ. This showed the development of ankylosis was characterized by localized and rapid mineralized tissue formation. Extensive rapid mineralization was also seen along the adjacent bone and root surfaces but with minimal extensions into the PDL space. This was particularly so along the adjacent root surface where the demarcation of labels and the root surface could be clearly distinguished. This appeared to correspond with the mineralization of cellular cementum-like deposits on the root surface, when compared with adjacent stained sections. This suggests that where ankylosis did occur, it appeared to be a spatially and temporally controlled event. The presence of inhibitory molecules within the central region of the periodontal ligament may have prevented complete mineralization of a wider zone of the PDL [6].

It is interesting to note that areas of ankylosis, as seen on adjacent stained sections did not pick up any label when the corresponding adjacent unstained section was viewed under fluoresecent light ie: sections from the treated rat 7 in Group 2. It is probable that the surface of the ankylotic region may have been at a resting, resorptive or reversal stage with no concurrent mineral deposition during the period of label administration [123].

10.3 Mineral tissue adaptation

10.3.1 Bone

The observation that the alveolar bone crest is the site of greatest mineral apposition among the 3 mineralized tissue surfaces is consistent with other studies that have used bone labels [51, 74]. The results for MAR bone in the left molars are in the ranges reported in other studies of male rats of comparable ages [9, 52].

Greater resorptive activity was noted along the treated bone surface between days 7 and day 28. This difference from the control teeth was most marked at day 14 and could be due to the removal of sterile necrotic tissue along the alveolar bone surface. This could have been a result of surface resorption by osteoclast-like cells within the PDL as inflammatory cells were not present. Surface resorption was also the most common pattern of resorption observed by Hammarström et al[94] and mainly occurred in teeth where the PDL was still vital.

The freezing stimulus appeared insufficient to induce complete and prolonged cell death as increased cellularity within the PDL with functional orientation of its collagen fibres had returned by day 28. The presence of osteoclasts in situ may have accounted for the continuing elevated levels of bone and root resorption till the last observation period of day 28. Alternatively, the activated osteoclasts may have been derived from the early presence of regenerating vascular channels, which has been postulated to be a recruitment source of mononuclear precursor cells of osteoclasts and odontoclasts [34, 66].

Mineral apposition increased between days 7 and 14 within the treated molars, consistent with a repair response. While there was a wide variation in the natural anatomy of the

alveolar bone surface, no widening of the bone marrow channels was observed during the earlier time periods which were most marked by a reduced cellular density in the PDL. This would suggest the blast-like cells in the PDL were more likely to have been derived from pool of undifferentiated mesenchymal cells apical to the interradicular region [83], or from osteoprogenitor cells in the perivascular region [18]. The decline in the levels of mineralized tissue apposition by day 28 may be partly explained by the remodeling of the woven bone into a lamellar bone type, which has a lower rate of mineralization[111]. A decrease in the remodeling rate of mineralized tissues over the four weeks was unlikely to have accounted for the late decline trend of apposition and resorption levels in alveolar bone, as this trend was not observed in the control teeth. This is in contrast to the findings reported by Misawa et al [9], who found significant decreases in mineral apposition rate in male Winstar rats from 8 to 12 weeks. This may be related to differences in nutrition, storage and handling conditions as the average weight gain of the rats was greater that that observed in the present study.

Discrete bone nodules were also observed in the PDL space apparently unattached to the bone and root surface. The nodules were seen in two rats, one with root resorption and cellular cementum repair but no sign of ankylosis (Day 21, rat 1) and the other with cellular cementum repair and ankylosis (Day 14, rat 7). They appeared reactive in nature with occasional active surface mineralization. Lindskog and Blomlof[83] observed islands of cells resembling epithelial cell rests in close proximity to these non-attached bone-like tissue, and suggested that these did not develop further into ankylosis. However, Wesselink and Beertsen[125] found no correlation between the prevalence of epithelial cell rests and the resolution of ankylosis by resorption, following the termination of bisphosphonate therapy in rats. The findings from this study suggests the nodules may

157

have been the initial nidus in the development of ankylosis as where ankylosis was
established, the ankylotic body was nodular in shape connected by finger-like extensions
to the bone and root surface, and lined by a rim of unmineralized matrix, with an
concentration of labels in situ. This supports the finding Hammarström [94], who observed
that ankylosis started with the formation of bone-like tissue in the central region of the
PDL, which then fused with newly formed hard tissue on the root surface and socket
wall.

The close interrelationship between mineral apposition on the bone surface and bone
resorption suggests a highly regulated and coordinated nature between the resorptive and
formative processes on the alveolar bone surface. This suggests a possible inbuilt
homeostatic mechanism within the periodontium to maintain the width of the periodontal
ligament.

10.3.2   Pulp

The time delay in the peak of reactive hard tissue formation in the treated molars may be
due to the 20 minute thermal insult initially resulting in partial pulpal cell death,
including the odontoblasts, and the time required for the differentiation of odontoblast-
like cells. This was a sterile necrosis as no inflammatory cells were seen in the pulp
chamber. The early increase in the number of small blood vessels could be due to an
initial vasodilation during the initial stages of an inflammatory process and new
microvessel formation[126] . This early repair response suggests the vascular supply to the
pulp was not irreversibly compromised by the thermal insult and that enough cells may
have survived to maintain mineral apposition rates similar to the untreated left side.

The reactive hard tissue seemed to have the characteristics of reparative dentine (one of the 2 subtypes of tertiary dentine) as no continuity of tubules was noted in this dentine and the underlying primary dentine. Trowbridge[127] stated that the atubular junctional zone between the reparative dentine and the overlying dentine seemed to limit the diffusion of irritants into the pulp. The increase in mineral apposition seen at day 21 and day 28 were from odontoblast-like cells that presumably replaced the primary odontoblasts. These cells could have arisen from metaplasia of the pulpal fibroblasts or from stem cells and endothelial cells within the pulp [127]. The rate of tertiary dentine formed was between 2.88-4.35µm/day (Table 9). This had similar temporal characteristics to other studies that investigated tertiary dentine beneath deeply restored cavities, where the appositional rate ranged from 3.3-3.95µm/day. A similar time lag of approximately 2 weeks post insult (ie: cavity preparation) was observed in its formation in monkey teeth, with the rate of formation declining in the later time periods [128].

The concurrent presence of large mineralized deposits within the pulp and ankylosis within the periodontal ligament was also noted in other studies, which was suggested to be related to a more extensive injury [76, 129]. The pulp chamber did not appear to undergo remodeling, with the labeling lines always regular and continuous across all 4 time periods. Progressive mineralized tissue deposition and an absence of resorption were seen, concurrent with a decrease in the physical size of the pulp chamber. However, these observations were mainly of teeth where only small focal regions of ankylosis were seen, over a short period of time. Resorption of extensive mineralized deposits within the pulp has been observed to occur between 60 to 120 days in replanted rat molars [76]. Yu and Abbott stated that resorption within the pulp was more likely to occur with replantation injuries, where the apical blood supply has been severed [130]. As such, the absence of

resorption within the pulp chamber in this study may be related to the mild nature of the thermal insult.

In one of the rats with ankylosis, bone-like tissue surrounded by hematoxyphilic cells was observed in the region of the pulp where the odontoblast layer was discontinuous. Vascular pericytes have been found to be a source of stem cells of the osteoblast lineage[131] . It is postulated that the osteoblast/cementoblast-like cells that formed the bone-like tissue may have been derived from the vascular pericytes as only the blood vessels in the vicinity of this bone-like tissue were lined by hematoxyphilic cells.

Comparing the histological changes that occurred within the pulp to that seen during orthodontic tooth movement, it would suggest that a 20 minute dry ice insult does provoke a more pronounced response. [132] Yet the ongoing vitality and cellular regenerative capacity of the pulp suggests a highly adaptive response to injury.

10.3.3   Root

The root surface had the smallest mineral apposition rate amongst the three mineralized tissue surfaces studied; the bone, root and pulp surfaces. The increase in mineral apposition noted on the root surface at days 14 and 21 also coincided with the time periods where ankylosis was most prevalent. In the rats with ankylosis, no lamellae were observed within the irregular whorls and finger-like projections of cellular cementum-like mineral deposits attached to the root surface. The matrix had a similar morphological appearance to woven bone under polarized light but it was not possible to distinguish between these two types. Bone-like tissue deposited on the root surface has been noted in previous studies on ankylosis [81, 86, 93, 94].

Based on the labeling pattern and the physical extensions of the cellular cementum-like deposits on the root surface into the PDL space, the amount of mineralized tissue formed seemed to be more than just the replacing the tissue lost by root resorption and possibly represents an exuberant repair response by cementoblast or osteoblast-like cells, which was postulated by Dreyer[93] to occasionally lead to ankylosis.

Within the PDL, the freezing insult appeared to have caused a partial necrosis of cells at day 7, including the original cementoblasts. However, this was followed by a marked cellular response at day 14 concomitant with extensive deposits on the root surface. As cementoblasts are terminally differentiated cells, the source of these cells at day 14 could have been derived from undifferentiated mesenchymal cells within the PDL, carried into the area by blood vessel growth during the early stages. The differentiation into active cementoblasts during the repair of root resorption may also have been assisted by epithelial cell rests of Malassez [44].

The significantly greater root resorption observed along the root surface of the right molar compared with the left molar during the earlier time periods was expected as this model was adapted from one first developed as a model for generating root resorption [53]. Root resorption levels were sustained at day 28, as also suggested by the sparse lining of labels along the root surface and its absence in regions of root resorption. This is consistent with DiIulio's [98] findings, though different methods were used to assess resorption.

It may be that the root surfaces were in the reversal stage of the remodeling cycle and/or active resorption may still have been present. In contrast, earlier studies utilizing this

hypothermic model found a decline in resorptive activity by day 28 [68, 93], with a reduction in clast cell presence. However, these studies also had a higher incidence of ankylosis, associated with acellular areas within the PDL. Shaboodien[68] also found the extent of ankylosis was more extensive over time. While the above studies all utilized a similar freezing duration, the variations in findings on resorption and ankylosis and PDL architecture suggest a milder type of insult in the present study, characterized by the rapid re-establishment of cellular architecture and absence of ankylosis and inflammatory cells within the PDL at day 28. Technical and operator variables to account for these differences in findings are discussed further in section 10.6.

Morphological signs of repair of resorption lacunae with deposition of cellular cementum-like deposits were evident from day 14, which continued till day 28, as seen by the smoother root surface. The variabilities in its presence and the reduced incidence of these deposits in the day 28 rats could be due to an ongoing, dynamic remodeling along the root surface where the root resorption in the later time periods may have had a role in eliminating areas of focal apposition along the root surface, as found by Wesselink et al [88], and postulated in other studies[87, 94, 125]. This is supported by the findings of Diiulio et al [98], who found a reduced frequency of ankylosis at the day 28 observation periods. This was associated with adjacent resorptive areas which usually did not show signs of repair. Interestingly, the ankylotic areas in DiIulio's study were all associated with an intact cementum surface.

As the day 28 rats in this study were among the first treated, with a postulated mild type of insult, it is probable that less cellular cementum-like deposits may have formed along the root surface. Any improved masticatory stimulation by day 28 was unlikely to have

played a role in this reduced incidence of ankylosis as increased mastication was found to partly prevent ankylosis, instead of eliminating areas of established ankylosis [99].

Root resorption was seen in the untreated control left molar but this was superficial and infrequent. There was no apparent predilection for any particular zone within the region of interest. This may have arisen as a result of increased masticatory function on the left molars after the right side thermal insult [93]. Cellular cementum-like deposits were also absent from the root surface.

10.4   Periodontal ligament width

The widening of the PDL width may be possibly attributed to an increased swelling within the PDL, associated with an increase in the number and/or size of existing blood vessels. The blood vessels within the PDL were most prominent during the earlier time periods but were not as noticeable by day 28. A decline in fluid extravasation from the blood vessels would also partially explain the decrease in PDL width in the later observation periods.

The treatment molars were probably also relatively hypofunctional, but investigation of the rats' right or left masticatory preference was beyond the scope of this study.

Several other reasons are hypothesized to account for the significantly larger (p<0.0001) mean PDL width on the right molar across days 7, 14, 21 and 28 days:

1. Areas of ankylosis in the treated molars were excluded from the calculations of PDL width.

2. Resorption along the bone and root surfaces seen from day 7. This continued to remain elevated till day 28. Where ankylosis was observed in localized focal

regions, adjacent resorption of the bone and root surfaces were seen. This may

also have also contributed to a net overall slight increase in width.

3. Problems with oblique sections. Even though measurement protocols were
    adhered to when taking measurements, some discretion was still needed in
    outlining the area of the PDL to be measured where there were sudden increases
    in PDL width towards the buccal or palatal as this would not have been in the
    furcation region. This would have equally affected the left and right side
    measurements and should be random in its effect.

4. The surface margins of alveolar bone were occasionally indistinct in sections,
    especially for recently formed mineralized tissue which had the tendency to form
    in irregular whorls and finger- like projections instead of regular lamellar sheets.

10.5 Treatment and sham rats

Frost has termed the non-specific elevation of bone formation and resorption which
follows noxious stimulation as a regional acceleratory phenomenon (RAP) [77] which has
been noted in regional areas and the contralateral side in other studies[79, 133]. From the
quantitative MAR and resorption data, labeling pattern and PDL width, no regional
acceleratory phenomena were seen in the internal control molars compared with the sham
control specimens. This suggests the use of the unfrozen contralateral molar in treated
rats may be a valid control to use to examine the mineralized tissue responses.

10.6 Ankylosis

Where ankylosis was observed, the close proximity to blood vessels in the earlier
observation periods was consistent with the pattern of formation of woven bone occurring
adjacent to newly formed blood vessels during the healing of tooth extraction sockets

[134]. The vascular pericytes may have been one of the sources of the precursor stem cells of the osteoblast/ cementoblast lineage [27]. However, the blood vessels may have also facilitated resorption within the periodontium. Castelli et al[135] found a higher vascular density within the PDL of replanted monkey incisors in areas of root cementum resorption than in areas of ankylosis. They suggested that a higher oxygen tension promotes osteoclasis. Similar observations on the proximity of vascular structures and osteoclasts within the PDL were noted by Biancu et al [136].

The hypothermic injury could have been insufficient to have produced ankylosis at day 28, yet enough to induce persistent active bone and root resorption for the stimulation of ongoing phagocytosis. As inflammatory cells were absent within the PDL, non-inflammatory mediators such as TGF-β and M-CSF, possibly mediated by osteoblasts[19, 24, 137], may have had a role in this surface resorption on the root surface, so it could extend beyond its normal 2-3 weeks duration, subsequent to the initial insult [38].

It was surprising that the most predictive mineralized tissue turnover parameters in this aseptic root resorption model reflected mineralized tissue formation and resorption on the root surface, where differences with the left control side were most significant, instead of the bone surface. This greater role of the root surface and associated formative and resorptive cells in this focal pattern of ankylosis, has been postulated to be due to a greater extent of cellular damage on the root side than the bone side of the PDL[86]. This would be expected with its closer proximity to the thermal insult. A more pronounced initial formative activity along the root surface was also seen by Dreyer et al [93].
The greater appositional activity along the bone surface compared with the root surface with a postulated reduced extent of cellular damage could have explained the spike in

woven bone formation at day 14 but, overall, no significant differences in mineral apposition along the bone surface over the four observation periods between the treated and control molars were noted.

The ongoing vitality of the PDL at day 28 appears to be related to the regression of ankylosis. The active root and bone resorption at the later time periods appear to be a protective mechanism to remove regions of reactive hard tissue. This resorption and possibly the source of clast-like cells were associated with vital parts of the PDL[87] and was postulated by Hammarström et al[94] to be a factor in the regression of ankylosis. In the study by Shaboodien [68], where a decline in resorptive activity within the PDL by day 28 occurred concomitantly with an increased distribution of ankylosis, numerous avital areas were noted in the associated PDL. This was not seen in this study. Technical factors, which were also postulated by Di Iulio[98], may have accounted for the intragroup variability and decreased incidence of ankylosis compared with earlier studies [53, 68, 93]. These are:

1. inter-rat variabilities in the thickness of dentine and/or enamel on the ground occlusal surface.

2. Tooth surface to which the dry ice pellets was applied. Dreyer al al [53] suggested the occlusal surface was the best surface for the application of the cold stimulus as better thermal conductivity occurs when the stimulus is applied parallel to the dentinal tubules. Due to the small size of the occlusal surface of the molars, inadvertent differential buccal surface application may have occurred.

3. Inconsistency in the physical size of the pellets applied or replaced. This would have affected the surface area of contact with the tooth surface and thermal conductivity. Large pellets would have a diminished area of contact with the

occlusal surface, with an increased air-insulating effect. During the 20 minute

duration, the pellets had to be frequently replaced as they diminished in size from

evaporation.

Examination of the photos taken during dry ice application suggested that variabilities in

physical size of the pellets applied may have partly explained the variations in the

histological responses seen. Future studies using this model should take into

consideration a method of standardizing the size of the dry ice pellets applied.

Based on the above studies and this study's findings, it is postulated that with a longer

freezing period, the incidence, permanence and progressiveness of dentoalveolar

ankylosis would eventually be established.

10.7   Clinical Implications of study

Ankylosis may form, but does not establish itself in the presence of a vital PDL[46, 86, 94].

Cells within the PDL are still responsible for the maintainence of the PDL width, as has

been found in other studies with PDL fibroblasts [39, 45, 47, 48, 138, 139]. The role of the

epithelial rests of Malessez in maintainence of the PDL width remains controversial [48,

125].

This thermal model was originally developed to be a more simplified experimental setup

to simulate the root resorption occurring during orthodontic tooth movement. This study

supports the role of root resorption in eliminating focal regions of ankylosis within the

PDL such as in rare case of spontaneous reeruption after secondary retention[84, 97, 140].

However, the pathogenesis of ankylosis differs, depending on the cause, and this may not

be extrapolated to the more common clinical scenario of physically traumatized incisors.

While studies have found masticatory function to be beneficial in the repair of the PDL and prevention of ankylosis[88, 99], it would be clinically relevant to conduct a biological study on the influence of orthodontic force application on traumatized teeth in the development of ankylosis to further explore the role of root resorption during ankylosis development.

10.8   Areas of further study

From this study, it appears that ongoing bone and root resorption, in conjunction with a decline in the mineralized tissue formation along the bone and root surface, were predominant factors in maintainence of a uniform PDL width. The increased cellularity within the PDL with the recovery of cellular vitality within the pulp chamber in the later time periods may be linked to this regression of ankylosis [66, 135].

Little is known on the molecular basis of the initiation of ankylosis. It has been suggested that a balance in the activities of bone sialoprotein and osteopontin may contribute to maintaining an unmineralized PDL region[6]. The paravascular regions in rodents are a common region for fibroblast progenitors [139]. In this regard, the protective role of fibroblasts, as has been suggested in other studies, in particular the competing activities of RANK and osteoprotegerin for the RANK-L ligand, should be further investigated. [6, 39, 88]

Further research is required into developing cellular labels or markers to trace the movement of the progenitor cells within the PDL during wound healing. This would hopefully improve our understanding into the factors stimulating their differentiation into different cellular phenotypes.

11. CONCLUSIONS

The following conclusions can be drawn from the results of the present study:

1. The low incidence of ankylosis seen in this study may have been due to a mild nature of thermal insult. Interoperator variation in technique may explain the differences, compared with other studies using the same model [53, 68, 98].

2. The ankylosis seen in this study was of a focal pattern, characterized by rapid mineralization within the ankylotic area and along the connecting root surface, across areas characteristic of resorbed and unresorbed areas. Cellular cementum-like tissue was always present. This supports the hypothesis of ankylosis being associated with an exuberant repair response to resorption along the root surface.

3. Discrete mineralized nodules within the periodontal ligament were associated with reactive hard tissue deposits along the root surface. These nodules may have a concurrent role in the initial formation of ankylosis.

4. The absence of ankylosis at day 28 could have been due to the absence of formed ankylosis or mineralized tissue resorption within the PDL and/or along the root surface may have had a role in in removing focal ankylotic deposits during this periodontal healing.

5. A time lag was observed in the formation of mineralized tissue along the walls of the pulp chamber, compared to along the bone and root surfaces, due to the cell death of odontoblasts from the thermal insult and the differentiation of new odontoblast-like cells.

6. Consistent uptake of both bone labels into alveolar bone was not reproducible as the tissue was of a woven bone type.

7. The periodontal ligament width had an initial widening, possibly associated with a reactive vascular response, and tended to return towards its original width in the

later observation periods, concomitantly with a healing response observed within the pulp and periodontal ligament.

8. In the rats with no signs of ankylosis and the sham rats, appositional activity was greatest along the interradicular alveolar bone surfaces in both treated and control teeth. Appositional activity was least along the furcal root surfaces.

9. The use of the untreated side molar as an internal control to assess mineralized tissue responses was a valid control.

10. The null hypotheses that a single prolonged thermal insult on a rat molar has no effect on mineralized tissue adaptation within the periodontium and pulp chamber and that the periodontal ligament width within the interradicular region does not change in response to this thermal trauma were rejected.

12. APPENDICES

12.1 Specimen Preparation

Tissue Dehydration and Processing Protocol

The following procedure was used for the impregnation of tissues with methylmethacrylate. All the procedures below except the last stage occurred in a vacuum chamber. Each specimen was placed in individual 25ml polypropylene tubes. At the last stage, to facilitate polymerization of the methylmethacrylate, the polypropylene tubes were tightly sealed and placed in a water bath in a 37°C temperature regulated oven. For each time interval, the old solution was discarded and fresh solution replenished:

Fixation-	70% ethanol	1hr
Dehydration-	70% ethanol	4hours
	70% ethanol	Overnight
	85% ethanol	4 hours
	85% ethanol	4 hours
	85% ethanol	Overnight
	95% ethanol	4 hours
	95% ethanol	4 hours
	95% ethanol	Overnight
	100% ethanol	4 hours
	100% ethanol	4 hours
	100% ethanol	Overnight
	100% ethanol	4 hours
	100% ethanol	Overnight
Defat	100% ethanol	1 hour
	100% ethanol	1 hour

	Acetone	24 hours
Infiltration	Methylmethacrylate monomer (MMA)	5 days
	MMA+Hardener	5 days
	MMA+Hardener+Initiator	2-3 days

The hardener was Polyethyleneglycol 400 added to MMA in the ratio of 1 part
Polyethyleneglycol 400 and 10 parts MMA.

The initiator was Bis(4-tert-butyl cyclohexyl) peroxydicarbonate with a measured 0.4%
(w/v of the combined volume of MMA+Hardener) in grams dissolved in the
MMA+Hardener solution to commence initiation of polymerization.

12.2   Slide Preparation And Section Processing Protocol

12.2.1 Slide coating procedures for undecalcified bone sections

All slides were coated with gelatine solution according to the following procedure.
Precoating of slides facilitates adherence of sections. All slides were obtained precleaned.

1. 10 grams of gelatine was dissolved in one litre of deionized water, heated to 60ºC
    and left to cool.

2. 1 gram of chromic potassium sulphate was then added with the assistance of a
    stirrer. This acted as an antifungal.

3. Place slides in racks

4. Each rack was placed in gelatine for a few seconds, then left on extraction
    overnight to dry.

12.2.2 Slides with unstained sections- processing

1. Remove filter paper and plastic

2. Soak slides in acetone (using a coplin jar or slide rack) for 10-15 minutes to remove methyl methacrylate

3. Clear in 2 series of xylene and place coverslip with adhesive

12.2.3 Slides with undecalcified sections- processing for VK/H&E staining

1. Repeat steps 1 and 2 in Appendix 3

2. Wash gently with distilled water 3x

3. Add 1% silver nitrate (made up in distilled water). This was made from stock 5% silver nitrate (stored at 4°C) with 1 part 5% silver nitrate and 4 parts distilled water.

4. Place slides in front of UV source for 1 hour. (the copland jar or slide rack is rotated once or twice during this time.

5. Wash gently with distilled water 3x.

6. Add 2.5% sodium thiosulphate for 5 minutes. This is made from stock 5% sodium thiosulphate solution.

7. Wash gently with distilled water 3x.

8. Place slides in haematoxylin for 10 minutes

9. Wash in running tap water for 1 minute

10. Differentiate with acid alcohol (couple of dips)

11. Wash in running tap water for 1 minute

12. Blue in saturated lithium carbonate (25 seconds)

13. Rinse in running tap water (30 seconds)

14. Stain with eosin for 2-4 minutes

15. Dehydrate with a 2 series of 100% ethanol, clear with 2 series of xylene and place coverslip with adhesive

12.2.4 Slides with decalcified sections- processing for H&E staining

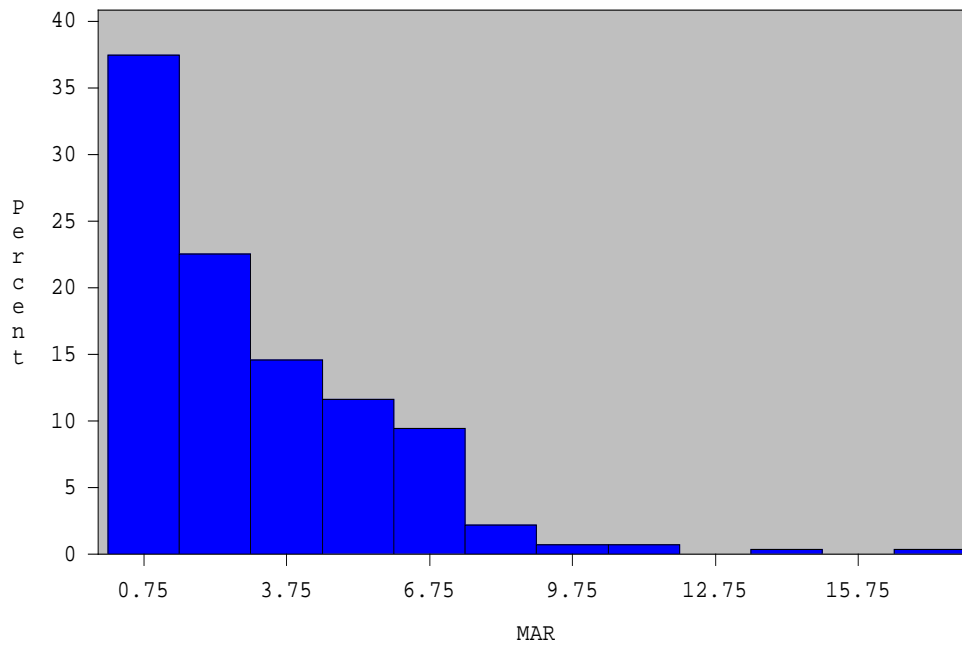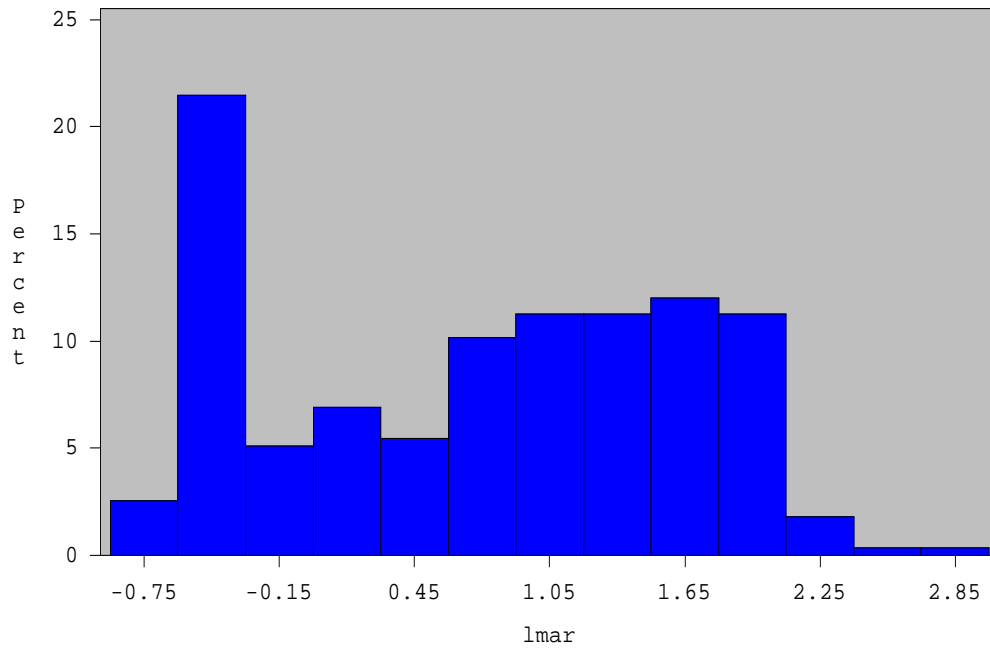1. Repeat steps 1 and 2 in Appendix 3
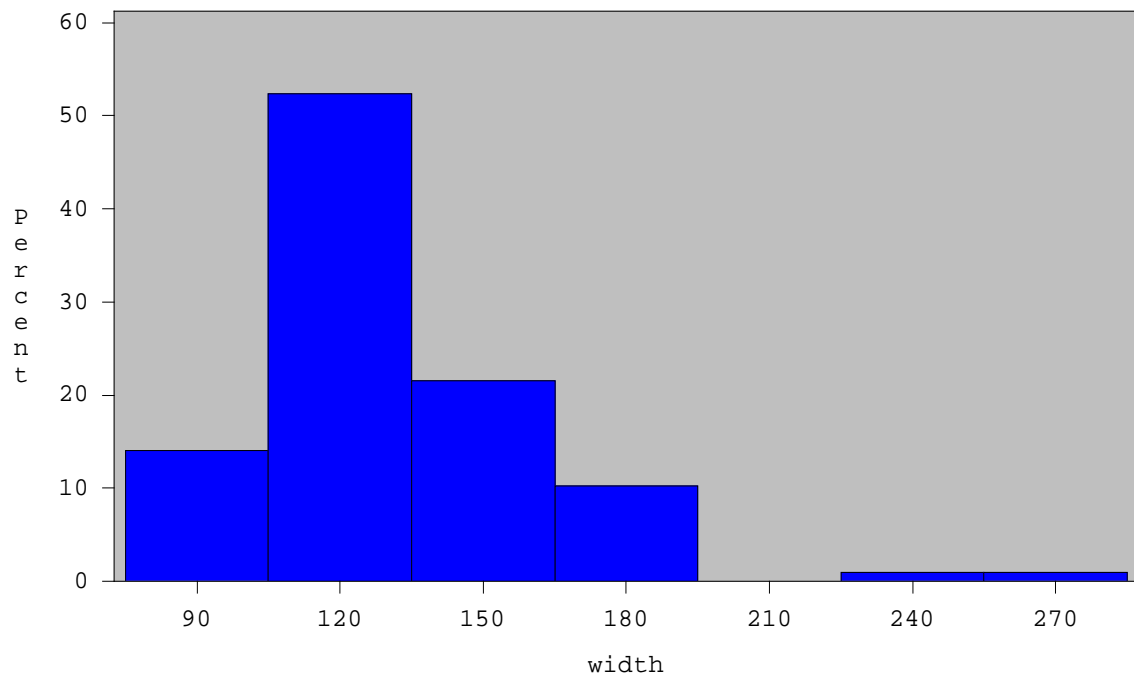
2. Repeat steps 7-15 in Appendix 4

12.3 Statistical Data

12.3.1 Histogram plot of MAR distribution

12.3.2 Histogram plot of log MAR distribution

12.3.3 Histogram plot of PDL width distribution

12.3.4 MAR dataset

Adjusted mean MAR for the time*side*location interaction

Effect	side	location	time	Log MAR	Mean MAR	Standard error
time*side*location	left	bone	7	1.6760	5.34417	0.78760
time*side*location	left	pulp	7	0.6644	1.94332	0.28484
time*side*location	left	root	7	-0.5039	0.60414	0.08295
time*side*location	right	bone	7	1.3330	3.79231	0.58158
time*side*location	right	pulp	7	0.4979	1.64531	0.24116
time*side*location	right	root	7	-0.2996	0.74115	0.10176
time*side*location	left	bone	14	1.7409	5.70227	0.77435
time*side*location	left	pulp	14	0.9481	2.58069	0.35041
time*side*location	left	root	14	-0.1768	0.83791	0.11378
time*side*location	right	bone	14	2.0205	7.54195	1.05918
time*side*location	right	pulp	14	1.1092	3.03188	0.44136
time*side*location	right	root	14	0.5571	1.74562	0.24387
time*side*location	left	bone	21	1.3768	3.96205	0.50559
time*side*location	left	pulp	21	0.6107	1.84164	0.27420
time*side*location	left	root	21	-0.4595	0.63161	0.09400
time*side*location	right	bone	21	1.5363	4.64742	0.61097
time*side*location	right	pulp	21	1.4723	4.35906	0.59612
time*side*location	right	root	21	0.2817	1.32535	0.17413
time*side*location	left	bone	28	1.7053	5.50286	0.74208
time*side*location	left	pulp	28	0.5947	1.81251	0.25284
time*side*location	left	root	28	-0.4426	0.64237	0.08270
time*side*location	right	bone	28	1.6543	5.22918	0.70522
time*side*location	right	pulp	28	1.0589	2.88310	0.42008
time*side*location	right	root	28	-0.3832	0.68169	0.09508

Differences of adjusted means (p values) for time*side*location interaction

Effect	time	side	location	time	side	location	p-value
time*side*location	7	left	bone	7	left	pulp	<.0001
time*side*location	7	left	bone	7	left	root	<.0001
time*side*location	7	left	bone	7	right	bone	0.0551
time*side*location	7	left	bone	14	left	bone	0.7495
time*side*location	7	left	bone	21	left	bone	0.1262
time*side*location	7	left	bone	28	left	bone	0.8853

176

Effect	time	side	location	time	side	location	p-value
time*side*location	7	left	pulp	7	left	root	<.0001
time*side*location	7	left	pulp	7	right	pulp	0.3320
time*side*location	7	left	pulp	14	left	pulp	0.1624
time*side*location	7	left	pulp	21	left	pulp	0.7971
time*side*location	7	left	pulp	28	left	pulp	0.7347
time*side*location	7	left	root	7	right	root	0.1921
time*side*location	7	left	root	14	left	root	0.0962
time*side*location	7	left	root	21	left	root	0.8269
time*side*location	7	left	root	28	left	root	0.7478
time*side*location	7	right	bone	7	right	pulp	<.0001
time*side*location	7	right	bone	7	right	root	<.0001
time*side*location	7	right	bone	14	right	bone	0.0013
time*side*location	7	right	bone	21	right	bone	0.3154
time*side*location	7	right	bone	28	right	bone	0.1221
time*side*location	7	right	pulp	7	right	root	<.0001
time*side*location	7	right	pulp	14	right	pulp	0.0038
time*side*location	7	right	pulp	21	right	pulp	<.0001
time*side*location	7	right	pulp	28	right	pulp	0.0081
time*side*location	7	right	root	14	right	root	<.0001
time*side*location	7	right	root	21	right	root	0.0025
time*side*location	7	right	root	28	right	root	0.6745
time*side*location	14	left	bone	14	left	pulp	<.0001
time*side*location	14	left	bone	14	left	root	<.0001
time*side*location	14	left	bone	14	right	bone	0.0820
time*side*location	14	left	bone	21	left	bone	0.0535
time*side*location	14	left	bone	28	left	bone	0.8527
time*side*location	14	left	pulp	14	left	root	<.0001
time*side*location	14	left	pulp	14	right	pulp	0.3413
time*side*location	14	left	pulp	21	left	pulp	0.0970
time*side*location	14	left	pulp	28	left	pulp	0.0709
time*side*location	14	left	root	14	right	root	<.0001
time*side*location	14	left	root	21	left	root	0.1636
time*side*location	14	left	root	28	left	root	0.1578
time*side*location	14	right	bone	14	right	pulp	<.0001
time*side*location	14	right	bone	14	right	root	<.0001
time*side*location	14	right	bone	21	right	bone	0.0131
time*side*location	14	right	bone	28	right	bone	0.0614
time*side*location	14	right	pulp	14	right	root	0.0013
Time * Side * Location	14	right	pulp	21	right	pulp	0.0717
Time * Side * Location	14	right	pulp	28	right	pulp	0.8069
Time * Side * Location	14	right	root	21	right	root	0.1550

177

Effect	time	side	location	time	side	location	p-value
Time * Side * Location	14	right	root	28	right	root	<.0001
Time * Side * Location	21	left	bone	21	left	pulp	<.0001
Time * Side * Location	21	left	bone	21	left	root	<.0001
Time * Side * Location	21	left	bone	21	right	bone	0.3014
Time * Side * Location	21	left	bone	28	left	bone	0.0771
Time * Side * Location	21	left	pulp	21	left	root	<.0001
Time * Side * Location	21	left	pulp	21	right	pulp	<.0001
Time * Side * Location	21	left	pulp	28	left	pulp	0.9375
Time * Side * Location	21	left	root	21	right	root	<.0001
Time * Side * Location	21	left	root	28	left	root	0.9313
Time * Side * Location	21	right	bone	21	right	pulp	0.6920
Time * Side * Location	21	right	bone	21	right	root	<.0001
Time * Side * Location	21	right	bone	28	right	bone	0.5301
Time * Side * Location	21	right	pulp	21	right	root	<.0001
Time * Side * Location	21	right	pulp	28	right	pulp	0.0387
Time * Side * Location	21	right	root	28	right	root	0.0006
Time * Side * Location	28	left	bone	28	left	pulp	<.0001
Time * Side * Location	28	left	bone	28	left	root	<.0001
Time * Side * Location	28	left	bone	28	right	bone	0.7443
Time * Side * Location	28	left	pulp	28	left	root	<.0001
Time * Side * Location	28	left	pulp	28	right	pulp	0.0061
Time * Side * Location	28	left	root	28	right	root	0.7099
Time * Side * Location	28	right	bone	28	right	pulp	0.0004
Time * Side * Location	28	right	bone	28	right	root	<.0001
Time * Side * Location	28	right	pulp	28	right	root	<.0001

12.3.5 Resorption dataset

12.3.5.1   % surface resorption

Adjusted means for the time*side*location interaction

Variable	days	side	Location	Mean % surface resorption, $R_{bone\ or\ root}$	Standard Error
time*side*location	7	left	bone	5.955	0.007264
time*side*location	7	left	root	0.748	0.006592
time*side*location	7	right	bone	6.600	0.017429
time*side*location	7	right	root	12.981	0.032547
time*side*location	14	left	bone	9.984	0.015973
time*side*location	14	left	root	1.900	0.005721

Variable	days	side	Location	Mean % surface resorption, $R_{bone\ or\ root}$	Standard Error
time*side*location	14	right	bone	16.363	2.0302
time*side*location	14	right	root	21.907	3.8108
time*side*location	21	left	bone	11.602	4.6142
time*side*location	21	left	root	0.913	0.3943
time*side*location	21	right	bone	12.987	1.4204
time*side*location	21	right	root	20.387	3.5726
time*side*location	28	left	bone	9.562	1.6464
time*side*location	28	left	root	1.586	0.5269
time*side*location	28	right	bone	12.121	2.6503
time*side*location	28	right	root	23.564	3.1656

Differences of adjusted means (p values) for time*side*location interaction

Variable	Time	side	Location	Time	Side	Location	p-value
side*bone_root		left	bone		left	root	<.0001
side*bone_root		left	bone		right	bone	0.0709
side*bone_root		left	bone		right	root	<.0001
side*bone_root		left	root		right	bone	<.0001
side*bone_root		left	root		right	root	<.0001
side*bone_root		right	bone		right	root	0.0002
time	7			14			<.0001
time	7			21			0.0011
time	7			28			<.0001
time	14			21			0.5494
time	14			28			0.4320
time	21			28			0.9427

12.3.5.2 % number of lacunae

Adjusted means for the time*side*location interaction

Variable	Time	Side	Location	Mean % lacunae number, $N_{bone\ or\ root}$	Standard Error
time*side*location	7	left	bone	8.659	1.5548
time*side*location	7	left	root	7.85	0.6910
time*side*location	7	right	bone	11.129	2.8005
time*side*location	7	right	root	15.482	2.5171
time*side*location	14	left	bone	15.524	2.0338

Variable	Time	Side	Location	Mean % lacunae number, $N_{\text{bone or root}}$	Standard Error
time*side*location	14	left	root	3.140	1.0427
time*side*location	14	right	bone	22.264	2.0072
time*side*location	14	right	root	26.898	4.3811
time*side*location	21	left	bone	14.069	3.5143
time*side*location	21	left	root	2.157	0.5828
time*side*location	21	right	bone	16.651	1.2202
time*side*location	21	right	root	27.006	3.8581
time*side*location	28	left	bone	12.636	2.5295
time*side*location	28	left	root	2.297	0.8838
time*side*location	28	right	bone	15.414	3.2660
time*side*location	28	right	root	26.572	4.1160

Differences of adjusted means (p values) for time*side*location interaction

Variable	Time	side	Location	Time	side	Location	P-value
side*bone_root		left	bone		left	root	<.0001
side*bone_root		left	bone		right	bone	0.0241
side*bone_root		left	bone		right	root	<.0001
side*bone_root		left	root		right	bone	<.0001
side*bone_root		left	root		right	root	<.0001
side*bone_root		right	bone		right	root	0.0016
time	7			14			<.0001
time	7			21			<.0001
time	7			28			<.0001
time	14			21			0.2690
time	14			28			0.0922
time	21			28			0.6330

REFERENCES

1. Hassell, T.M., Tissues and cells of the periodontium. Periodontol 2000, 1993. 3: p. 9-38.

2. Berkovitz, B., Holland, GR, Moxham, BJ, A colour atlas and textbook of oral anatomy, histology and embryology. 1992, Wolfe. p. 111.

3. Bosshardt, D.D. and K.A. Selvig, Dental cementum: the dynamic tissue covering of the root. Periodontol 2000, 1997. 13: p. 41-75.

4. Gonçalves, P., Sallum, EA, Sallum, AW, Casati, MZ, Toledo, S, Nociti, FH, Dental cementum reviewed: development, structure, composition,regeneration and potential functions. Brazilian Journal of Oral Sciences, 2005. Vol. 4(No. 12, Jan./Mar. 2005): p. pp. 651-658.

5. Saygin, N., W. Giannobile, and M. Somerman, Molecular and cell biology of cementum. Periodontology 2000, 2000. 24(1): p. 73-98.

6. Nanci, A. and D.D. Bosshardt, Structure of periodontal tissues in health and disease. Periodontol 2000, 2006. 40: p. 11-28.

7. Ten Cate, A.R., Periodontium, in Oral Histology. Development, Structure & Function. 1994, Mosby. p. 276-312.

8. Marks, S., Schroeder, HE, Tooth eruption: Theories and facts. The Anatomical Record, 1996. 245(2): p. 374-393.

9. Misawa, Y., et al., Effect of age on alveolar bone turnover adjacent to maxillary molar roots in male rats: A histomorphometric study. Arch Oral Biol, 2007. 52(1): p. 44-50.

10. Schroeder, H.E., Cementum, in The Periodontium. 1986: Berlin, Germany. p. 23-128.

11. Bosshardt, D.D., Are Cementoblasts a Subpopulation of Osteoblasts or a Unique Phenotype? J Dent Res, 2005. 84(5): p. 390-406.

12. Yamamoto, T. and K.V. Hinrichsen, The development of cellular cementum in rat molars, with special reference to the fiber arrangement. Anat Embryol (Berl), 1993. 188(6): p. 537-49.

13. Bosshardt, D.D. and H.E. Schroeder, How repair cementum becomes attached to the resorbed roots of human permanent teeth. Acta Anat (Basel), 1994. 150(4): p. 253-66.

14. Bower, R.C., Furcation morphology relative to periodontal treatment. Furcation root surface anatomy. J Periodontol, 1979. 50(7): p. 366-74.

15.   Zander, H.A. and B. Hurzeler, Continuous cementum apposition. J Dent Res, 1958. 37(6): p. 1035-44.

16.   Amstad-Jossi, M. and H.E. Schroeder, Age-related alterations of periodontal structures around the cemento-enamel junction and of the gingival connective tissue composition in germ-free rats. J Periodontal Res, 1978. 13(1): p. 76-90.

17.   Sodek, J. and M. McKee, Molecular and cellular biology of alveolar bone. Periodontology 2000, 2000. 24(1): p. 99-126.

18.   Saffar, J.L., J.J. Lasfargues, and M. Cherruau, Alveolar bone and the alveolar process: the socket that is never stable. Periodontol 2000, 1997. 13: p. 76-90.

19.   Li, X., Jee, WS, Integrated Bone Tissue Anatomy and Physiology, in Current Topics in Bone Biology, H. Deng, Liu, YZ, Editor. 2005, World Scientific Printers: Singapore. p. 11-56.

20.   Vignery, A., Baron, R, Dynamic histomorphometry of alveolar bone remodeling in the adult rat. The Anatomical Record, 1980. 196(2): p. 191-200.

21.   Thilander, B., Rygh, P, Reitan, K, Tissue Reactions in Orthodontics, in Orthodontics: Current Principles & Techniques, T.M. Graber, Vanarsdall, R.L, Vig, K., Editor. 2005, Mosby: St Louis. p. 145-220.

22.   Teitelbaum, S.L., C.C. Stewart, and A.J. Kahn, Rodent peritoneal macrophages as bone resorbing cells. Calcif Tissue Int, 1979. 27(3): p. 255-61.

23.   Mundy, C.R., et al., Direct resorption of bone by human monocytes. Science, 1977. 196(4294): p. 1109-11.

24.   Feng, X., Zhou, H, Osteoclast Biology, in Current Topics in Bone Biology, H. Deng, Liu, YZ, Editor. 2005, World Scientific Printers: Singapore. p. 71-94.

25.   Arnett, T.R., Update on bone cell biology. Eur J Orthod, 1990. 12(1): p. 81-90.

26.   Miekle, M.C. The Biology of Skeletal Tissues, in Craniofacial development, growth and evolution. 2002, Bateson Publishing Diss, Norfolk, UK. p. 77-124.

27.   Connolly, M., Li, G, Skeletal Stem Cells, in Current Topics in Bone Biology, H. Deng, Liu, YZ, Editor. 2005, World Scientific Printers: Singapore. p. 57-70.

28.   Simonet, W.S., et al., Osteoprotegerin: a novel secreted protein involved in the regulation of bone density. Cell, 1997. 89(2): p. 309-19.

29.   Seibel, M.J., Molecular markers of bone turnover: biochemical, technical and analytical aspects. Osteoporos Int, 2000. 11 Suppl 6: p. S18-29.

30.   Roberts, E.W., Bone Physiology, Metabolism, and Biomechanics in Orthodontic Practice, Chapter 6 in Orthodontics: Current Principles and Techniques. 2005. Editors Graber TM, Vanarsdall RJ, Vig K. Mosby: St Louis. p. 221-292.

31.   McCulloch, C.A. and A.H. Melcher, Cell density and cell generation in the periodontal ligament of mice. Am J Anat, 1983. 167(1): p. 43-58.

32.   Mariotti, A., The extracellular matrix of the periodontium: dynamic and interactive tissues. Periodontol 2000, 1993. 3: p. 39-63.

33.   Domon, T., et al., Apoptosis of odontoclasts under physiological root resorption of human deciduous teeth. Cell Tissue Res, 2008. 331(2): p. 423-33.

34.   Kimura, R., et al., Dental root resorption and repair: histology and histometry during physiological drift of rat molars. J Periodontal Res, 2003. 38(5): p. 525-32.

35.   Domon, T., et al., Electron microscopic and histochemical studies of the mononuclear odontoclast of the human. Anat Rec, 1994. 240(1): p. 42-51.

36.   Domon, T., et al., Mononuclear odontoclast participation in tooth resorption: the distribution of nuclei in human odontoclasts. Anat Rec, 1997. 249(4): p. 449-57.

37.   Domon, T., et al., Increase in odontoclast nuclei number by cell fusion: a three-dimensional reconstruction of cell fusion of human odontoclasts. Anat Rec, 1998. 252(3): p. 462-71.

38.   Gunraj, M.N., Dental root resorption. Oral Surg Oral Med Oral Pathol Oral Radiol Endod, 1999. 88(6): p. 647-53.

39.   Lekic, P., McCulloch, CAG, Periodontal ligament cell populations: The central role of fibroblasts in creating a unique tissue. The Anatomical Record, 1996. 245(2): p. 327-341.

40.   Ten Cate, A.R., Development of the Periodontium, in Oral Histology. Development, Structure & Function. 1994, Mosby. p. 257-275.

41.   Grzesik, W.J. and A.S. Narayanan, Cementum And Periodontal Wound Healing And Regeneration. Crit Rev Oral Biol Med, 2002. 13(6): p. 474-484.

42.   Yamashiro, T., M. Tummers, and I. Thesleff, Expression of Bone Morphogenetic Proteins and Msx Genes during Root Formation. J Dent Res, 2003. 82(3): p. 172-176.

43.   Hasegawa, N., et al., Immunohistochemical characteristics of epithelial cell rests of Malassez during cementum repair. J Periodontal Res, 2003. 38(1): p. 51-6.

44.   Brice, G.L., W.J. Sampson, and M.R. Sims, An ultrastructural evaluation of the relationship between epithelial rests of Malassez and orthodontic root resorption and repair in man. Aust Orthod J, 1991. 12(2): p. 90-4.

45.   Melcher, A.H., On the repair potential of periodontal tissues. J Periodontol, 1976. 47(5): p. 256-60.

46.   Line, S.E., A.M. Polson, and H.A. Zander, Relationship between periodontal injury, selective cell repopulation and ankylosis. J Periodontol, 1974. 45(10): p. 725-30.

47.   Ogiso, B., et al., Fibroblastic regulation of osteoblast function by prostaglandins. Cell Signal, 1992. 4(6): p. 627-39.

48.   Lindskog, S., L. Blomlof, and L. Hammarström, Evidence for a role of odontogenic epithelium in maintaining the periodontal space. J Clin Periodontol, 1988. 15(6): p. 371-3.

49.   Yoshizawa, T., et al., Homeobox Protein Msx2 Acts as a Molecular Defense Mechanism for Preventing Ossification in Ligament Fibroblasts. Mol. Cell. Biol., 2004. 24(8): p. 3460-3472.

50.   Reitan, K. and E. Kvam, Comparative behavior of human and animal tissue during experimental tooth movement. Angle Orthod, 1971. 41(1): p. 1-14.

51.   Shimpo, S., et al., Compensatory bone formation in young and old rats during tooth movement. Eur J Orthod, 2003. 25(1): p. 1-7.

52.   King, G.J., et al., Alveolar bone turnover in male rats: site- and age-specific changes. Anat Rec, 1995. 242(3): p. 321-8.

53.   Dreyer, C.W., A.M. Pierce, and S. Lindskog, Hypothermic insult to the periodontium: a model for the study of aseptic tooth resorption. Endod Dent Traumatol, 2000. 16(1): p. 9-15.

54.   Bosshardt, D.D. and H.E. Schroeder, Cementogenesis reviewed: a comparison between human premolars and rodent molars. Anat Rec, 1996. 245(2): p. 267-92.

55.   Goldberg, M. and A.J. Smith, Cells and Extracellular Matrices of Dentin and Pulp: A Biological Basis for Repair and Tissue Engineering. Crit Rev Oral Biol Med, 2004. 15(1): p. 13-27.

56.   Laino, G., et al., A new population of human adult dental pulp stem cells: a useful source of living autologous fibrous bone tissue (LAB). J Bone Miner Res, 2005. 20(8): p. 1394-402.

57.   Tate, Y., et al., Odontoblast responses to GaAlAs laser irradiation in rat molars: an experimental study using heat-shock protein-25 immunohistochemistry. Eur J Oral Sci, 2006. 114(1): p. 50-7.

58.   Ten Cate, A.R., Dentine-Pulp complex, in Oral Histology. Development, Structure & Function. 1994, Mosby. p. 169-217.

59.   Andreasen, J.O., Relationship between surface and inflammatory resorption and changes in the pulp after replantation of permanent incisors in monkeys. J Endod, 1981. 7(7): p. 294-301.

60.   Hammarström, L. and S. Lindskog, General morphological aspects of resorption of teeth and alveolar bone. Int Endod J, 1985. 18(2): p. 93-108.

61.   Brudvik, P. and P. Rygh, Transition and determinants of orthodontic root resorption-repair sequence. Eur J Orthod, 1995. 17(3): p. 177-88.

62. Andreasen, J.O., Relationship between cell damage in the periodontal ligament after replantation and subsequent developmnet of root resorption. Acta Odontol Scand, 1981. 39: p. 15-25.

63. Andreasen, J.O., Effect of extra-alveolar period and storage media upon periodontal and pulpal healing after replantation of mature permanent incisors in monkeys. Int J Oral Surg, 1981. 10(1): p. 43-53.

64. Andreasen, J.O., Interrelation between alveolar bone and periodontal ligament repair after replantation of mature permanent incisors in monkeys. J Periodontal Res, 1981. 16(2): p. 228-35.

65. Tal, H., A. Kozlovsky, and S. Pitaru, Healing of sites within the dog periodontal ligament after application of cold to the periodontal attachment apparatus. J Clin Periodontol, 1991. 18(7): p. 543-7.

66. Tal, H. and S.S. Stahl, Healing following devitalization of sites within the periodontal ligament by ultralow temperatures. J Periodontol, 1986. 57(12): p. 735-41.

67. Wesselink, P.R., W. Beertsen, and V. Everts, Resorption of the mouse incisor after the application of cold to the periodontal attachment apparatus. Calcif Tissue Int, 1986. 39(1): p. 11-21.

68. Shaboodien, S., Traumatically induced dentoalveolar ankylosis in rats. Doctor of Clinical Dentistry 2005 thesis. University of Adelaide.

69. Brudvik, P. and P. Rygh, The repair of orthodontic root resorption: an ultrastructural study. Eur J Orthod, 1995. 17(3): p. 189-98.

70. Hebel, R., Stromberg, M.W, Osteology, in Anatomy of the Laboratory Rat. 1976, The Williams & Wilkins Company. p. 9-11.

71. Tran Van, P.T., A. Vignery, and R. Baron, Cellular kinetics of the bone remodeling sequence in the rat. Anat Rec, 1982. 202(4): p. 445-51.

72. Baron, R., R. Tross, and A. Vignery, Evidence of sequential remodeling in rat trabecular bone: morphology, dynamic histomorphometry, and changes during skeletal maturation. Anat Rec, 1984. 208(1): p. 137-45.

73. Vignery, A. and R. Baron, Effects of parathyroid hormone on the osteoclastic pool, bone resorption and formation in rat alveolar bone. Calcif Tissue Res, 1978. 26(1): p. 23-8.

74. Nakamura, Y., et al., Histology and tetracycline labeling of a single section of alveolar bone of first molars in the rat. Biotechnic & Histochemistry, 2000. 75(1): p. 1-6.

75. Licata, A.A., Discovery, clinical development, and therapeutic uses of bisphosphonates. Ann Pharmacother, 2005. 39(4): p. 668-77.

76. Komatsu, K., et al., Long-term effects of local pretreatment with alendronate on healing of replanted rat teeth. J Periodontal Res, 2008. 43(2): p. 194-200.

77. Frost, H.M., Bone Histomorphometry: choice of marking agent and labeling schedule, in Bone Histomorphometry: techniques and interpretation, R.R. Recker, Editor. 1983, CRC Press. p. 37-52.

78. Eriksen, E.F., Axelrod, D.W, Melsen, F, Histomorphometric indices, in Bone Histomorphometry. 1994, Raven Press: New York. p. 39-50.

79. Verna, C., D. Zaffe, and G. Siciliani, Histomorphometric study of bone reactions during orthodontic tooth movement in rats. Bone, 1999. 24(4): p. 371-379.

80. Andersson, L., et al., Tooth ankylosis. Clinical, radiographic and histological assessments. Int J Oral Surg, 1984. 13(5): p. 423-31.

81. Löe, H. and J. Waerhaug, Experimental replantation of teeth in dogs and monkeys. Arch Oral Biol, 1961. 3: p. 176-84.

82. Biederman, W., The problem of the ankylosed tooth. Dent Clin North Am, 1968: p. 409-24.

83. Lindskog, S. and L. Blomlof, Mineralized tissue-formation in periodontal wound healing. J Clin Periodontol, 1992. 19(10): p. 741-8.

84. Raghoebar, G.M., et al., Secondary retention of permanent molars: an assessment of ankylosis by scanning electron and light microscopy. Br J Oral Maxillofac Surg, 1992. 30(1): p. 50-5.

85. Hellsing, E., I. Alatli-Kut, and L. Hammarström, Experimentally induced dentoalveolar ankylosis in rats. Int Endod J, 1993. 26(2): p. 93-8.

86. Andreasen, J.O., Analysis of pathogenesis and topography of replacement root resorption (ankylosis) after replantation of mature permanent incisors in monkeys. Swed Dent J, 1980. 4(6): p. 231-40.

87. Andreasen, J.O. and M.R. Skougaard, Reversibility of surgically induced dental ankylosis in rats. Int J Oral Surg, 1972. 1(2): p. 98-102.

88. Wesselink, P.R. and W. Beertsen, Repair processes in the periodontium following dentoalveolar ankylosis: the effect of masticatory function. J Clin Periodontol, 1994. 21(7): p. 472-8.

89. Wesselink, P.R. and W. Beertsen, Ankylosis of the mouse molar after systemic administration of 1-hydroxyethylidene-1,1-bisphosphonate (HEBP). J Clin Periodontol, 1994. 21(7): p. 465-71.

90. Melcher, A.H., Repair of wounds in the periodontium of the rat. Influence of periodontal ligament on osteogenesis. Arch Oral Biol, 1970. 15(12): p. 1183-204.

91. Pindborg, J.J., Ankylosis of teeth, in Pathology of the dental hard tissues. 1970, W.B Saunders: Philadelphia. p. 362-366.

92.   Jacobs, S.G., Ankylosis of permanent teeth: a case report and literature review. Aust Orthod J, 1989. 11(1): p. 38-44.

93.   Dreyer, C.W., Clast Cell Activity in a Model of Aseptic Root Resorption. 2002. PhD thesis. The University of Adelaide: Adelaide.

94.   Hammarström, L., et al., Dynamics of dentoalveolar ankylosis and associated root resorption. The role of the necrotic periodontal membrane in cementum resorption and ankylosis. Endod Dent Traumatol, 1989. 5(4): p. 163-75.

95.   Giannobile, W.V., et al., Recombinant human osteogenic protein-1 (OP-1) stimulates periodontal wound healing in class III furcation defects. J Periodontol, 1998. 69(2): p. 129-37.

96.   Rygh, P., Reitan, K, Changes in the supporting tissues of submerged deciduous molars with and without permanent successors. Odontologisk tidskrift, 1964. 72: p. 345-360.

97.   Raghoebar, G.M., et al., Secondary retention of permanent molars: a histologic study. J Oral Pathol Med, 1989. 18(8): p. 427-31.

98.   Di Iulio, D.S., Relationship of epithelial cells and nerve fibres to experimentally induced dentoalveolar ankylosis in rats, Doctor of Clinical Dentistry 2007 thesis. University of Adelaide.

99.   Andersson, L., et al., Effect of masticatory stimulation on dentoalveolar ankylosis after experimental tooth replantation. Endod Dent Traumatol, 1985. 1(1): p. 13-6.

100.   Parfitt, A.M., et al., Bone histomorphometry: standardization of nomenclature, symbols, and units. Report of the ASBMR Histomorphometry Nomenclature Committee. J Bone Miner Res, 1987. 2(6): p. 595-610.

101.   Eriksen, E.F., Axelrod, D.W, Melsen, F, Bone Histology and Histomorphometry, in Bone Histomorphometry. 1994, Raven Press: New York. p. 33-38.

102.   Miller, S.C., et al., Intermittent parathyroid hormone administration stimulates bone formation in the mandibles of aged ovariectomized rats. J Dent Res, 1997. 76(8): p. 1471-6.

103.   King, G.J. and S.D. Keeling, Orthodontic bone remodeling in relation to appliance decay. Angle Orthod, 1995. 65(2): p. 129-40.

104.   King, G.J., S.D. Keeling, and T.J. Wronski, Histomorphometric study of alveolar bone turnover in orthodontic tooth movement. Bone, 1991. 12(6): p. 401-9.

105.   Ramirez-Yanez, G.O., et al., Prostaglandin E2 enhances alveolar bone formation in the rat mandible. Bone, 2004. 35(6): p. 1361-8.

106.   Parfitt, A.M., Bone histomorphometry: standardization of nomenclature, symbols and units (summary of proposed system). Bone, 1988. 9(1): p. 67-9.

107. Frost, H.M., Tetracycline-based histological analysis of bone remodeling. Calcified Tissue International, 1969. 3(1): p. 211-237.

108. Tam, C.S. and W. Anderson, Tetracycline labeling of bone in vivo. Calcif Tissue Int, 1980. 30(2): p. 121-5.

109. Sun, T.C., et al., Do different fluorochrome labels give equivalent histomorphometric information? Bone, 1992. 13(6): p. 443-446.

110. Frost, H.M., Bone Histomorphometry: Corrrection of the Labeling 'Escape Error', in Bone Histomorphometry: techniques and interpretation, R.R. Recker, Editor. 1983, CRC Press. p. 133-142.

111. Parfitt, A.M., The Physiologic and Clinical Significance of Bone Histomorphometric Data, in Bone Histomorphometry: techniques and interpretation, R.R. Recker, Editor. 1983.

112. Birkenhager-Frenkel, D.H. and J.C. Birkenhager, Bone appositional rate and percentage of doubly and singly labeled surfaces: Comparison of data from 5 and 20 [mu]m sections. Bone, 1987. 8(1): p. 7-12.

113. Yagishita, H., S. Iwatsubo,and T. Aoba, Confocal laser scanning microscopic studies on alveolar bone remodeling with orthodontic tooth movement and retention. Scanning Microsc, 1995. 9(3): p. 781-8.

114. Page, K.M., Stevens, A, Lowe, J, Bancroft, J.D, Bone, in Theory and Practice of Histological Techniques, J.D. Bancroft, Stevens, A, Editor. 1990, Churchill Livingstone: New York. p. 309-341.

115. Tuncay, O.C., D. Ho, and M.K. Barker, Oxygen tension regulates osteoblast function. Am J Orthod Dentofacial Orthop, 1994. 105(5): p. 457-63.

116. Zeger, S.L. and K.Y. Liang, Longitudinal data analysis for discrete and continuous outcomes. Biometrics, 1986. 42(1): p. 121-30.

117. Lee, J.H., et al., The use of GEE for analyzing longitudinal binomial data: a primer using data from a tobacco intervention. Addict Behav, 2007. 32(1): p. 187-93.

118. Bland, J.M. and D.G. Altman, Statistical methods for assessing agreement between two methods of clinical measurement. Lancet, 1986. 1(8476): p. 307-10.

119. Efron, B., "Bootstrap Methods: Another Look at the Jackknife". The Annals of Statistics, 1979. 7(1): p. 1-26.

120. Ogura, N., et al., Longitudinal observation of cementum regeneration through multiple fluorescent labeling. J Periodontol, 1991. 62(4): p. 284-91.

121. Compston, J.E., S. Vedi, and A.J. Stellon, Inter-observer and intra-observer variation in bone histomorphometry. Calcif Tissue Int, 1986. 38(2): p. 67-70.

122.   Brown, G.G., Processing of Tissue & Methods for Bone and Cartilage, in An Introduction to Histotechnology. 1978, Appleton-Century-Crofts. p. 52-83, 246-248.

123.   Hori, M., et al., A classification of in vivo bone labels after double labeling in canine bones. Bone, 1985. 6(3): p. 147-154.

124.   Martin, R.B., Label escape theory revisited: the effects of resting periods and section thickness. Bone, 1989. 10(4): p. 255-64.

125.   Wesselink, P.R. and W. Beertsen, The prevalence and distribution of rests of Malassez in the mouse molar and their possible role in repair and maintenance of the periodontal ligament. Arch Oral Biol, 1993. 38(5): p. 399-403.

126.   Grunheid, T., B.A. Morbach, and A. Zentner, Pulpal cellular reactions to experimental tooth movement in rats. Oral Surg Oral Med Oral Pathol Oral Radiol Endod, 2007. 104(3): p. 434-41.

127.   Trowbridge, H.O., Pulp biology: progress during the past 25 years. Aust Endod J, 2003. 29(1): p. 5-12.

128.   Fischer, F.M., A. el-Kafrawy, and D.F. Mitchell, Studies of tertiary dentin in monkey teeth using vital dyes. J Dent Res, 1970. 49(6): p. Suppl:1537-40.

129.   Nishioka, M., et al., Tooth replantation in germ-free and conventional rats. Endod Dent Traumatol, 1998. 14(4): p. 163-73.

130.   Yu, C. and P.V. Abbott, An overview of the dental pulp: its functions and responses to injury. Aust Dent J, 2007. 52(1 Suppl): p. S4-16.

131.   Doherty, M.J., et al., Vascular pericytes express osteogenic potential in vitro and in vivo. J Bone Miner Res, 1998. 13(5): p. 828-38.

132.   Anstendig, H.S. and J.H. Kronman, A histologic study of pulpal reaction to orthodontic tooth movement in dogs. Angle Orthod, 1972. 42(1): p. 50-5.

133.   Schaffler, M.B., et al., Skeletal tissue responses to thermal injury: an experimental study. Bone, 1988. 9(6): p. 397-406.

134.   Cardaropoli, G., M. Araujo, and J. Lindhe, Dynamics of bone tissue formation in tooth extraction sites. An experimental study in dogs. J Clin Periodontol, 2003. 30(9): p. 809-18.

135.   Castelli, W.A., et al., Vascular response of the periodontal membrane after replantation of teeth. Oral Surg Oral Med Oral Pathol, 1980. 50(5): p. 390-7.

136.   Biancu, S., I. Ericsson, and J. Lindhe, Periodontal ligament tissue reactions to trauma and gingival inflammation. An experimental study in the beagle dog. J Clin Periodontol, 1995. 22(10): p. 772-9.

137.   Chen, D., Chen, M, Yan, Y, Wang, YJ, Zhu, T, Regulation of Bone Remodeling, in Current Topics In Bone Biology. 2005. p. 279-298.

138.   Ogiso, B., et al., Fibroblasts inhibit mineralised bone nodule formation by rat bone marrow stromal cells in vitro. J Cell Physiol, 1991. 146(3): p. 442-50.

139.   Beertsen, W., C.A. McCulloch, and J. Sodek, The periodontal ligament: a unique, multifunctional connective tissue. Periodontol 2000, 1997. 13: p. 20-40.

140.   Raghoebar, G.M., W.A. van Koldam, and G. Boering, Spontaneous reeruption of a secondarily retained permanent lower molar and an unusual migration of a lower third molar. Am J Orthod Dentofacial Orthop, 1990. 97(1): p. 82-4.